MITOXANTRONE–LOADED ALBUMIN MICROSPHERES FOR LOCALIZED INTRATUMORAL CHEMOTHERAPY OF BREAST CANCER

By

BRETT ANTHONY ALMOND

A DISSERTATION PRESENTED TO THE GRADUATE SCHOOL
OF THE UNIVERSITY OF FLORIDA IN PARTIAL FULFILLMENT
OF THE REQUIREMENTS FOR THE DEGREE OF
DOCTOR OF PHILOSOPHY

UNIVERSITY OF FLORIDA

2002

To my parents, Barbara and Donald Almond, for their patient support of my prolonged academic pursuits.

ACKNOWLEDGMENTS

I would like to gratefully acknowledge the many people whose support made it possible for me to complete this research. I am permanently indebted to Dr. Eugene P. Goldberg for patiently sharing his knowledge and advice as he guided my graduate studies. I would also like to thank the other members of my graduate committee: Dr. Christopher Batich, Dr. Anthony Brennan, Dr. Allen Neims, and Dr. James Seeger. I must also acknowledge my appreciation of Dr. Lynn Peck and Dr. Sunder Shrestha for taking their time to teach me various procedures and sharing their extensive knowledge of animal husbandry. Additionally, Dr. Dietmar Siemann's generous donation of the 16/C MAC tumor line made this research possible. I also gratefully acknowledge Dr. Carol Detrisac whose speedy analysis of our histology slides made it possible for me to finish in a timely manner. Additionally, Jennifer Wrighton has provided considerable administrative support over the last several years.

I would also like to thank the other graduate students who offered consider help and moral support as I progressed through my studies. Dr. Ahmad "Bob" Hadba, who initiated these studies with me, taught me much about good lab practice, experimental design, and, most of all, the required self-discipline. Dr. James Marotta offered much advice regarding the laboratory, research, and life-in-general that I find invaluable to this day. I would also like to thank Dr. Kaustubh Rau, Dr. Drew Amery, Dr. Christopher Widenhouse and Dr. Jeanne McDonald for their lively discussions, knowledge, and support.

I would like to specifically like to thank the other students whose help allowed me to conduct these experiments. Dr. Ahmad "Bob" Hadba, Shema Freeman and Amanda York diligently traveled with me to the animal care facilities seven days a week and helped with many of my other experiments. Paul Martin who showed great patience in helping me obtain every electron micrograph. I would like to especially thank Amy Gibson whose help and support were absolutely invaluable throughout the dissertation process. I would also like to thank my other friends and collegues, which include but are not limited to: Clay Bohn, Brian Cuevas, Dan Urbaniak, Adam Feinberg, and Brian Hatcher.

I am indebted to my family who have patiently supported my overly long academic pursuits. I would specifically like to thank my parents, Donald and Barabara Almond, and my brother, Stephen Almond. My grandparents and the rest of my extended family are also deserving of my gratitude.

TABLE OF CONTENTS

page

LIST OF TABLES

LIST OF FIGURES

LIST OF ABBREVIATIONS

5-FU	5-Fluorouracil
ACS-UF	Animal Care Services (at the University of Florida)
ACS	American Chemical Society
AM	Ametantrone
ANOVA	Analysis of variance: a statistical test
AUC	Area under the curve: a pharmacokinetic term referring to the integration of the drug concentration versus time curve
BSA	Bovine serum albumin: the matrix material for all micro and mesospheres used in the studies reported herein
CAB	Cellulose acetate butyrate: a dispersing agent used in the suspension crosslinking process used to produce microspheres
CBC	Complete blood cell count
CBC w/diff	Complete blood cell count with a differential count of each type of leukocyte
CDC	Centers for Disease Control and Prevention: an agency of the U.S. Department of Health and Human Services
DCE	1,2-Dichloroethane
DMPL	Detoxified monophosphoryl lipid A: an immunomodulating agent
DNA	Deoxyribonucleic acid
DOX	Doxorubicin: an anthracycline chemotherapeutic drug
EDB	Enzymatic digestion buffer
EDTA	Ethylenediamine tetraacetic acid sodium salt dihydrate: a metal ion chelator

FDA	Food and Drug Administration
F-MXN	Free mitoxantrone in a saline or Tsaline vehicle
GLM	General linear method: a statistical test
GTA	Glutaraldehyde
H&E	Hematoxylin and eosin staining
HPLC	High performance liquid chromatography
IACUC	Internal Animal Care and Use Committee (at the University of Florida)
IT	Intratumoral
IV	Intravenous
KPBS	Phosphate buffer solution with an osmolality of 300 mOsm (calculated not measured) adjusted using a combination of KCL and NaCl
LPS	Lipopolysaccharide(s): a class of naturally occurring immunomodulators frequently found in bacterial cell walls
MCT	Multiple comparisons test(s): statistical tests performed after the results of an ANOVA are found to be significant
MRI	Magnetic resonance imaging
MS-MXN	Microsphere or mesosphere-loaded mitoxantrone
MTD	Maximum tolerated dose
MXN	Mitoxantrone (Novantrone™, Lederle / Immunex): 9,10-Anthracenedione, 1, 4-dihydroxy-5,8-bis[[2-[(2-hydroxyethyl)amino]ethyl] amino]-, dihydrochloride: other abbreviations sometimes used for MXN: DiOHA, DHAD and DHAQ HCl
NCI	National Cancer Institute: a component of NIH
NIH	National Institutes of Health: an agency of the U.S. Department of Health and Human Services
NTW	Normalized tumor weight

NTABW	Normalized tumor-adjusted body weight: the TABW on day n divided by the TABW on day 0
PBS	Phosphate buffer solution with the osmolality adjusted to 300 mOsm using NaCl
PMP	Polymethylpentene
R^2	Coefficient of determination
RNA	Ribonucleic acid
SEM	Scanning electon micrograph or scanning electron microscopy.
SPE	Solid phase extraction: a technique used to purify samples prior to HPLC analysis
SRI	Southern Research Institute: located in Birmingham, Alabama
TABW	Tumor-adjusted body weight: the mouse's body weight minus the estimated weight of the tumor
TCA	Trichloroacetic acid
Tsaline	0.5% Tween 80 in normal saline: a surfactant solution used to suspend microsphere formulations for injection

Abstract of Dissertation Presented to the Graduate School
of the University of Florida in Partial Fulfillment of the
Requirements for the Degree of Doctor of Philosophy

MITOXANTRONE–LOADED ALBUMIN MICROSPHERES FOR LOCALIZED INTRATUMORAL CHEMOTHERAPY OF BREAST CANCER

By

Brett Anthony Almond

December 2002

Chair: Dr. Eugene P. Goldberg
Department: Materials Science and Engineering

The safety and efficacy of conventional chemotherapy is limited by its toxicity. The direct intratumoral injection of free or microsphere-loaded antineoplastic drugs is a promising modality for the treatment of solid tumors. Intratumoral chemotherapy delivers high localized doses of cytotoxic drugs to the tumor tissues than does systemic (intravenous) chemotherapy and it decreases systemic drug concentrations and toxicities. The use of drug-loaded microspheres also provides a prolonged release of drug into the surrounding tumor tissues, increasing exposure of the neoplasm to therapeutic levels of the cytotoxic drug.

Mitoxantrone and 5-fluorouracil–loaded albumin microspheres were synthesized. The microspheres were synthesized using a suspension crosslinking technique and a glutardehyde crosslinking agent. The particle-size distribution of the microspheres was controlled by adjusting the emulsion energy and the concentration of cellulose acetate butyrate, the emulsion stabilization agent. Both microsphere size and crosslink density

(glutaraldehyde concentration) were found to affect the *in vitro* release of loaded drugs in *in vitro* infinite sink conditions.

The *in vivo* efficacy and toxicity of intratumoral chemotherapy with free and microsphere-loaded mitoxantrone were evaluated in a 16/C murine mammary adenocarcinoma model. Intratumoral chemotherapy with free mitoxantrone significantly improved survival and decreased toxicity compared to intravenously delivered drug. The efficacy of two size distributions of mitoxantrone-loaded albumin microspheres, corresponding to mean diameters of 5 to 10 μm and 20 to 40 μm, were evaluated delivered both alone and in combination with free mitoxantrone. Intratumoral injection of mitoxantrone-loaded microspheres was found to allow the safe delivery of increased doses compared to free drug. The maximum tolerated doses were approximately 40 mg/kg compared to 12 mg/kg, respectively. Intratumoral chemotherapy using free and/or microsphere-loaded mitoxantrone significantly improved survival time compared to controls. Cure rates as high as 80% were achieved after a single treatment with some microsphere formulations compared to 0% for untreated controls. The combination of mitoxantrone-loaded microspheres followed by the surgical excision of the tumor produced the most promising results with up to 100% survival in some treatment groups. Based on results of these studies, the initiation of a Phase-I clinical trial in human breast cancer patients may be warranted.

CHAPTER 1
INTRODUCTION

The safety and efficacy of conventional intravenous chemo- and immunotherapies are severely limited by their toxicities. Although significant advances have been made in the fields of cancer diagnosis and biology, little improvement has been seen in cancer mortality. Based on the Center for Disease Control (CDC) estimates for the past 20 years, there has only been a 2% decline in breast cancer mortality and a 77% increase in lung cancer mortality (estimated to be 41,000 and 157,000 respectively in 2000).[1, 2] The cytotoxic activity of most chemotherapeutic drugs has been shown to be highly dose-dependant. However, systemic toxicities such as myelosuppression, mucositis, and cardiomyalgia prevent the use of higher therapeutic doses. In a 1991 editorial on the evolution of breast cancer treatment, Edward Scanlon, a former president of the American Cancer Society, made the following statement.

> Over a period of 100 years, breast cancer treatment has evolved from no treatment to radical treatment and back again to more conservative management, without having affected mortality. Adjuvant treatment has been attempted with irradiation, hormones, chemicals, and a lengthy list of other regimens, including home remedies. Aside from earlier diagnosis, little progress has been made to reduce breast cancer mortality. Much has been accomplished however in reducing morbidity and improving the patients quality of life, even though quality is difficult to quantitate. Often studies that involve a narrow margin of statistical significance can alter the treatment practices of thousands of physicians. In diseases like breast cancer, future physicians must exercise care when evaluating the statistical analyses of treatment modalities.

Scanlon's statements regarding breast cancer treatment and his warnings regarding the overemphasis of studies with small, but statistically significant, differences in treatment outcomes are still valid today.[3]

Most current breast-cancer treatment regimens include some surgery in combination with chemotherapy and hormonal therapy (if the tumor is hormone receptor positive).

Some progress has been made during the last decade in the chemotherapeutic treatment of breast cancer after a long period of little advancement. As of 1995, only eight cytotoxic drugs had approval by the US Federal Drug Administration (FDA) for the treatment of breast cancer: cyclophoshamide, docetaxel, doxorubicin, 5-fluorouracil, methotrexate, mitomycin-C, paclitaxel, and vinblastine. Of those eight, Taxol (paclitaxel, approved in 1994) and Taxotere (docetaxel, approved in 1996) were the only cytotoxic drugs to have been approved within the last 20 years. Nolvadex (tamoxifen citrate), an anti-estrogen, was approved for delaying the recurrence of breast cancer after treatment in 1986. Arimedex (anastrozole), another hormonal agent was approved in 1995. As a result of the dearth of advancements, great emphasis was put on the development and testing of new chemotherapeutics. Over a relatively short period of 10 years, paclitaxel progressed from its first clinical trials in 1983 to general acceptance as an efficacious treatment of metastatic breast cancer by 1993.[4]

Since 1996, several drugs received approval for use in the treatment of breast cancer. Fareston (toremifene citrate) and Femara (letrozole) were approved in 1997. Herceptin (trastuzumab), an antibody against the HER2 protein which is overexpressed in some breast cancer cells, and Xeloda (capecitabine), which is converted intracellularly to 5-fluorouracil, received FDA approval in 1998. Ellence (epirubicin hydrochloride), a drug similar to doxorubicin, was approved for adjuvant therapy in 1999. Aromasin (exemestane), an irreversible aromatase inhibitor, was also approved in 1999.[5] It is

readily apparent that most newly approved drugs for the treatment of breast cancer are hormonal antagonists or new derivatives of previously approved drugs, with taxanes being the only new class of cytotoxic agents recently approved. And, it should be noted that the efficacy of systemically delivered taxanes is limited by their significant toxicities, as with previous cytotoxic agents.

One proposed mechanism for overcoming this shortcoming of conventional cancer therapy is the use of locally, or regionally, delivered chemotherapy. The rationale for this treatment modality is a pharmacokinetic one. The exposure of a tumor mass to chemotherapeutic drugs can be dramatically increased if the drugs are injected into the arteries feeding the tumor, into a tumor-bearing compartment (such as the sub-arachnoid space), or more specifically directly into the tumor itself. Local chemotherapy modalities used to date (clinically or experimentally) include intraperitoneal, intraventricular, intrathecal, intrapleural, intraarterial (upstream of the tumor), and direct intratumoral (intralesional) injection.

Another technique used to increase efficacy, while decreasing toxicity, is continuous infusion of chemotherapeutics. This technique is also justified based on a pharmacokinetic rationale. Most chemotherapy drugs have relatively short half-lives. This means that after bolus infusion, the drugs are only available at therapeutic concentrations for a relatively short time, and high peak concentrations lead to increased toxicities. The use of continuous-infusion pumps allows drug levels to be maintained at therapeutic concentrations, while limiting peak concentrations and associated toxicities.[6]

The rationale for the use of intratumorally injected drug-loaded microspheres is based on the rationales for both regional chemotherapy and continuous infusion

chemotherapy. Intratumorally injected microspheres will release loaded chemotherapeutic agents into the tumor mass, providing high local concentrations of cytotoxic drugs. Additionally, the microspheres will provide a prolonged continuous release of drug into the tumor environment through diffusion of the drug out of the matrix and biodegradation of the protein matrix *in vivo*. Any of the released drug not taken up by the tumor cells will diffuse into the local lymphatic and venous drainage and be carried to the draining lymph nodes and the rest of the body. Thus, intratumoral (IT) injection of drug-loaded microsphere formulations provides prolonged high local doses of cytotoxic drugs, while limiting systemic exposure and therefore toxicities. In January 2002 our research group published the most comprehensive review of this chemotherapeutic approach to date.[2]

Microspheres are homogeneous particles ranging in size from 1 to 1000 μm, while mesospheres are represent the subset of microspheres that are between 1 and 10 μm in diameter. Protein microspheres are most commonly produced by suspension crosslinking. This process consists of dispersing an aqueous protein solution (the dispersed or discontinuous phase) in an immiscible organic liquid (the continuous phase) with a paddle mixer, vortex mixer, ultrasonicator, or homogenizer. After a stable suspension has formed, a crosslinking agent is added, and the resulting particles are collected. These protein microspheres can be loaded with drugs, such as cytotoxic chemotherapeutics, immuno-modulating agents, or antibiotics; either during the suspension crosslinking step or after the stable particles are collected.

Previous studies showed that the release characteristics of drug-loaded microspheres are a function of particle size and crosslink density as well as drug-matrix

interactions. Higher crosslink densities lead to slower release of drugs (probably due to decreased particle swelling), and therefore slower diffusion of drug from the particle, and decreased rate of biodegradation. Larger particles have a slower release because of the reduced ratio of surface area to volume as the spheres increase in size. Mesosphere formulations (1 to 10 μm particles) are believed to be advantageous, compared to larger microsphere formulations, because their smaller size facilitates their injection through smaller gauge needles and provides for better perfusion of the particles within the tumor tissue.

The object of the research reported here was to perform *in vivo* evaluations of the safety and efficacy of the intratumoral injection of mitoxantrone both as free drug and loaded into albumin microspheres and mesospheres. These evaluations were performed in the 16/C murine mammary carcinoma model, which is a rapidly dividing high-grade breast-cancer line grown subcutaneously in immunocompetent C3H/HeJ mice. Mitoxantrone (MXN) is an anthracenedione that has significant activity as an antineoplastic drug. It is similar in activity and mechanism of action and toxicity to doxorubicin (DOX), a common chemotherapeutic drug. However MXN causes less toxicity, and specifically less cardiotoxicity, than DOX although it is not active against as many tumor types.[7] The MXN-loaded albumin microspheres were produced from bovine serum albumin using the suspension crosslinking techniques previously developed by Hadba, with some modification to achieve the desired size distribution and percent drug loading.[8, 9]

Initially, a large statistically designed study was performed to compare the efficacy of intratumorally injected free MXN compared to intravenous (IV) injections

with or without tumor excision 10 days after treatment. Dose escalation studies were performed using both MXN-loaded microspheres (20 to 40 μm average diameter) and mesospheres (6-8 μm average diameter) to determine the appropriate dose for optimum efficacy with minimum toxicity with direct comparison to intratumoral injections of free MXN.

Optimum doses were then further evaluated when the MXN-loaded microspheres or mesospheres were intratumorally injected suspended in a free drug solution. It was felt that this combination of free drug with the microsphere-loaded drug would provide an initial loading dose of MXN as it perfused the tumor mass followed by a prolonged continuous exposure as MXN was released from the microspheres (mesospheres). The efficacy of 3 injections scheduled one week apart was also evaluated in an attempt to more closely mimic the scheduled chemotherapy regimens used clinically to treat breast cancer. Another study was performed to investigate the effect of timing of tumor excision after intratumoral chemotherapy, with complete blood counts performed to assess toxicity and histological evaluation of the excised tumor tissue to determine the extent of perfusion by the drug and microspheres and to determine degree of necrosis of the neoplastic tissue.

Other studies were performed to develop synthesis conditions for 5-fluorouracil–loaded albumin microspheres. This was done to facilitate future *in vivo* studies designed to evaluate the efficacy of intratumoral injections 5-Fluorouracil (5-FU) as free drug or as microsphere-loaded drug. There is interest in delivering 5-FU–loaded microspheres in combination with MXN-loaded microspheres because the two drugs have been found to exhibit synergistic effects when used in combination.[7] In fact, the combination

chemotherapy regimen of cyclophosphamide, an anthracyline (i.e. DOX), and 5-FU delivered systemically is regarded as effective, and is the currently favored adjuvant chemotherapy regimen for treatment of breast cancer.

It is important to note that although this research was directed to the evaluation of intratumoral chemotherapy of breast cancer, it is reasonable to believe that the results will be applicable to most solid tumors. Previous studies from this laboratory (Goldberg laboratory, University of Florida) in the Lewis lung, murine ovarian, and line-10 guinea pig hepatoma cancer models in fact suggest that this is the case.

CHAPTER 2
BACKGROUND

2.1 Breast Cancer

Aulus Cornelius Celsus (42 BC – 37 AD) described breast cancer based on the four cardinal signs of inflammation: heat, redness, pain, and swelling. In his description of breast cancer 2000 years ago, Celsus advised that treatment was pointless. Seventeen hundred years later in France, Jean Louis Petit performed the first radical mastectomies in an attempt to treat breast cancer. In the late 1800s, William Halstead described the radical mastectomy essentially as it is still performed today.[3] Current National Institutes of Health (NIH) treatment guidelines for the treatment of breast cancer recommend the use of adjuvant chemotherapy in conjunction with mastectomy in node-positive or node-negative women with tumors greater than 1 cm in diameter. Additionally, hormonal therapy, such as tamoxifen, is recommended for women whose tumors test positive for hormone receptors. Radiation therapy should be considered for women at high risk for local-regional tumor recurrence (women with advanced primary tumors or four or more positive lymph nodes).[10]

It is estimated that approximately 1 in 8 women (13.24%) in the United States will be diagnosed with breast cancer during their lifetime (see Table 2-1). With the exception of skin cancers, breast cancer is the most commonly diagnosed cancer in women and the second leading cause of cancer death in women (after lung cancer). The National Cancer Institute (NCI) estimates that there were 193,700 new cases of breast cancer and 40,600 breast cancer related deaths in 2001 in the United States. In the period

from 1950 to 1998, there has been a 63.1% increase in the incidence of breast cancer, but only a 14.7% decrease in mortality. This corresponds to a -0.1% estimated annual percent change in breast cancer mortality in the US. A woman diagnosed with breast cancer between 1989 and 1997 had an 86.8% chance of surviving 5 years from the time of initial treatment.[11-13]

Table 2-1 Chances of a woman in the US developing breast cancer (by age group).

Age 30 to 40	1 in 257
Age 40 to 50	1 in 67
Age 50 to 60	1 in 36
Age 60 to 70	1 in 28
Age 70 to 80	1 in 24
Ever	1 in 8

Approximately 95% of breast cancers are diagnosed as adenocarcinomas, usually infiltrating ductal carcinomas.[14] At diagnosis, 35 to 50% of patients have detectable metastases in their lymph nodes.[15] Known risk factors for the development of breast cancer include early age at menarche, late age at menopause, late age at first full-term pregnancy, nulliparity, heavy body weight, and long-term use of oral contraceptives or hormonal replacement therapy. These risk factors are believed to represent cumulative exposure of breast tissue to the hormones estrogen and progesterone. These hormones are hypothesized to play a role in carcinogenesis because they influence the rates of mitosis (cell division) within the breast epithelium. Women with previously detected benign breast disease are 3 to 5 times more likely to develop breast cancer. Meta-analysis has also suggested a dose-response relationship between alcohol consumption and the development of breast cancer. Familial inheritance of mutations in the BRCA1 and BRCA2 are also associated with an increased risk of breast cancer, although less than 10% of breast cancers in Western countries are believed to be attributable to genetic factors. Instead, environmental factors are believed to be more influential based on

studies of the incidence of breast cancer among migrants to the United States from foreign regions with lower incidence rates.[14, 16]

2.2 Chemotherapeutic Treatment of Breast Cancer

2.2.1 Rationale for Cytotoxic Chemotherapy

At the turn of the 20th century, Paul Ehrlich observed that certain histological stains were selectively concentrated intracellularly in microorganisms. He hypothesized that if such "stains" could be found that were toxic to the microrganisms, they might have a therapeutic value. In his search for an effective treatment for syphilis, he used the term *chemotherapy* to describe the use of such selectively toxic compounds. Such selective chemotherapeutic substances make use of the differences between hostile bacteria and the normal cells of the body. However, cancer cells are naturally similar in structure and function to normal eukaryotic cells. Therefore, very small differences in cellular environment and metabolism have been capitalized on to develop antineoplastic agents. The difference most commonly used in cancer chemotherapy is the higher rate of mitosis, or cell division, found in tumor cells.[17]

Fundamental work in the understanding of cancer biology and the role of cytotoxic chemotherapy in its treatment was conducted in the 1970s at the Southern Research Institute in Alabama. This work led to the formulation of the Skipper-Schabel-Wilcox model of tumor growth and what have become known as Skipper's Laws. His first law states that the doubling time of cancer cells is constant, which leads to the exponential growth of the tumor mass. Skipper's second law states that the "cell kill" of cytotoxic drugs follows first-order kinetics. This simply means that for a given dose, a certain fraction of exposed cells will be killed, regardless of the number of cells exposed. This leads to the use of the term "log-kill" for a treatment (e.g., a 3 log-kill means 99.9%

of exposed cells will be killed). These laws allow the mathematical rationalization of how cancers can be cured, and cure probabilities can be calculated and have been confirmed experimentally in some tumor lines. However, Skipper's Laws were developed based on experiments with mouse leukemia cell lines. Skipper's first law does not hold for solid tumors because they quickly outgrow their blood supply leading to a necrotic, or dying, fraction of the cell population in addition to the proliferating fraction. Instead of exponential growth, solid tumors tend to exhibit Gompertzian, or sigmoid, growth curves as a result of the balance between proliferating and dying cells within the population. Small tumors have a higher growth fraction and are therefore more sensitive to cytotoxic chemotherapeutics. When treating solid tumors, it is then clear (based on Skipper's second law) that the highest probability of achieving cures occurs when treating small tumors.[17, 18]

2.2.2 Combination Chemotherapy

The term combination chemotherapy refers to the use of more than one antineoplastic drug in a chemotherapy regimen. This was originally done based on empirical evidence of an increased, or even synergistic, effect when using multiple drugs. In 1979, the Goldie-Coldman hypothesis was published, mathematically rationalizing the use of combination chemotherapy based on the development of drug resistance within the cancer cells. Simply put, if a cell has a 10^{-5} probability of spontaneous mutation to develop resistance to a drug and a 1 g tumor contains 10^{9} cells, then that tumor will contain up to 10^{4} resistant cells. However if two such drugs (with independent mechanisms of resistance) are used, then less than one cell in 10^{10} (10^{5} X 10^{5}) should be resistant. Thus, the use of multiple drugs, with independent resistance mechanisms, reduces the chances of resistant cells surviving the chemotherapy treatment.[17, 19]

This hypothesis combined with empirical evidence and experience led to the development of three principles of combination chemotherapy. First, each of the drugs should be active as single agents against the tumor being treated. Second, drugs with differing mechanisms of action, and therefore resistance, should be used. And third, agents with different dose-limiting toxicities should be used so that each can be given at or near its maximum therapeutic dose. This third principle has been difficult to implement in practice since the toxicities of most antineoplastic agents are developed in the same healthy tissues; the ones characterized by rapid cell division (bone marrow, gastrointestinal epithelium, etc.). Therefore, some dose reduction has been necessary in most combination chemotherapy regimens.[17, 20]

2.2.3 High-Dose Chemotherapy

One avenue of study to increase breast cancer survival is the use of high-dose chemotherapy combined with hematological growth-factor support or bone marrow transplant. The rational for high-dose therapy is that in laboratory models of cancer, the dose intensity of cytotoxic agents correlates with curative therapy, whereas higher cumulative doses are associated with longer survival for those not cured.[21] Although several early clinical studies of high-dose (or dose-intense) chemotherapy trials produced promising results, larger trials reported to date have produced less exciting outcomes. This combined with the discreditation of a promising South African study led to what Dr. Rodenhuis (who was involved in a large Dutch study with favorable outcomes) described as “unreasonably negative” expectations since 1999 for high-dose chemotherapy in breast cancer.

This negativity is unfounded since many of the studies that have failed to detect differences between high and normal dose groups lacked sufficient statistical power to

detect a 30% difference in outcomes. Indeed, only two of the eight reported studies (that are relevant and have not been discredited) randomized more than 200 patients. Both of those studies (the Cancer and Leukemia Group B (CALGB) and the Dutch insurance industry studies) found trends in relapse-free survival favoring high-dose chemotherapy. Additional follow-up data from 11 randomized trials are expected to be reported within the next few years.[22-24] It would therefore be prudent to wait for the results of these trails before making decisions concerning the efficacy of high-dose chemotherapy.

2.2.4 Local-Regional Chemotherapy

The rationale for the local, or regional, delivery of antineoplastic drugs is to expose the tumor to active agents at concentrations beyond the levels safely achievable by conventional systemically delivered chemotherapy. This desire for increased tumor exposure encompasses both increased peak concentrations and prolonged time of exposure (quantified as the area under the concentration-time curve (AUC)). Mechanisms for delivering local chemotherapy include direct intratumoral injection, intraarterial injection of agents into arteries feeding the tumor(s), and injection of the agent into tumor-bearing compartments or potential spaces (intraperitoneal, intrapleural, intrathecal, intraventricular, etc.).[25-27] Of these techniques, intrathecal and intraventricular chemotherapy are perhaps the most clinically accepted. This is because it is necessitated by the poor diffusion across the blood-brain barrier with the ratio of drug levels in the cerebrospinal fluid to the plasma ranging from 0.30 to not detectable for most chemotherapeutic agents.[26]

Markman detailed four ways to optimize the efficacy of regionally administered antineoplastic c agents.[28]

- Increase tumor exposure to cytotoxic agents (both peak concentrations and area under the curve (AUC))
- Prolong tumor exposure to cytotoxic agents
- Decrease toxicity compared with systemically (IV) delivered agents
- Increase opportunity for concentration-dependant synergy between combinations of agents

2.2.5 Continuous Infusion Chemotherapy

Because most cytotoxic chemotherapeutic drugs have a low therapeutic index and short metabolic life, selection of an optimal dose and schedule to maximize efficacy while limiting toxicity is important. Continuous infusion of chemotherapeutics allows the concentration of the cytotoxic agents to be maintained within the narrow window above the therapeutic concentration and below the severely toxic levels. The maintenance of therapeutic drug levels also increases the proportion of cells exposed to the agent while they are actively cycling, which is when the majority of cytotoxic drugs are most effective. The reduction of peak concentrations associated with IV bolus infusions has been shown in preclinical and some clinical studies to decrease the toxicities of the chemotherapy.[6]

In both preclinical and clinical studies DOX, a chemotherapy drug similar in chemical structure and mechanism of action to mitoxantrone, delivered as a continuous infusion or in regular divided doses, demonstrated therapeutic benefits compared DOX delivered as a bolus injection. Preclinical studies in a variety of animals have demonstrated a reduction in cardiomyopathy, a major toxicity associated with the use of DOX, when DOX was given at low doses over long periods of time compared to high doses over short periods of time. The clinical experience to date with continuous

infusion of DOX has been limited to Phase I and II, nonrandomized, studies. The studies generally demonstrated a similar to enhanced level of efficacy for infusional treatments with a reduction in treatment-associated toxicities.[6]

The antimetabolite 5-FU is another antineoplastic agent that has benefited from continuous infusion chemotherapy compared to traditional bolus therapy. Some studies suggested that time of exposure may be more important than concentration of 5-FU in determining its cytotoxicity.[29] Other pharmacokinetic studies have shown that 5-FU levels in bone marrow are 50 to 1000 times lower in patients treated with continuous infusion compared to bolus injection.[30] A meta-analysis of six trials involving 1,219 patients with advanced colorectal cancer found that continuous infusion of 5-FU resulted in increased tumor-response rates, increased overall survival, and decreased hematological toxicities. The continuous infusion therapy was associated with a higher rate of hand-foot syndrome occurrence.[31] In summary, experience with 5-FU administered as a continuous infusion shows improved outcomes probably as a result of decreases in severe toxicities.[6]

2.2.6 Chemotherapeutic Drugs Used to Treat Breast Cancer

2.2.6.1 Mitoxantrone

Chemical characteristics. Mitoxantrone (MXN) is an anthracenedione, a group of synthetic chemotherapeutic drugs that were originally synthesized as stable dyes and inks. It is one of many derivatives of ametantrone that were originally synthesized by the American Cyanamid laboratories in a search for compounds with potential chemotherapeutic activity (Figure 2-1). Of the derivatives synthesized, MXN is the most potent. MXN received FDA approval in 1987, and is the only anthracenedione currently approved for clinical use. Anthracenediones are often compared to the naturally

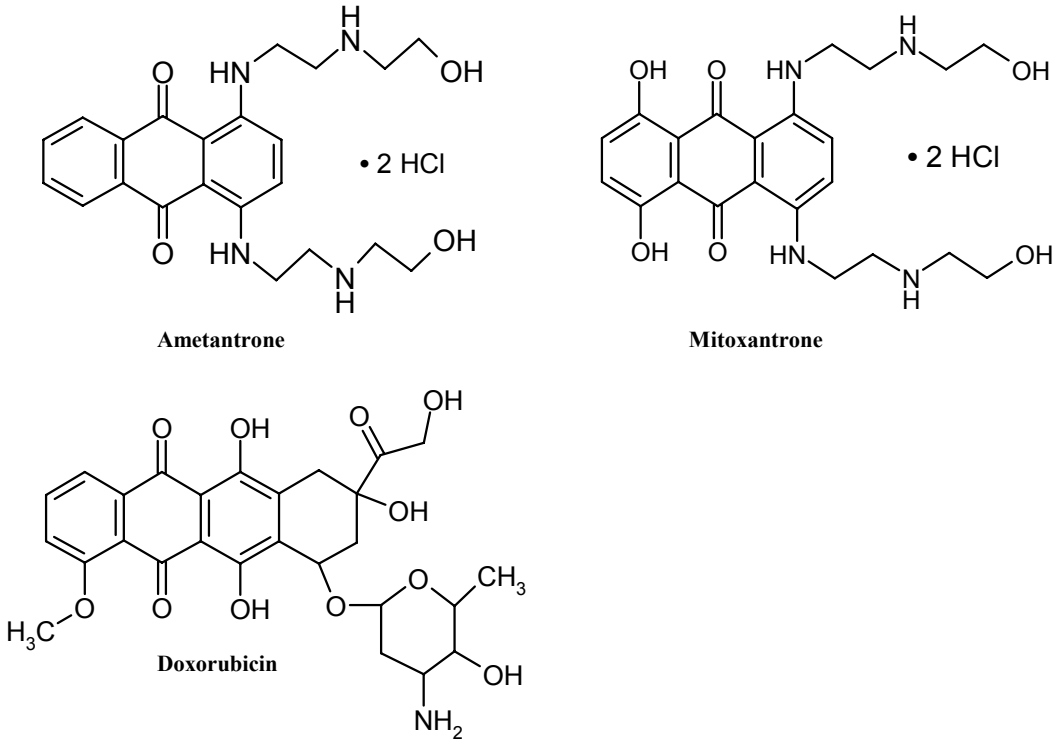

Figure 2-1 Chemical structures of the anthracenediones ametantrone and mitoxantrone, and the anthracycline doxorubicin.

occurring antitumor antibiotics, which include the anthracyclines (e.g., DOX and daunorubicin), bleomycin, and mitomycin C) because of their similar chemical structures, mechanisms of action, antitumor activities, and toxicities.[32, 33]

The chemical name for mitoxantrone is 1,4-dihydroxy- 5,8 bis[(2-(2-hydroxyethyl) amino) ethyl] amino- 9,10-anthracenedione dihydrochloride ($C_{22}H_{28}N_4O_6 \bullet 2HCl$, molecular weight = 517.4 g/mol). It is a planar polycyclic aromatic molecule with two basic side chains. It is a dark blue compound with absorbance peaks in the visible spectrum at approximately 610 and 658 nm. Two pKa values, 5.99 and 8.13, have been reported for MXN, although they have not been attributed to any specific functionality in the molecule. The solid is readily soluble in water, physiologic saline, and methanol, but will decompose in alkaline solutions. Lederle Parentals, Inc. manufactures MXN for Immunex Corporation, which markets it under the brand name

Novantrone®. It is available in 10, 12.5, or 15 mL vials at a concentration equivalent to 2 mg/mL MXN free base. Currently, it is FDA approved for the treatment of acute nonlymphocitic leukemia, pain in advanced hormone-refractory prostate cancer, and chronic multiple sclerosis. In the experimental setting, it has been used to treat advanced breast cancer, non-Hodgkins lymphoma, multiple myeloma, bladder carcinoma, hepatocellular carcinoma, and advanced ovarian cancer among others.[7, 34, 35]

Pharmacodynamics. Although the precise mechanism of cytotoxicity for MXN is not certain, identified potential mechanisms include single- and double-strand deoxyribonucleic acid (DNA) breaks, peroxidation of cell membranes and mitochondrial lipids, cell surface cytotoxicity, and inhibition of glutathione synthesis. It is believed that the planar electron-rich ring structure of MXN allows it to intercalate DNA, while the basic side chains electrostatically crosslink the phosphate groups on the exterior of the DNA helix. MXN is also known to inhibit the enzyme Topoisomerase II. This nuclear enzyme catalyses the cleavage and resealing of supercoiled DNA during repair, replication, and transcription. MXN stabilizes the enzyme-DNA intermediate complex, which leads to double-strand breaks in the DNA.[36] Additionally, MXN is believed to undergo oxidative activation *in vivo* producing free radical intermediates, which cause nonprotein-associated DNA strand breaks and membrane-lipid peroxidation.[7, 37] However, a recently published study calls into question the importance of free radical production in MXN's cytotoxity. In this study, thirty-six anthraquinone derivatives were synthesized with structures similar to MXN, but with side chains of varying charge and redox activity. It was found that at least one cationic substituent, such as the 2-(dimethylamino)ethylamino moiety, was required for *in vitro* cytotoxic activity against

the P388 murine leukemia cell line. Derivatives that possessed redox potential, but no cationic substituents, were not cytotoxic *in vitro*.[38]

A steep dose-response curve has been observed in *in vitro* studies of MXN's cytotoxicity.[39] MXN is about 5 to 7 times more potent than DOX. One study found that greater than 90% of both dividing and nondividing cells died when exposed to 0.5 mg/mL of MXN for 2 hours. However, concentrations as low as 1 to 10 ng/mL of MXN are sufficient to block the progression of mammalian cells from the G2 to the M phase of the cell cycle (Figure. 2-2).[32] This suggests that MXN, although not phase specific, is most effective against actively cycling cells.

Like all cytotoxic drugs MXN has a variety of toxicities associated with its use. However, MXN has been demonstrated to be significantly more tolerable to patients (less toxic) than the anthracyclines DOX and daunorubicin.[7] When delivered at equivalently efficacious doses as DOX, MXN was found to cause less nausea, emesis, alopecia, stomatitis, cardiotoxicity, and weight loss (leading to better performance statuses in

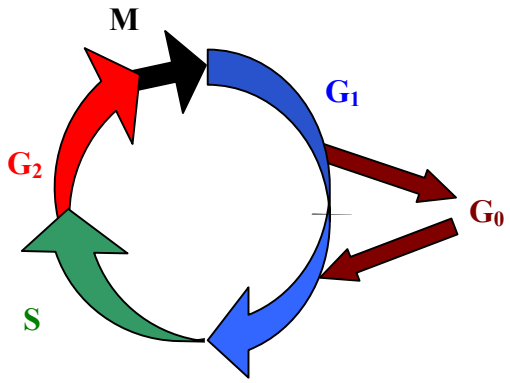

Figure 2-2 The cell cycle and its phases. M is the period of mitosis (cell division); G_1 is the period of normal metabolism without DNA synthesis (referred to as G_0 if for a prolonged period); S is the period of DNA synthesis and chromosome replication; G_2 is a short period of growth before cell division. Many cells will enter the G_0 phase and remain there until death (also known as apoptosis).

patients). The dose-limiting toxicity of MXN is leukopenia, predominately granulocytopenia, in patients treated for solid tumors. White-cell nadirs typically occur 10 to 14 days after treatment with cell counts usually recovering 21 days of treatment. Severe leukopenia (< 1000 cells/μL) occurs in approximately 6% of patients receiving 12 to 14 mg/m^2 of MXN. At the same dose, about 1% of patients will develop severe thrombocytopenia (<25,000 platelets/μl).[7, 33, 40, 41]

When delivered at standard doses, MXN (12 mg/m^2) and DOX (60 mg/m^2) produce similar levels of myelosuppression (as demonstrated by similar cell nadirs and times to nadirs and recovery). Despite their similar hematological effects, one study comparing the tolerability of MXN to DOX found that 96% of patients receiving MXN were still receiving the full initial dose by the sixth drug cycle compared to 77% of DOX recipients.[42] Cardiac toxicity is occurs less often in patients treated with MXN than those treated with DOX. Approximately 3% of adults will develop signs of cardiac toxicity with an estimated worst case incidence of congestive heart failure of 1.3% (compared to 2.2% for DOX).[7] Furthermore, MXN-induced cardiac abnormalities appear to be reversible in animal (and some human) studies, whereas DOX-induced changes are cumulative and non-reversible. The reduced cardiotoxicity of MXN compared to DOX led to it being the preferred drug for high-dose chemotherapy trials incorporating autologous bone marrow transplant rescue.[4, 33] Tables 2-2 and 2-3 list incidences of significant adverse events and laboratory abnormalities observed in a study of 149 multiple sclerosis patients receiving MXN at two dose levels (as reported in the MXN for injection package insert, Immunex Corporation, 2000). Most adverse events were considered to represent mild to moderate levels of toxicity. Nausea was the only event

Table 2-2 Adverse events of any intensity occurring in ≥ 5% of patients in any dose group of Novantrone and that were numerically greater than in the placebo group.

	Percent of patients		
Adverse event	Placebo (n = 64)	5 mg/m^2 Novantrone (n = 65)	12 mg/m^2 Novantrone (n = 62)
Nausea	20	55	76
Alopecia	31	38	61
Menstrual disorder *	26	51	61
Amenorrhea *	3	28	43
Upper respiratory tract infection	52	51	53
Urinary tract infection	13	29	32
Stomatitis	8	15	19
Arrythmias	8	6	18
Diarrhea	11	25	16
Urine abnormal	6	5	11
ECG abnormal	3	5	11
Constipation	6	14	10
Back pain	5	6	8
Sinusitis	2	3	6
Headache	5	6	6

* Percentage of female patients

Table 2-3 Laboratory abnormalities occurring in ≥ 5% of patients in either dose group of Novantrone and that were numerically greater than in the placebo group.

	Percent of patients		
Laboratory abnormality	Placebo (n = 64)	5 mg/m^2 Novantrone (n = 65)	12 mg/m^2 Novantrone (n = 62)
Leukopenia [a]	0	9	19
Gamma-GT increased	3	3	15
SGOT increased	8	9	8
Granulocytopenia [b]	2	6	6
Anemia	2	9	6
SGPT increased	3	6	5

* Assessed using World Health Organization toxicity criteria

a. < 4000 cells/mm^3

b. < 2000 cells/mm^3

occurring with severe intensity in more than one patient (occurring in 3 patients (5%) in the 12 mg/m^2 group).

MXN is also known to have several potentially clinically import actions other than its cytotoxicity. For one, it is known to inhibit cytochrome P-450 drug metabolism in the liver. It has an antiplatelet aggregation effect similar to that of aspirin, and inhibits the production of prostaglandin E2 and thromboxane B2 in epinephrine stimulated platelets. This may lead to the reduction of the angiogenic response in tumors.[7]

Pharmacokinetics. The detection of MXN in biological samples and its pharmacokinetic properties have been reported by numerous researchers. Accurate determination of MXN's pharamacokinetics has been difficult because of its instability at room temperature, significant binding to proteins in samples, its nonspecific adsorbtion to filters and glassware, and its prolonged terminal half-life. Although many different techniques have been used to detect MXN, high performance liquid chromatography (HPLC) is currently the preferred method. Sample preparation typically involves the precipitation of proteins followed by solid phase extraction (SPE) using XAD-2 beads or reverse-phase silica gel. The drug and its two major metabolites, the mono and the dicarboxylic acid derivatives of the terminal hydroxyl groups, are then separated using reverse-phase C18 or C8 HPLC columns. Acidic mobile phases with acetonitrile or methanol organic modifiers are typically used allowing the elution of MXN within 15 minutes. Ametantrone, bisantrene, or anthracenedione diacetate may be used as internal standards to control for MXN lost during sample preparation. The drug is typically detected using spectrophotometry at either 658 or 611 nm. Alternatively, electrochemical oxidation detection of MXN has been reported to be approximately an

order of magnitude more sensitive than spectrophotometry, and the use ^{14}C labeling allows the radiochemical detection of the drug in samples.[43-50]

Adequate prediction of the pharmacokinetics of MXN *in vivo* requires the use of a 3-compartment model. Following IV administration, the drug rapidly leaves the plasma, binding to endothelial surfaces and the cellular components of the blood ($t_{1/2}\,\lambda_1$ from 4.1 to 10.7 minutes). Plasma levels of MXN typically fall to 1 ng/mL or less within 12 to 24 hours. This is followed by a second phase in which the drug is distributed throughout the body ($t_{1/2}\,\lambda_2$ from 0.3 to 3.1 hours). After its distribution to the deep tissue compartment, MXN is eliminated from the body very slowly ($t_{1/2}\,\lambda_3$ from 7 to 12 days). MXN is primarily metabolized by the liver with up to 56% of a ^{14}C-labeled dose being recovered in 120 hours after excretion into the bile and recovered in the feces of rats. Less than 14% of a dose was recovered in the urine in the same time period.[45] In at least one study, the interpatient pharmacokinetics of MXN varied significantly with a greater than 7-fold difference in peak plasma concentrations (64 to 490 ng/mL) after an infusion of 10 mg/m^2, and the terminal half-lives ranged from 42 to 189 hours (shorter than previously reported in Ehninger's review of the pharmacokinetics of MXN). This variability led to an almost 13-fold difference in AUC between patients (80 to 1030 ngh/mL).[47]

2.2.6.2 5-Fluorouracil

Chemical characteristics. The drug 5-fluorouracil (5-FU) belongs to the group of antineoplastic compounds known as the antimetabolites. 5-FU was synthesized in 1957 as a pyrimidine antagonist by substituting a fluorine atom for hydrogen on the pyrimidine nucleotide uracil (Figure 2-3). Its chemical name is 5-fluoro-2,4(1H,3H)-pyrimidinedione ($C_4H_3FN_2O_2$, molecular weight = 130.08 g/mol). 5-FU is a white, to

nearly white, odorless crystalline powder. Its solubility in water is limited to 10 to 13 mg/mL. The maximum UV absorption occurs at approximately 266 nm. The compound will undergo hydrolysis at high pH and temperatures. The solubility in water increases with increased pH because of salt formation, and aqueous solutions at pH 9 are stable at room temperature for up to 3 years if protected from light.[51] At physiological pH, the drug is a mixture of the neutral form and the two tautomeric monoanions formed by the dissociation of the N-1 and N-2 protons (pKa = 7.71 at 25°C).[51, 52] The minimum lethal dose in humans is 450 mg/kg over 30 days (oral) or 6 mg/kg over 3 days (IV).[53] 5-FU has been used to treat a variety of cancers including breast, colorectal, gastric, pancreatic, bladder, cervical, and cutaneous carcinomas among others.

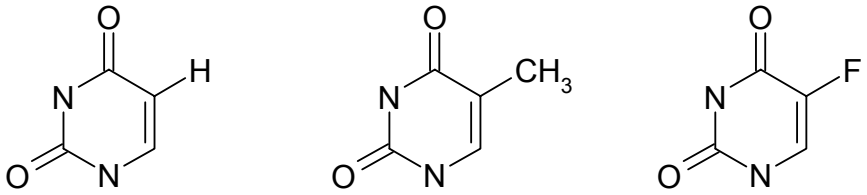

Figure 2-3 The chemical structures of the pyrimidines, uracil and thymine, and the antimetabolite, 5-fluorouracil, respectively.

Pharmacodynamics. The antimetabolite chemotherapeutics are similar in chemical structure to naturally occurring compounds. This similarity allows them to incorrectly serve as substrates for enzymes, thereby disrupting normal cellular metabolism. 5-FU is structurally similar to the pyrimidine nucleotide uracil. This allows it to substitute for uracil and thymine during ribonucleic acid (RNA) and DNA synthesis and repair. The disruption of DNA synthesis explains the cytotoxicity of 5-FU, as well as why it is most effective during the S-phase of the cell cycle. 5-FU is considered a cell-cycle specific chemotherapeutic and is most cytotoxic to tissues (healthy or neoplastic) that have a high rate of mitosis. 5-FU also incorporates itself into all types of

RNA (tRNA, mRNA, etc.). Its incorporation into RNA is believed to play a significant role in 5-FU's cytotoxicity. However, RNA-directed toxicity occurs at higher drug concentrations than are required for DNA-directed toxicity. Heidelberger intentionally designed 5-FU in 1957 to inhibit the enzyme thymidylate sythase (TS), which catalyzes the conversion of deoxyuridine monophosphate (dUMP) into deoxythymadine monophosphate (dTMP). When FdUMP serves as the substrate for TS, a stable covalent complex of FdUMP, TS, and tetrahydrofolate is formed. The inactivation of the TS enzyme leads to a depletion of available thymadine triphosphate (TTP) and an abundance of FdUMP and deoxyuridine triphosphate (dUTP) within the cell, which are then incorrectly incorporated into DNA during synthesis and repair. Their incorporation presumably activates the DNA excision-repair process leading to DNA strand breaks.[54]

The intracellular pathways leading to 5-FU's inhibition of DNA and RNA synthesis are shown in Figure 2-4.[52, 55] In summary, 5-FU exerts its cytotoxic action through three mechanisms: the inhibition of TS by accumulating FdUTP in the cell, incorporation of FdUTP into DNA, and incorporation of FUTP into RNA. It is uncertain at this time which of these mechanisms is essential for antineoplastic efficacy.[52, 56]

Like all cytotoxic chemotherapeutic drugs, 5-FU has a number of toxicities that limit the dose that can be safely administered intravenously. The dose limiting toxicity of 5-FU is often mucositis, which manifests as stomatitis, diarrhea, nausea and anorexia. 5-FU also produces significant myelotoxicity, most significantly leukopenia with cell nadirs usually occurring between 9 and 14 days after the first dose. Additional toxicities that may occur include thrombocytopenia, anemia, alopecia, dermatitis, and occasionally cardiotoxicity.[54]

Pharmacokinetics. 5-FU is most commonly administered intravenously as either a bolus, continuous infusion, or bolus followed by continuous infusion for the treatment of noncutaneous cancers because of its poor bioavailability following oral administration (25 - 30%). Approximately 10% of an administered dose is bound to plasma proteins. An additional 11% of a dose is distributed within the cellular elements of blood.[57] The plasma half-life after IV administration is short (10 to 20 min), and 7 to 20% of a dose is excreted unchanged in the urine within 6 to 24 hours. Another 22 to 45% of the dose is metabolized in the liver by the enzyme dihydropyrimidine dehydrogenase, which inactivates 5-FU by reducing the pyrmidine ring structure. This enzyme is also found in the intestinal mucosa and other tissues that serve as secondary sites for the inactivation of 5-FU. [54, 55]

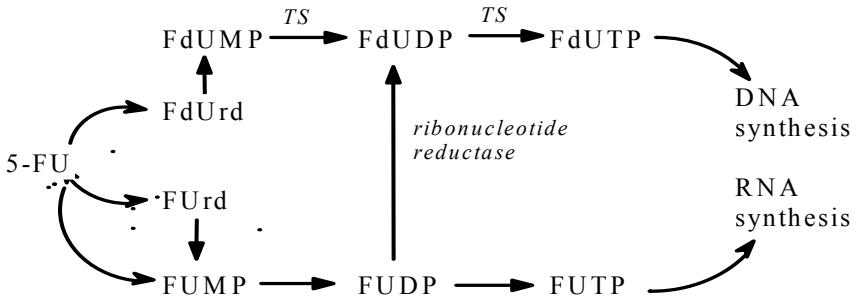

Figure 2-4 The intracellular pathways for 5-FU metabolism, based on figures in Gutheil and Parker.[52, 55]

2.3 Intratumoral Chemotherapy of Cancer

2.3.1 Intratumoral Chemotherapy with Free Drugs

The direct IT injection of chemotherapeutic agents, either as free drugs or in controlled release devices, has gained increased attention. The first clinical reports of IT chemotherapy were made in the late 1950s by Bateman. The treatment of a variety of far-advanced cancers with two phosporamide drugs was reported with a positive response in 66% of the 177 mammary adenocarcinomas treated.[58, 59] Little further research on IT

chemotherapy was reported until the late 1970s. In 1978, McLaughlin et al reported the efficacy IT mitomycin-C in the line-10 guinea pig hepatoma. This study also demonstrated the induction of immunity to further inoculations with the tumor line when mytomycin treatments were followed by IT injections of a BCG cell wall emulsion.[60] Bast et al, Borsos et al, Cantrell et al, and McLaughlin & Goldberg also reported such IT treatment-associated induction of immunity to tumor lines.[61-64]

Increased interest in the IT treatment of cancer has developed over the past 20 years. Reports of such studies are too numerous to list here and the reader is instead referred to a number of reviews of this treatment modality. Tomita, Walter et al, and Haroun & Brem have written review focused on the efficacy of intratumoral treatments of brain cancers.[65-67] Theon published a review narrowly focused on the veterinary applications of IT chemo- and immunotherapy for the treatment of equine tumors.[68] McLaughlin & Goldberg and Brincker have written broader reviews of the IT treatment of multiple types of cancer.[64, 69] The most current and inclusive review of IT chemo- and immunotherapy to date was published in January of 2002 by this research group.[2]

One exciting development is that a Bulgarian group recently reported the intra- or peritumoral injection of MXN in human breast cancer patients.[70] In this study, 0.5 mL (1.0 mg) of MXN was injected into two sites in the primary tumor and surrounding tissues either intraoperatively, 0.5 to 3 h preoperatively, 20 h and 0.5 to 3 h preoperatively, or daily for 3 days preoperatively. Unfortunately, this was a small study of 37 patients focused on the use of MXN to stain the sentinel lymph nodes of the patients rather than the direct treatment of their tumors. Therefore, the maximum amount of time elapsed between the first injection and mastectomy was three days. Because of

the varied treatments used and the alternative focus of this study, it does not truly represent a Phase I trial of IT chemotherapy with MXN. However it is important to note, the IT treatments (using up to 6.0 mg MXN cumulative doses) were well tolerated with "insignificant" local erythema occurring in only two patients (without patient complaint), and no local-regional recurrence or distant metastases were observed at a median follow-up of 19.2 months (range 8 to 30 months).

2.3.2 Rationale for the Use of Drug-Loaded Microspheres

The rationale for controlled release of chemotherapeutic agents from microspheres implanted directly within a tumor mass is that it combines the advantages of both high dose chemotherapy and continuous infusion chemotherapy. The drug-loaded microspheres release a high dose of chemotherapeutic agent into the local tumor environment with the drug diffusing from the microsphere through the extracellular fluid to the nearby tumor cells. The extent of diffusion of the drug through the tumor mass and its uptake by the tumor cells before it is lost to the lymphatic and vasculature drainage is dependant upon both the characteristics of the drug itself and the local tumor environment.[71] The slow diffusion of the drug from the microsphere matrix and the release of additional drug as the microsphere biodegrades provides a sustained release of drug, resulting in prolonged high dose exposure of the tumor cells to the cytotoxic agent as in infusional chemotherapy, theoretically at higher, and therefore more efficacious, concentrations.[2, 64, 72]

Currently the only FDA approved polymeric drug release device for the treatment of cancer is the Gliadel wafer (Guilford Pharmaceuticals, Baltimore, MD). Gliadel is a carmustine-impregnated polyanhydride wafer, which was approved in 1996 for implantation after the surgical debulking of gliomas. Guilford Pharmaceuticals is also in

Phase I clinical trials of the Paclimer microsphere drug release system for the treatement of ovarian and non-small cell lung cancer. Paclimer microspheres are composed of paclitaxel loaded into a proprietary polyphosphoester microsphere matrix. In one preclinical study of the Paclimer system, IT injected microspheres were found to increase the doubling time of tumors to approximately 5 times the rate of IP treated animals.[73]

2.3.2 Research Experience at the University of Florida

The laboratory of Professor Goldberg at the University of Florida has studied the synthesis and efficacy of intratumoral chemo- and immunotherapy and drug-loaded microspheres for more than 20 years. Results of these earlier studies are briefly outlined here.

Iwata and Longo developed the original procedures for protein microsphere synthesis upon which later work within the group has been based. Prior to their work, earlier techniques for the synthesis of albumin microspheres using vegetable oil dispersions and high temperature protein denaturing produced hydrophobic microspheres that were not readily dispersed in aqueous solvents for postsynthesis modification or *in* vivo delivery. Protocols for the synthesis of albumin (from human and several animal sources) and dextran microspheres loaded with the antineoplastic agents DOX and bleomycin and the antibiotics streptomycin and gentamycin were developed.

Iwata and Longo developed a novel synthesis in which a stable emulsion of protein dissolved in the discontinuous aqueous phase is crosslinked by addition of a crosslinking agent such as glutaraldehyde, diisocyanates, or aldehyde sucrose dissolved in the continuous organic phase.[74, 75] This technique produced relatively hydrophilic microspheres that were readily dispersible in aqueous mediums. The microsphere size could be controlled by adjusting the appropriate processing parameters. It was further

shown that the loading of cationic drugs, such as DOX, could be increased by blending polyanionic polymers, such as polyglutamatic acid or carboxymethyl dextran, into the polymer matrix. The initial *in vivo* studies performed with antineoplastic drug-loaded microspheres were largely concerned with demonstrating the safety and reduced toxicity of these formulations. One important finding of these preliminary studies was that DOX-loaded microspheres injected IP did not produce the ulceration and necrosis characteristic of free DOX formulations, and the drug could be safely delivered at much higher doses with little to no observed toxicity.[74, 76-79]

Other later work at the University of Florida was focused on developing chemotherapeutic microspheres using the protein casein instead of albumin. Casein is a high molecular weight amphiphilic protein found in milk. Knepp and Jayakrishnan showed that the drug loading efficiency and in vitro release characteristics of casein were comparable to those of similar albumin formulations. Intratumorally injected MXN-loaded 20% polyglutamic acid / 80% casein microspheres were also effective in slowing tumor growth in a mouse Lewis lung carcinoma model. [80-82]

Jayakrishnan continued research on the synthesis and efficacy of casein microspheres at Sree Chitra Tirunal Instituite for Medical Sciences and Technology in India after leaving the University of Florida. He reported a synthesis of smooth, round albumin and casein microspheres using a polyurethane dispersing agent at much lower concentrations than had previously been used.[83] In another study, casein microspheres were loaded with 5-FU, and biodegradation studies of nonloaded casein microspheres found they persisted in muscle tissue for about six months, approximately three times longer than albumin microspheres.[84] Microspheres were also formed from the

polysaccharide chitosan and loaded with MXN. When these microspheres were injected IP into rats bearing Ehrlich ascites carcinoma, 62.5% of the microsphere treated mice survived for 60 days as compared to 0% of the control mice.[85]

At the University of Florida, Kirk and Quigg performed a series of experiments to synthesize bovine serum albumin microspheres (not blended with polyanionic polymer) loaded with a variety of active agents and using three different crosslinking chemistries. Active agents were successfully incorporated into microspheres included the antineoplastic agents methotrexate and MXN, the immunomodulator detoxified monophosphoryl lipid A (DMPL, a modified endotoxin, in collaboration with John Cantrell of Ribi Immunochem), and acid phosphatase (as a model for enzyme incorporation and release). Experiments were conducted utilizing three different crosslinking chemistries: the traditional glutaraldehyde, multivalent metal ions, and thermal gelation using microwave energy.

Two notable *in vivo* experiments performed under the supervision of Dr. Quigg and reported by Kirk were the evalution of MXN-loaded albumin microspheres in the Lewis lung carcinoma model and in the murine ovarian teratocarcinoma model (with Dr. Cantrell). Significant results were obtained in the Lewis lung carcinoma model (a metastatic squamous cell carcinoma model) with up to 75% survival in mice treated with microsphere formulations delivered as dispersions in free drug solutions and an impressive 92% survival when the same treatment was combined with tumor excision 10 days after treatment. None of the untreated control animals survived longer than 24 days in this study. In the ovarian tumor model, mice were treated with IP injections of either free or microsphere-loaded MXN. Once again microspheres incorporating MXN proved

to be an effective treatment with 80 to 90% of the treated animals surviving compared to 0% of the untreated. Another interesting result was that 100% of the animals treated with 250 μg of free MXN survived even though this was well above the published LD_{50} for IP MXN.[86]

Hadba continued research with albumin microspheres. With the help of Marotta, the first full scale statistically designed experiments to model particle-size as a function of processing parameters during synthesis was conducted.[9, 87, 88] It was also shown that release of highly protein bound drugs such as MXN is not fully described by the *in vitro* release experiments conducted in saline or buffer solutions typically reported. The release profile for the same microsphere formulation varied greatly when comparing phosphate buffer solution (PBS) and human plasma mediums in *in vitro* experiments.[8, 9] Hadba also performed several *in vivo* experiment in collaboration with research reported here. IV treatment was compared with IT free MXN, with or without tumor excision after treatment. Another experiment compared the efficacy and toxicity of MXN-loaded albumin microspheres with intratumoral injection of free MXN. Preliminary results of these experiments were presented in Hadba's dissertation and a review of intratumoral chemotherapy published from our research group.[9, 89] However, the complete results are reported here.

2.3.3 Reported Use of MXN and 5-FU-Loaded Microspheres

A few other research groups have reported the use of MXN or 5-FU loaded microspheres for localized chemotherapy. Independently, an Austrian group Luftensteiner et al has published experiments that are similar to those of Hadba. They conducted a statistically designed study to determine the process parameters that influenced particle size using a modification of the processing technique published by

Longo et al. However, there were some differences between the Hadba and Luftensteiner studies in the specific parameters that were tested.[90]

Perhaps the most significant difference with the results published by Luftensteiner et al is that the *in vivo* studies have focused on the evaluation of IP injection of microspheres. The Austrian group performed a thorough comparison of the pharmacokinetics of free and microsphere loaded MXN injected IP at 30, 60, or 120 mg/m^2. Microsphere formulations produced lower peak concentrations of MXN during the first 4 hours after administration in both the peritoneal fluid and plasma. The two delivery mechanisms produced comparable drug concentrations in both the peritoneal fluid and plasma in the period from 4 to 72 hours, which was the extent of the study.[91] It would have been valuable to have data past the first 72 hours to determine if the microspheres provided a prolonged release of MXN to thereby produce higher concentrations of drug at later time points compared to the free drug injections.

In a comprehensive analysis of the toxicity of IP delivered MXN, either free drug or loaded in albumin microspheres (average diameter of approximately 30 μm) in healthy rats, Luftensteiner et al found that animals treated with 30 mg/m^2 MXN in microspheres injected every 3 weeks for three treatment cycles had significantly increased survival compared to those treated with free drug. However, no significant difference was detected in animals treated with a single injection, and significant mortality occurred with both MXN treatment regimens. This mortality was probably attributable to the relatively high dose of MXN delivered IP. Serial complete blood cell counts (CBCs) found significant leucopenia and anemia in both the microsphere and the free drug treatment groups with cell nadirs occurring around seven days after treatment followed by gradual

recovery. No significant difference was seen between the two treatment groups CBCs, however measurements of body weight, food and water intake, and urine production showed that the microsphere bound drug was better tolerated than free drug.[92] Although this study provided valuable information regarding the reduced toxicities of IP MXN-loaded microspheres, it was limited by the high doses which caused severe chemoperitonitis, as evidenced by peritoneal bleeding, hemorrhagic ascites, and peritoneal adhesions on necropsy.

The preparation of 5-FU–loaded microspheres has been previously reported in the literature. The majority of these formulations have used PLGA as the microsphere matrix.[93-95] Other microsphere materials used have included ethylcellulose, gelatin, and alginate.[96-98] Sugibayashi et al have reported the preparation of 5-FU–loaded microspheres, but they had a low percent drug loading and were hydrophobic (prepared from a vegetable oil emulsion).[99] One Indian group, that included Jayakrishnan, reported the loading and release of 5-FU from casein microspheres prepared similarly to the technique used by this laboratory. At this point, the synthesis of *in situ* 5-FU–loaded hydrophilic albumin microspheres prepared using a suspension-crosslinking technique similar to that of Hadba have not been reported.

2.4 Animal Model of Breast Cancer

2.4.1 C3H/HeJ Mouse Strain

The C3H/HeJ mouse strain is a substrain of the C3H mouse, one of the most common mouse strains used in research. In 1920, Strong developed the C3H parent strain by crossing a BALB albino mouse with a DBA male. The resulting offspring were selected for a high incidence of spontaneous mammary tumor development.[100, 101] This high incidence of mammary tumors was a result of infection of the strain with the

retrovirus now identified as the mouse mammary tumor virus (MMTV). In the C3H strains, this virus is passed from the mother to suckling pups in the breast milk and leads to a greater than 90% incidence of tumor development by one year of age. Thus, C3H mice fostered on a nonviremic mother will be virus and tumor free. However since MMTV is a retrovirus, it has now become apparent that endogenous MMTV provirus exists integrated into the germline, and some mouse strains, such as GR, will develop virus-associated tumors even if fostered at birth. It is important to note for general mouse colony health reasons that fostered C3H strains will not develop tumors from endogenous integrated proviruses. In fact it is estimated, that most, if not all, inbred mouse strains contain 2 to 8 endogenous proviruses which do not produce infectious viruses.[102, 103]

The C3H/He substrain was developed by Heston in the 1940s as a model of mammary carcinogenesis and is probably the most widely used of the C3H substrains. This strain was passed to The Jackson Laboratory in 1947, and their line was termed C3H/HeJ. At some point during the 1960s, a spontaneous genetic mutation occurred in the C3H/HeJ strain making it endotoxin (lipopolysaccharide) resistant.[100, 104] In 1999, the Jackson Laboratory rederived its C3H/HeJ strain in order to improve overall colony health. Since that time, C3H/HeJ mice have been free of infectious MMTV.[101, 105] These are the main differences between the C3H/HeJ strain and other C3H/He mice maintained by other breeders.

2.4.2 16/C Murine Mammary Adenocarcinoma Model

The 16/C murine mammary adenocarcinoma model was first isolated and developed at the Southern Research Institute (SRI) in Birmingham, Alabama. In the mid to early 70s, Schabel and coworkers at SRI were searching for a suitable breast cancer model in mice that would accurately represent the clinical course and drug sensitivities of

breast cancer in women. To this end, a colony of retired breeder C3H/He mice, which were known to have a high incidence of spontaneous mammary tumors was maintained and observed for tumor development. It was desired to isolate a tumor line that maintained a high metastatic potential. It was known that existing murine tumor models failed to maintain their metastatic potential when the tumor line was maintained by the serial subcutaneous passage of primary tumor tissue. Therefore, when a mouse developed a spontaneous tumor, it was sacrificed, its lungs dissected, and lung fragments trocared subcutaneously into another mouse. If this mouse then developed a tumor, its lungs were dissected and implanted into another mouse. It was theorized that if the tumor was highly metastatic, there would be a sufficient number of tumor cells in the transplanted lung tissue to propagate new tumor growth. A highly metastatic murine mammary adenocarcinoma, the 16/C tumor model, was isolated using this method in 1974.[106] The 16/C murine mammary adenocarcinoma tumor line has a a high take rate following transplantation and produces grade III tumors with rapid growth rate, doubling in volume approximately every 2 to 3 days.

Of importance to the research reported here, the activity of the anthracenediones and other common chemotherapeutic drugs in this tumor model has been studied and reported in the literature. Mitoxantrone was found to have a significant therapeutic efficacy in this tumor line, similar to that of adriamycin, when delivered IV. Mitoxantrone was also found to have therapeutic synergy when delivered in combination with several other common chemotherapeutics including cyclophosphamide, 5-FU, Ara-C, and vincristine.[106-108]

2.5 Purpose of These Studies

In view of the foregoing and with the basic goal of establishing preclinical data for IT chemotherapy which would facilitate the commencement of a Phase I human breast cancer trial, the studies reported here were initiated. These studies investigate the use of IT injection of MXN, either as free drug or albumin microsphere-loaded drug, for the treatment of breast cancer.

CHAPTER 3
MATERIALS AND METHODS

3.1 Materials

Mitoxantrone (MXN) was donated by Lederle Laboratories. The MXN was reported by the manufacturer to have a purity of 82.74%, and it was used without any further purification. 5-Fluorouracil was purchased from Sigma Chemical Company (St.Louis, MO). Ametantrone (AM) was provided by Dr. Schultz at the Drug Synthesis and Chemistry Branch of the National Cancer Institute in Bethesda, Maryland. The purity was not reported, and the AM was used as received as an internal standard in the HPLC assay of MXN. The anesthetic Vetamine (Ketamine HCl, 100 mg/mL) and the analgesic Banamine (Flunixin Meglumine, 50 mg/mL) were produced by Schering-Plough Animal Health. Xylaxine (20 mg/mL) was produced by The Butler Company (Columbus, OH). Vetamine was diluted with normal saline to 50 mg/mL, Xylazine to 6.67 mg/mL, and Banamine to 1 mg/mL, prior to use. Metofane (Methoxyflurane) was diluted in a 1 to 1 ratio with mineral oil. Mice were briefly anesthetized by placing them into 50 mL centrifuge tubes with a piece of cotton gauze coated with the Metofane/mineral oil mixture.

All proteins, enzymes, and chemical reagents were purchased from Sigma Chemical Company, unless other wise specified. Heparin Sodium Salt from Porcine Intestinal Mucosa (151 USP k units/mg) was dissolved in normal saline to prepare a 100 unit/mL solution which was used to coat syringes prior to blood collection. Bovine serum albumin, Fraction V initial fractionation by cold alcohol precipitation, (BSA) was

used to prepare albumin microspheres. Glutaraldehyde (Grade II, 25 % w/w aqueous solution) was distilled and used to prepare 40 mg/mL solutions of glutaraldehyde in DCE for use in microsphere synthesis.

Ultapure water was prepared in the laboratory using a Barnstead/Thermolyne NANOpure Ultrapure Water System (model 04754). All ultrapure water was purified until its resistance was greater than 17.0 MΩ-cm. Absolute ethanol (200 proof USP) was produced by AAPER Alcohol and Chemical Company and purchased from University of Florida Hospital Stores. Acetonitrile, HPLC grade, and Methanol, Optima or HPLC grade, were purchased from Fisher Scientific. All other solvents and salts were purchased from Fisher Scientific and at least Certified A.C.S. grade.

General medical and surgical supplies were generally obtained through University of Florida Health Center Stores, Henry Schein (Melville, NY), or Webster Veterinary Supply (Sterling, MA). All hypodermic needles were Monoject (Sherwood Medical) except the 30 Ga. needles which were PrecisionGlide (Becton Dickinson). Prior to surgery, the surgical site was shaved with a scapel blade, and the site and the surgeons hands were disinfected with Surgical Scrub and Handwash (2 % Chloroxylenol, Vet Solutions, Inc.). During surgery, animals' eyes were protected with a thin layer of petrolatum ophthalmic ointment (Puralube Vet Ointment, Pharmaderm, Melville NY). A 0.5 % solution of Tween 80 (donated by ICI Americas Surfactants) in normal saline was used to suspend microspheres prior to intratumoral injection.

3.1.1 Buffer Solutions

Phosphate buffer solution. Isotonic phosphate buffered saline (PBS) was prepared in-house for both *in vitro* and *in vivo* use. Stock 50 mM solutions of monobasic

and dibasic sodium phosphate were prepared in ultrapure water. PBS was prepared by adding monobasic solution to the dibasic solution until the desired pH was reached. Typically, a 1:2.9 monobasic to dibasic volume ratio was required for a pH 7.4 buffer. The necessary amount of sodium chloride to prepare an isotonic solution was determined by preparing standards ranging from 0 to 10 mg/mL NaCl in buffer solution. A μOsmette osmometer (Precision Instruments) was then use to measure the osmolality of each standard and a linear calibration plot prepared. The appropriate amount of NaCl to prepare a 300 mOsm buffer solution, as determined from the calibration plot, was added and the PBS sterile filtered through a 0.20 μm filter.

Other strength (mM) buffers were prepared using the same technique. Typically, large volumes of buffer (4 L) were prepared to reduce day-to-day variability in experiments. Small volumes of these stock buffers were sterilized by filtration using disposable Corning or Osmonics sterile filtering (pore size < 0.22 μm) apparatus just prior to use in the *in vivo* experiments.

HPLC mobile phase. An ammonium formate / acetonitrile solution was used as the mobile phase for HPLC analysis of MXN in mouse serum. First, a 0.5 M ammonium formate salt solution was prepared. Ammonium formate (102 g) was dissolved in 1.5 L of ultrapure water to make a 1.0 M solution. The pH of this solution was adjusted to 3.5 with concentrated HCl. This was then diluted to 3 L to make a 0.5 M salt solution. This ammonium formate solution was then vacuum filtered through a 0.10 or 0.20 μm filter (Anodisc 47) and used to make the HPLC mobile phase, which was 80% ammonium formate solution / 20% acetonitrile / 0.05% trifluoroacetic acid. The mobile phase was degassed by sparging with argon before use.

Saline for microsphere injections (Tsaline). The addition of a surfactant to the saline used to inject microspheres was required to stabilize the microsphere suspension. The surfactant also prevented the microspheres from adhering to the sides of the syringe, and to each other, during injections. Tween 80 was chosen as an ideal surfactant that was safe for injection in the *in vivo* experiments. Therefore, a 0.5% (w/v) Tween 80 in isotonic saline solution was prepared and sterile filtered through a sterile 0.20 μm filter into sterile vials for storage prior to use. This modified saline will be referred to as Tsaline in the remainder of this work.

Neutral buffered formalin. A 10% neutral buffered formalin solution was used to fix tissue samples prior to processing for histology. This buffer was prepared by dissolving 6.5 g of sodium phosphate dibasic and 4 g of sodium phosphate monobasic in 900 mL of ultrapure water. This solution was then diluted to 1000 mL with 40% w/v formaldehyde solution. The pH of the resulting solution was then adjusted to 7.0 using either 1 N HCl or NaOH as needed prior to filtration through a 0.22 μm Durapore filter (Millipore Corp.).

Enzymatic digestion buffer. Microspheres were digested in an enzyme solution in order to determine the concentration of drug in the loaded microspheres. The composition for the enzymatic digestion buffer (EDB) was based on prior work by Hadba[9] and Quigg (unpublished laboratory notebooks). This solution was prepared by dissolving 720 mg ethylenediamine tetraacetic acid sodium salt dihydrate (EDTA), 80 mg L-cysteine HCl hydrate, 50 mg papain, 50 mg bacterial protease type VIII, and 50 mg L-ascorbic acid (Aldrich Chemical Co.) in 100 mL of 0.1 M PBS (pH 7.0). The antioxidant L-ascorbic acid was added to this formulation to prevent the oxidative

degradation of MXN during the digestion. The EDB solution was prepared fresh prior to each use.

3.1.2 Reagent Solutions

Protein solutions. Albumin solutions must be characterized after preparation because the solid albumin powder is hygroscopic, absorbing approximately 10% of its weight in water, and solutions foam when prepared making the use of volumetric flasks difficult at best. Solutions for microsphere synthesis were prepared by dissolving approximately 110% of the desired amount of BSA in slightly less ultrapure water than is needed for the final volume of the solution. The BSA solution will foam significantly when mixed. After complete mixing, the foam can be broken by centrifuging, and the solution diluted to the final volume. The concentration of the resulting solution must then be determined. The weight % albumin is then determined by drying a sample on a Mettler LJ16 Moisture Analyzer at 130°C for 60 minutes. A sufficient volume of solution is dried to leave at least 1 g of dried albumin. The density of the solution is then determined gravimetrically. The density and the weight percent protein are then be used to determine the weight per volume concentration of the albumin solution.

Glutaraldehyde in 1,2-dichloroethane. The solution of glutaraldehyde (GTA) in 1,2-dichloroethane (DCE) used to crosslink albumin during microsphere synthesis was prepared as described by Hadba.[9] Aqueous glutaraldehyde was vacuum distilled. The resulting distillate was dissolved in DCE to a concentration of 40 mg/mL.

3.2 Methods

3.2.1 Standard Microsphere Synthesis

Hydrophilic albumin microspheres were prepared using the standard suspension crosslinking procedure developed by Hadba based on previous work reported by Longo,

Quigg, and Kirk.[9, 74, 77-79, 86] Albumin microspheres were synthesized by crosslinking a discontinuous aqueous BSA phase dispersed in a continuous DCE organic phase. A typical synthesis protocol is described. Three mL of a 20 % w/v BSA solution was dispersed in 47 mL of a 4 % cellulose acetate butyrate (CAB) in DCE solution in a 300 mL Labconco lyophilization flask with a Lightnin Lab Mixer (model LIU08, General Signal, Dublin, Ireland) or a Caframo BDC6015 Mixer (Caframo, Wiarton, Ontario, Canada) using a two inch two-blade stirrer. A top for the lyophilization flask was always used, and the space around the stirrer shaft covered with parafilm to decrease solvent evaporation during microsphere synthesis. The mixture was stirred for 20 min at 1250 RPM to allow an equilibrium emulsion to form prior to the addition of GTA in DCE to crosslink the BSA. After the addition of crosslinking agent, the solution was stirred for 2 hr at 600 RPM, then 50 mL of acetone was added and stirring continued for an additional hour to dehydrate the protein microspheres. The microspheres were centrifuged at 5000 RPM (3444 xg) in a Beckman Model J2-21 centrifuge (Beckman Coulter, Fullerton, MA) with a JA-17 rotor. Alternatively, a Dynac II benchtop centrifuge (Clay Adams) was used. The supernatant was decanted, the resulting microspheres washed by resuspension in approximately 30 mL of acetone, and the suspension centrifuged again. This microsphere washing procedure was repeated 4 times and the microspheres were left to dry at room temperature overnight. These standard synthesis conditions yield approximately 600 mg of microspheres.

3.2.1.1 Synthesis of MXN-loaded albumin microspheres

In situ MXN-loaded microspheres were produced by dissolving the appropriate concentration of MXN in the aqueous BSA solution prior to dispersion. The dispersion

energy (stirring speed) and CAB concentration were adjusted to produce microspheres with the desired size distribution.

3.2.1.2 Synthesis of 5-FU–loaded albumin microspheres

A study was performed as a "proof of concept" for the development of 5-FU–loaded BSA microspheres. Three different microsphere formulations were prepared with varying crosslink densities corresponding to 2, 4, and 8 % (w/w) GTA. The microspheres were prepared using the standard albumin microsphere synthesis protocol. The specific processing parameters used are shown in Table 3-4.

It was known that the use of different mixers produced slight variations in the particle size of the microspheres. This is presumable due to variations in the shear field produced by specific mixer and blade combinations. In order to reduce the impact of these variations on this study, the three samples for each crosslink density were randomized as best possible between the two mixers. Table 3-5 shows the run order and mixer randomization for each sample prepared.

One significant difference in the preparation of 5-FU–loaded microspheres compared to MXN-loaded microspheres lies in the method of incorporating the drug into the aqueous solution. When preparing MXN-loaded microspheres, the drug is added to the aqueous solution after the BSA concentration is determined. This is not feasible when using 5-FU because of the poor solubility of 5-FU in water. Instead an aqueous solution of 5-FU is formed by adding crystalline 5-FU to ultrapure water and adjusting the pH with 1 M NaOH (and 1 N HCL if necessary) to a pH of 9.0. A stable solution of 5-FU at concentrations greater than 30 mg/mL can be formed this way, although the solution must frequently be heated to achieve the initial dissolution of the 5-FU. This solution is used to form the BSA solution and this 5-FU/BSA solution is then

characterized. The amount of the 5-FU solution used to prepare the 5-FU/BSA solution is used to calculate its final 5-FU concentration. This is done to account for the volume expansion caused by the dissolved BSA.

Table 3-4 Processing conditions used for the synthesis of 5-FU–loaded BSA microspheres. All variables were held constant, except for GTA concentration which was 2, 4, or 8%.

Processing conditions	Level
GTA cocentration (% w/w relative to BSA)	2, 4, 8
BSA concentration (% w/v)	24.8
CAB concentration (% w/v)	3.0
Aqeous phase (mL)	2.5
DCE phase (mL)	47.5
D/C ratio	5.3
Stirring rate during emulsion stabilization (RPM)	1250
Stirring rate during crosslinking (RPM)	600

Table 3-5 Study design for the synthesis of 5-FU–loaded BSA microspheres. Three samples of each GTA concentration were prepared. Run order and mixer used were randomized. Each sample is designated by %GTA - ID#.

Run Order	Caframo mixer	Lightnin' mixer
1	4% GTA - 1	8% GTA - 2
2	2% GTA - 3	2% GTA - 2
3	4% GTA - 2	8% GTA - 1
4	8% GTA - 3	2% GTA - 1
5		4% GTA - 3

3.2.2 Microsphere Particle Size Characterization

3.2.2.1 Scanning electron microscopy

Scanning electron microscopy (SEM) was used to visually examine the particle morphology, surface topography, and size distribution of prepared albumin micro- and mesospheres. Micro/mesosphere samples were mounted on aluminum SEM stubs with double-sided tape. In order to perform SEM on nonconducting materials, such as protein

microspheres, the sample's surface must first be coated with a conducting material to prevent electrical charging of the surface. A gold/palladium coating was applied to the microspheres' surface with a Technix Hummer V sputter coater. The microspheres were coated for approximately five minutes using a 20 mAmp current. These conditions are known to deposit a 300 Å coating in four minutes. Relatively thick coatings were used when imaging microspheres in order to decrease the surface charging effects which alter and distort the image. A JOEL 6400 SEM (JOEL, Ltd., Peabody, MA) was used to image the coated microspheres. Electron microscopy was performed with a 5 KeV accelerating voltage, 15 mm working distance, and a condenser lens setting of 10. Paul Martin assisted with all electron microscopy, and exemplar images were digitally captured and archived.

3.2.2.2 Laser diffraction particle sizing

Particle size distributions of the prepared microspheres were measured using laser diffraction. This was done using the Coulter LS 230 particle sizer with the small volume module (Beckman Coulter, Fullerton, MA) at the University of Florida Engineering Resource Center. A 1 to 2% suspension of microspheres was analyzed using HPLC grade methanol as the suspension and analysis medium. This suspension was added drop-wise to the sample chamber until the obscuration reached 9 to 12%. The BSA optical model was used to calculate the particle sizes of the microspheres. The particle size distribution and distribution statistics were generated using the Coulter LS32 (v3.01) particle characterization software. The mean, median, standard deviation, and particle size distribution quartiles were calculated for each distribution obtained. The mean to median ratio was also calculated and used as a measurement of the distribution symmetry.

3.2.3 Determination of Microsphere Drug Content

After synthesis, it was necessary to determine the drug content in the loaded microspheres formulations. This was done spectrophotometrically after enzymatically digesting the microsphere protein matrix to release the loaded active drug. Approximately 5 mg of microspheres were incubated in 10 mL of EDB solution for two days at 37°C in a TBS incubator (Triangle Biomedical Sciences, Durham, NC). Each microsphere formulation was incubated in triplicate along with two controls. Each control consisted of 200 μl of a 1000 μg/mL drug solution in 10 mL of EDB. One control additionally had 50 mg of BSA. These controls were used to determine the percent MXN lost during the protein precipitation or to degradation during incubation. After 48 hours, the degradation solution was observed with a light microscope to ensure complete degradation of the microspheres. (Microspheres with a high crosslink density, such as 8% GTA, never completely degraded.) After digestion, 2 mL of each solution was placed in a test tube to which 2 mL of a 10% (w/v) trichloroacetic acid (TCA) in PBS was added and the samples were left at room temperature for 30 minutes to precipitate dissolved proteins. After the proteins precipitated, the samples were centrifuged and the supernatant collected for spectrophotometric analysis. Drug standards were prepared in a 5% TCA matrix. These standards were used to prepare a linear calibration curve using a Shimadzu UV-2401PC UV-VIS spectrophotometer (Shimadzu Scientific Instruments, Inc., Norcross, GA). A coefficient of determination (R^2) of at least 0.990 was obtained for each calibration curve, or new standards were prepared and a new calibration performed. Any unknown with an absorbance above the range of the standards was diluted by half until its absorbance fell within the valid range

for the calibration curve. Analysis of MXN-loaded microspheres was performed in polystyrene or acrylic disposable cuvettes (Fisher Scientific) at 658 nm with standards ranging from 1 to 50 μg/mL.

Analysis of 5-FU was performed using analogous methods except absorption at 266.5 nm was used to quantify the solution concentration. Additionally, since the digestion buffer also has some absorbance at this wavelength, all procedures should be performed upon EDB controls in triplicate, and the average absorption for the EDB subtracted from the absorbance of the 5-FU containing unkowns before calculating the concentration of 5-FU.

3.2.4 *In Vitro* Microsphere-Loaded Drug Release

The *in vitro* release of MXN and 5-FU from loaded microspheres was determined in PBS (0.05 M, pH 7.4). Roughly 20 mg of drug-loaded microspheres were suspended in 100 mL of PBS in 125 mL polymethylpentene (PMP) Erlenmyer flasks (Nalgene). These flasks were placed in the TBS incubator and maintained at a temperature of 37°C while rotating constantly. At selected time points a 1.000 mL aliquot of the supernatant was removed and placed in semimicro acrylic cuvettes, which were stored at 4°C until analysis. Nonloaded microspheres were also incubated with a known quantity of free drug to serve as controls. Each aliquot removed was replaced with an equivalent volume of fresh PBS. Each microsphere formulation was analyzed in triplicate. The amount of released drug was quantified using the Shimadzu UV-VIS spectrophotometer measuring the absorbance of the solution at either 266.5 nm for 5-FU or 658 nm MXN, as described previously. It is likely that the actual release of drugs *in vivo* would be influenced by drug binding to physiologic proteins. Therefore, the *in vivo* drug release of loaded

microspheres would also be dependant upon the local microenviroonment of the tumor and peritumoral tissues.

3.2.5 Passage of Tumor

The 16/C murine mammary adenocarcinoma cell line was a gift from Dr. Dietmar Seiman (Dept. of Radiation Oncology, University of Florida). The tumor line was maintained in C3H/HeJ mice since this cell line is non-viable *ex vivo*. In order to passage this tumor, mice with the tumor were euthanized with CO_2. Then within five minutes, the tumor mass was excised and finely minced under aseptic conditions. The tumor was then resuspended in calcium-free PBS to a concentration of approximately 25 mg of tumor per 50 mL injection. The mice receiving the tumor were anesthetized using Metofane, and 50 μL of the tumor suspension was injected subcutaneously with a 23 Ga needle into the flank of each mouse. This inoculation resulted in the development of a 500 mg tumor 10 to 14 days after inoculation. It should be noted that transplantation of metastatic foci is required in order to maintain metastatic potential in the 16/C tumor line. Because the tumor line used for these experiments was maintained by serial subcutaneous transplantation of primary tumor tissue (not metastatic foci), the model was not expected to produce metastases.

3.2.6 Standard *In Vivo* Experiment Protocol

All animals were housed in the University of Florida Animal Care Services (ACS-UF) facilities. They were housed five mice or less per cage, maintained on a 12 hour light schedule, and had access to food and water *ad libium*. Syngenic female mice, C3H/HeJ (Jackson Laboratories, Bar Harbor, ME) were used for all experiments with the 16/C mammary adenocarcinoma tumor model. Mice were 10 to 14 weeks old adults when they were inoculated with the 16/C tumor line, unless otherwise noted. All animal

procedures were approved by the University of Florida Institutional Animal Care and Use Committee (IACUC).

Approximately ten to 14 days after the induction of the tumor, when the tumor was 10 mm in its largest dimension (which for a 1 X 1 cm tumor corresponded to 0.5 g or 2.5% of body weight), the mice were randomly assigned to one of the treatment groups. Each group then received either a 100 μL intratumoral injection of free drug in normal saline, microsphere-bound drug suspended in Tsaline, or microsphere-bound drug suspended in a free drug in Tsaline solution using a 25 Ga needle. Alternatively, IV injection of free drug in saline was performed through the lateral tail veins using a 30 Ga needle. Doses were calculated based on an average mouse weight of 20 g, and all mice in each dose group received the same dose. Animals were briefly anesthetized with Metofane to facilitate injections. The intratumoral injections were administered through four injections around the perimeter of the tumor and one in the center (20 μL per injection site, 100 μL total dose). This was done to ensure that perfusion of the drug or microspheres throughout the tumor tissue was achieved.

After treatment, animals were observed once daily. Any animal showing clinical abnormalities in attitude, hydration, activity was monitored more closely. Animal weights and tumor sizes were recorded at least every two days for 60 days after treatment. The tumor mass was monitored by measuring the tumor dimensions with vernier calipers then calculating the mass using the following relation based on the volume of an ellipse:

$$Tumor\ Weight\ (g) = \frac{ab^2}{2000}$$

where *a* is the diameter of the tumor along its largest dimension in mm and *b* is the diameter orthogonal to *a* in mm. Any animal with persistent signs of malaise, or whose body weight loss, adjusted for the weight of the tumor mass, reached or exceeded 20% of its starting body weight, was considered to be suffering from drug toxicity and euthanized in a CO_2 chamber. If the tumor mass of an animal exceeded 10% of its total body mass, it was considered a treatment failure and the animal euthanized and the tumor excised for examination. Animals surviving tumor free 60 days after initial treatment were considered "cured".

3.2.7 Blood Collection for CBCs

Blood (about 200 μL) for complete blood cell count with differential cell counts (CBC) was collected from the ventral tail artery of the mice. This was done by first disinfecting the tail with a povodone iodine solution or 70% alcohol, then nicking the ventral artery with a scalpel and collecting the blood directly into a pediatric EDTA blood collection tube. The ACS-UF clinical lab then performed CBCs with differentials on the collected blood. This was done to determine if there was any evidence of leukopenia, which is indicative of myelosuppression the dose-limiting toxicity of mitoxantrone.

3.2.8 Histology of Tissue Specimens

Tissue samples were taken from each mouse after euthanasia for histological analysis. Tumor tissue was dissected from the skin and the underlying fascia and muscle for histological analysis of cellular composition, organization, and tumor grade. Samples of liver tissue were also obtained for analysis of signs of toxicity since it is the primary organ of MXN metabolism and excretion. Tissue specimens were placed in clearly labeled 15 mL centrifuge tubes and fixed with 10% neutral buffered formalin for at least 24 hours. They were then stored in 75% ethanol/water until further processing. Samples

were then dehydrated with serial ethanol washes (75%, 90%, 95%, and dry 100% ethanol for at least 15 minutes, 3 washes per concentration) prior to clarification with xylene and paraffin embedding. Samples were then sectioned and Hematoxilin and Eosin (H&E) stained using standard techniques. Tissue processing and staining was performed by Regeneration Technologies, Inc. (Alachua, FL) or the Research Histology Core Lab (Department of Pathology, Immunology, and Laboratory Medicine, College of Medicine, University of Florida). All slides were evaluated and interpreted by Dr. Carol Detrisac (Department of Pathobiology, College of Veterinary Medicine, University of Florida) who has been kind enough to collaborate in these studies.

3.2.9 Experimental Design of *In Vivo* Efficacy Studies

3.2.9.1 IV versus IT neoadjuvant chemotherapy with F-MXN

A study was performed to compare IV to IT delivered chemotherapy. Few published studies have directly compared IT chemotherapy to the standard IV chemotherapy used clinically, and none have done this using MXN. Treatment groups were included that received a single injection of MXN free drug either IT or IV followed by surgical resection of the tumor mass (neoadjuvant chemotherapy), as well as groups that only received chemotherapy with no surgical intervention. Two different doses of MXN were used for this study, 4 and 8 mg/kg. Control groups consisted of mice receiving no treatment or surgery only. Surgical resection of the tumor mass was originally scheduled for 10 days after the initiation of treatment for those groups receiving surgery. However, the tumor's rapid rate of growth necessitated tumor excision on day 5 for the surgical control group. The study was originally designed with 12 mice in each treatment group (10 groups X 12 mice = 120 mice). Because little was known of the tolerable doses for MXN delivered IT, the animals receiving the 8 mg/kg doses were

studied in the first leg of the study. The treatment groups receiving 4 mg/kg doses were studied in a second leg. Control animals were included in all study legs to ensure similar tumor growth characteristics. Samples of tumor and liver tissue were taken during necropsy of each mouse. These tissue samples were fixed in 10% neutral buffered formalin, and standard H & E stained sections were prepared for histological examination.

It was hypothesized that the IT treatment groups would have significantly lower tumor growth rates, increased survival times, and increased number of cured animals, as well as tolerate higher doses of MXN. The secondary hypothesis was that animals receiving neoadjuvant (preoperative) chemotherapy would have better outcomes than those receiving chemotherapy alone.

This study was performed using the standard protocol for tumor inoculation, treatment initiation, injection procedure, and study endpoints described in section 3.2.6. A diagram of the treatment groups included in the design of this study is shown in Figure 3-5.

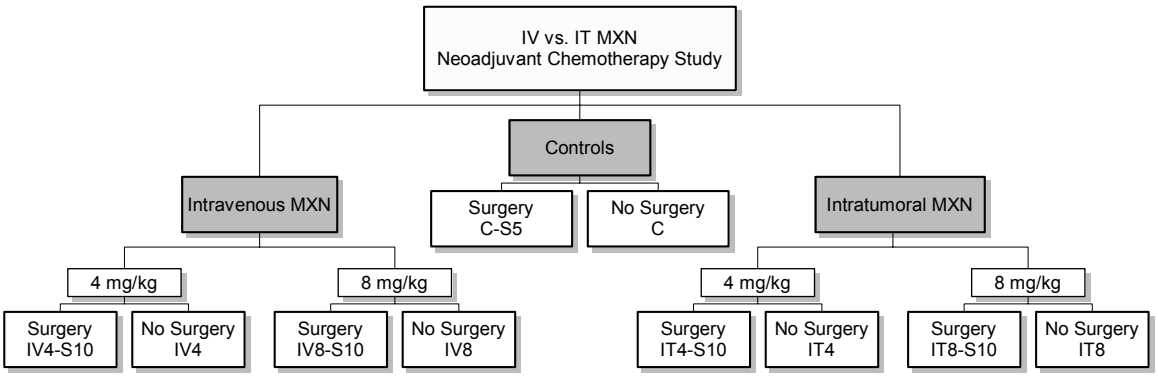

Figure 3-5 Study design for the comparison of the efficacy and toxicity of intravenous (IV) compared to intratumoral chemotherapy (IT) using mitoxantrone with and without surgery performed on Day 10 (after randomization) following chemotherapy treatment on Day 5 for untreated controls. (n = 12 per group)

3.2.9.2 Intratumoral therapy with free or 20 to 40 μm microsphere-loaded MXN

This was a pilot study comparing the efficacy of intratumoral injection of free MXN (F-MXN) with albumin microsphere-loaded MXN (MS-MXN). Treatment consisted of a single treatment on Day 0 initiated when the 16/C MAC tumor reached 10 mm in longest dimension as described in the Section 3.2.6. It was known from the previous comparison of IT to IV chemotherapy with F-MXN that 8 mg/kg IT was well tolerated. However, it was not known what the maximum tolerated dose (MTD) of MS-MXN would be. Therefore this study was also considered a pilot study to determine what doses of albumin MS-MXN would be well tolerated. Initial groups consisted of F-MXN delivered at 4, 8, 16, 24 mg/kg or MS-MXN delivered at 8, 16, or 24 mg/kg. In the initial studies, the MS-MXN dose was suspended in saline. As the study progressed additional groups consisting of 24, 32, and 48 mg/kg doses of MS-MXN delivered in a 0.5% Tween 80 in normal saline solution (Tsaline) were added to the study. Control groups consisting of untreated tumors, IT injection of Tsaline, and non-loaded albumin microspheres were included in the study.

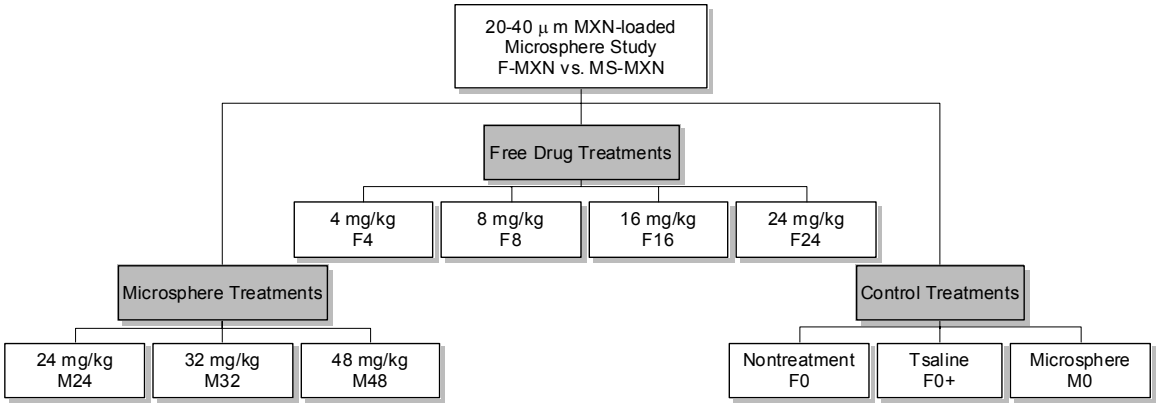

Figure 3-6 Study design for the evaluation of a single intratumoral injection of 20 to 40 μm MS-MXN compared to F-MXN delivered on Day 0. (n = 4 per group)

This study was performed using the standard protocol for tumor inoculation, treatment initiation, injection procedure, and study endpoints described in section 3.2.6. A diagram of the treatment groups included in this study design is shown in Figure 3-6.

3.2.9.3 Intratumoral therapy with 20 to 40 μm microspheres combined with free MXN

The object of this study was the *in vivo* evaluation of the safety and efficacy of intratumoral injection of MXN both as a combination of free drug with drug-loaded albumin microspheres. Treatment groups consisted of intratumoral MS-MXN delivered in combination with F-MXN or in a control vehicle (Tsaline). Control groups also included included nontreated, intratumorally injected Tsaline, and nonloaded albumin microspheres with similar size and crosslink density to the MS-MXN formulation. The dose levels of 24 and 32 mg/kg MS-MXN for the treatment groups were chosen based on the results of the previous study of 20 to 40 μm MS-MXN and F-MXN. The free drug delivery vehicle used to deliver the MXN-loaded albumin microspheres consisted of 4 or 8 mg/kg of MXN in Tsaline.

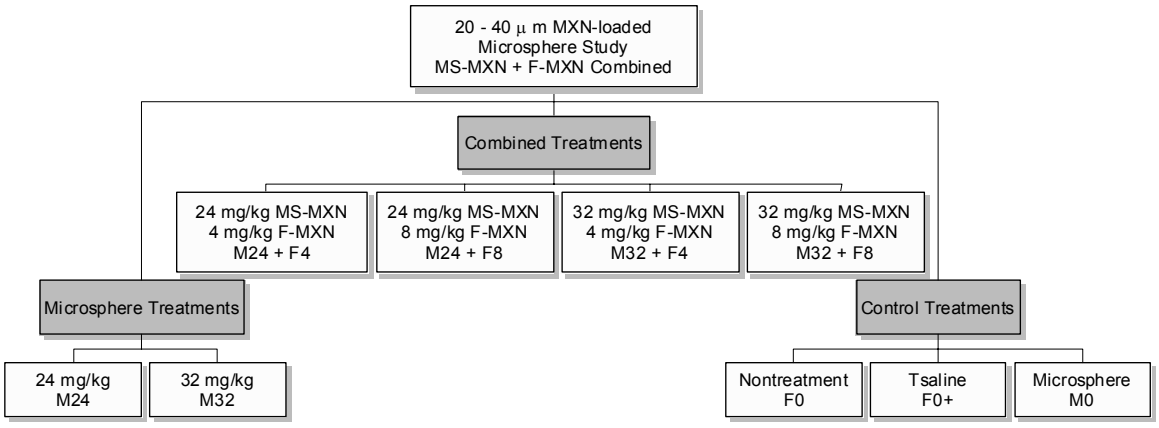

Figure 3-7 Study design for the evaluation of a single intratumoral injection of 20 to 40 μm MS-MXN combined with F-MXN delivered on Day 0. (n = 4 per group)

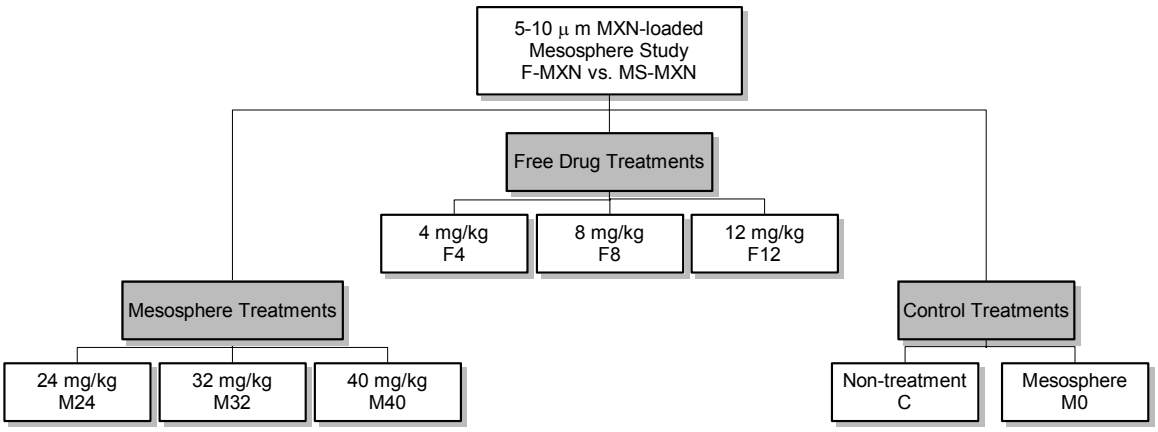

Figure 3-8 Study design for the evaluation of a single intratumoral injection of 5 to 10 μm MS-MXN compared to F-MXN delivered on Day 0. (n = 5per group)

This study was performed using the standard protocol for tumor inoculation, treatment initiation, injection procedure, and study endpoints described in section 3.2.6. A diagram of the treatment groups included in this study is shown in Figure 3-7.

3.2.9.4 Intratumoral therapy with free or 5 to 10 μm mesosphere-loaded MXN

This study was similar in design and purpose to the previous 20 to 40 μm MS-MXN pilot study except that smaller 5 to 10 μm MXN loaded mesospheres (MS-MXN) were used. Microsphere formulations were injected using the Tsaline delivery vehicle. Control groups consisted of untreated tumors and nonloaded albumin microspheres with a similar size and crosslink density to the MS-MXN formulation. A Tsaline control group was not included. Not all animals used for this study were of the same age and weight. Therefore, three 10 to 14 week old mice (approximately 20 g) and two older 18 to 22 week old mice (approximately 24 g) were included in each study. The number of animals from each weight/age group was constant for each treatment group in order to prevent any confounding of the survival data. All animals received MXN doses calculated as though they weighed 20 g. This was done in order to make the doses equivalent to those used in earlier studies on a dose per tumor basis.

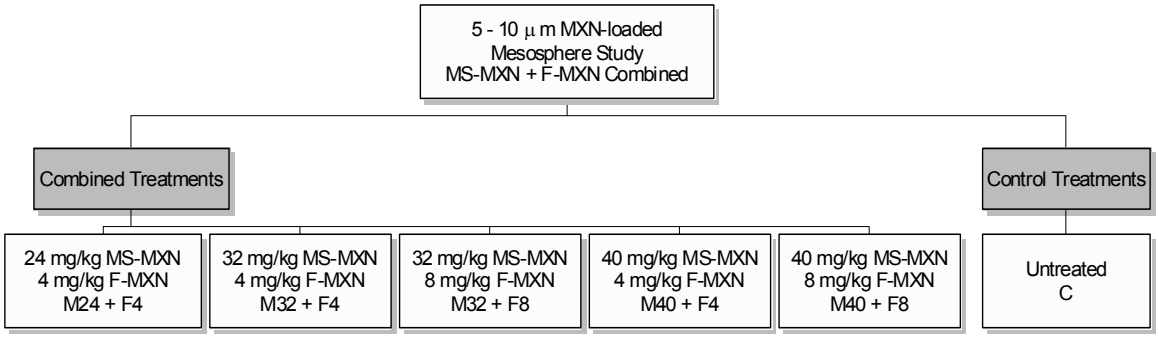

Figure 3-9 Study design for the evaluation of a single intratumoral injection of 5 to 10 μm MS-MXN combined with F-MXN delivered on Day 0. (n = 5 per group)

Other than the differences noted above, this study was performed using the standard protocol for tumor inoculation, treatment initiation, injection procedure, and study endpoints described in section 3.2.6. A diagram of the treatment groups included in this study is shown in Figure 3-8.

3.2.9.5 Intratumoral therapy with 5 to 10 μm mesospheres combined with free MXN

This study was analogous to the pilot study of 20 to 40 μm MS-MXN combined with F-MXN. Each group received a single treatment on Day 0. Treatment groups were chosen based on the results of the previous study of a 5 to 10 μm MS-MXN. Control groups in this study consisted of untreated tumors. Nonloaded microsphere and Tsaline controls were not included.

This study was performed using the standard protocol for tumor inoculation, treatment initiation, injection procedure, and study endpoints described in section 3.2.6. A diagram of the treatment groups included in this study is shown in Figure 3-9.

3.2.9.6 Histology and efficacy of neoadjuvant intratumoral chemotherapy

This was a study of the clinical and histological pathology of intratumoral treatment with F-MXN or MS-MXN. As an adjunct to the histological aspects, the study

also served as a pilot experiment to evaluate the timing of tumor excision following the use of IT MXN as a neoadjuvant therapy. Mice bearing the 16/C MAC were treated with IT injection of F-MXN alone or MS-MXN combined with F-MXN on delivered on Day 0. Two MS-MXN formulations were used for this study, both were delivered in a 4 mg/kg F-MXN in Tsaline delivery vehicle (and were therefore a combination treatment of F-MXN and MS-MXN). One formulation had a low crosslink density while the other was the higher crosslink density formulation used in previous experiments (crosslink densities corresponded to 2 and 8% GTA). Both MS-MXN formulations fell within the 5 to 10 μm range for median mesosphere diameter. Each mouse was randomized to treatment and to receive surgery on day 1, 5 or 14 after IT treatment. Animals receiving surgery on day 1 or 14 also received CBCs with differential cell counts. The tumors were surgically excised under aseptic conditions as described in section 3.2.6. The excised tumors were fixed in 10% neutral buffered formalin prior to the preparation of H & E stained slides for histological examination.

The histological examination and evaluation of the tumor samples was performed by Dr. Carol Detrisac (Department of Pathobiology, College of Veterinary Medicine, University of Florida). The histological evaluation of the tumor samples specifically included: evidence and distribution of necrosis; the presence, distribution, and degradation of microspheres; visible presence of drug within the tumor; whether necrosis was associated with the microspheres; inflammatory response to the tumor, including cell types and if it is associated with the presence of microspheres; whether the viable tumor cells exist as a cell mass or as tendrils of cells within fibrosis; mitotic figures per 40x high power field; cellular pleomorphism (on an ordinal scale with 1 = all the same to 3 =

high degree of variability); presence of peritumoral fibrosis; and whether the surgical borders were "clean".

This study used the standard protocol for tumor inoculation, treatment initiation, injection procedure, study endpoints and analysis described in section 3.2.6. The treatment groups and timing of surgery and laboratory measurements obtained are detailed in Table 3-6.

3.2.9.7 Scheduled injections of intratumoral chemotherapy

Another study was designed to evaluate the efficacy of multiple scheduled IT injections of F-MXN or MS-MXN. Treatment groups consisted of 24 mg/kg MS-MXN (5 to 10 μm, 8% GTA) delivered in a 4 mg/kg F-MXN vehicle on days 0, 7 and 14, or F-MXN delivered at a dose of 8 mg/kg on day 0 and 4 mg/kg on Days 7 and 14. Doses were chosen to be at or close to the MTD based on previous studies of single IT treatments. Additionally, an untreated control group was included for comparison. Any animal suffering from a tumor adjusted body weight (TABW) loss greater than 15% compared to its TABW on Day 0 at the time of the second or third injection did not receive that injection. Additionally, any animal whose tumor was judged to have

Table 3-6 The histology and neoadjuvant chemotherapy study design. Mice were treated on Day 0 with high or low crosslink density mesospheres in combination with F-MXN, F-MXN alone, or control nontreatment. (n = 3 per time point)

Treatment (Day 0)	Day 1	Day 7	Day 14
MS-MXN (2% GTA)	T, CBC	T	T, CBC
MS-MXN (8% GTA)	T, CBC	T	T, CBC
F-MXN	T, CBC	T	T, CBC
Control	T, CBC	T	N/A

T= H&E stained slide of tumor tissue, CBC= Complete Blood Cell Count w/ differential

completely regressed at the time of the second or third injection did not receive that injection.

The study was performed using the standard protocol for tumor inoculation, treatment initiation, injection procedure, and study endpoints described in section 3.2.6. The treatment groups and dose schedule are outlined in Table 3-7.

3.2.10 Statistical Analysis

Each animal was randomly assigned to a treatment group at the time of treatment (on Day 0). An enrollment schedule of treatments was randomly generated at the beginning of each experiment. At the time of initial treatment, each animal received the next treatment on the randomized enrollment schedule of treatments. The randomization was blocked in such away as to insure that all treatments were distributed throughout the enrollment schedule.

Statistical analysis of the experimental data was performed using MINITAB Statistical Software Release 13.31 (Minitab, Inc., State College, PA).

Survival data were analyzed using the nonparametric Kaplan-Meier method. Data were Type I censored (right censored for time) at Day 60 (or the last day of the study). The log-rank statistical test was performed on the set of survival curves for each

Table 3-7 Scheduled injection study design. Mice were treated with 3 injections spaced 7 days apart of either combination MS-MXN and F-MXN, F-MXN alone, or control nontreatment. (n = 10 per treatment group)

Drug formulation	Day 0 dose	Day 7 dose	Day 14 dose
MS-MXN + F-MXN combined	24 mg/kg MS-MXN + 4 mg/kg F-MXN	24 mg/kg MS-MXN + 4 mg/kg F-MXN	24 mg/kg MS-MXN + 4 mg/kg F-MXN
F-MXN	8 mg/kg F-MXN	4 mg/kg F-MXN	4 mg/kg F-MXN
Control	untreated	untreated	untreated

experiment. If a statistically significant difference was detected within the experiment ($P < 0.05$), pair-wise comparisons of appropriate treatment groups were performed with no adjustment for the use of multiple comparisons.

Continuous data, such as tumor or body weight on day n, were analyzed using the appropriate statistical tests. Evaluation of the effect of one factor with more than two levels on a continuous response variable was performed using one-way ANOVA, if the study data were balanced, or the General Linear Model ANOVA, if the data were unbalanced. If the groups were significantly different ($p < 0.05$) based on the ANOVA test, Tukey's multiple comparisons tests (MCT) were performed on each possible factor level combination. Significance for the Tukey's MCT was set at a family error rate of 0.05 or 0.10 depending on the number of samples and comparisons performed. The significance level used for each comparison is clearly stated in the discussion of the results. Analysis of response variables with one independent factor and two levels was performed using Student's T-test with a $p < 0.05$ considered evidence of a significant difference in the means.

CHAPTER 4
RESULTS AND DISCUSSION OF *IN VITRO* EXPERIMENTS

4.1 Synthesis and Characterization of MXN-Loaded BSA Microspheres

Five different BSA microsphere formulations were prepared for use in the *in vivo* studies. Initial studies were done using MXN-loaded BSA microspheres with a mean diameter between 20 to 40 μm and a crosslink density corresponding to 8% GTA. Nonloaded microspheres with a similar mean diameter and crosslink density were used for the control microsphere treatment groups. These 20 to 40 μm BSA microspheres were originally synthesized and characterized by Ahmad Hadba.

Smaller MXN-loaded BSA mesospheres with a mean diameter between 5 and 10 μm were also desired for use in the *in vivo* studies since it was expected that smaller mesospheres might more efficiently perfuse the tumor mass. These mesospheres were prepared based on the synthesis techniques and model of particle size as a function of processing parameters developed by Hadba.[9] Three different BSA microsphere formulations were prepared in this size range. Two were MXN-loaded with crosslink densities corresponding to 2 and 8% (w/w) GTA. Nonloaded BSA microspheres prepared with 8% (w/w) GTA were also prepared for use as microsphere controls in the *in vivo* studies utilizing these smaller mesospheres. The process parameters found to produce the desired microsphere sizes is shown in Table 4-8. The particle morphology and size distribution of all five microsphere formulations were characterized. The percent MXN loading and *in vitro* MXN release from the MXN-loaded microspheres were also determined.

Table 4-8 BSA meso- and microsphere synthesis conditions. MXN-loaded microspheres were prepared using a 15% (w/w MXN/BSA) solution.

Processing conditions	5 - 10 μm BSA MS's	20 - 40 μm BSA MS's
GTA cocentration (% w/w relative to BSA)	8	8
BSA concentration (% w/v)	20	30
CAB concentration (% w/v)	4.0	2.0
Aqeous phase (mL)	3	2.5
DCE phase (mL)	47	47.5
D/C ratio	6.4	5.3
Emulsification time (min)	20.0	20.0
Crosslinking time (min)	180.0	180.0
Stirring rate during emulsion stabilization (RPM)	1250	1250
Stirring rate during crosslinking (RPM)	600	600

The crosslink density in these studies is represented by the processing parameter of weight % GTA (relative to the total weight of the microsphere). GTA preferentially reacts to crosslink BSA through the amines found on the side chain of the amino acid lysine. There are 59 lysine amino acids, or 0.901 mmol, per gram of BSA. Each weight % GTA corresponds to 0.1 mmol GTA per gram of BSA.[9] Therefore, each % GTA corresponds to a 1:9 molar ratio of GTA to lysine, and assuming 100% reaction 4.5% GTA would correspond with complete reaction of all lysine groups (with each GTA molecule reacting with 2 lysines). However, complete reaction does not occur and GTA is known to react through other amino acids than just the lysine. Additionally GTA may also self polymerize to form a dimer, or even higher order polygluteraldehyde. This polygluteraldehyde may also react to form crosslinks between BSA molecules.

4.1.1 MXN-Loaded Microsphere Characterization

The amount of drug loaded into each MXN microsphere formulation was determined by enzymatically digesting the albumin microspheres and measuring the

amount of released drug spectrophotometrically. The results for the analysis of the MXN-loaded microspheres used in the *in vivo* studies are summarized in Table 4-9. It was felt that the MXN loading value obtained by enzymatic digestion of the microspheres would be more reliable for measuring the MXN that would be bioavailable after intratumoral injection compared to values obtained by measuring the amount of MXN lost from the synthesis and wash solutions (the MXN depletion assay). The MXN-depletion assay would likely overestimate the amount of drug loaded into the albumin microspheres because of failure to account for drug adsorption to the laboratory glassware or drug covalently bound and inactivated by GTA. However, it must be noted that the MXN loading measured by enzymatic digestion may also underestimate the amount of drug incorporated into the microspheres because some drug may remain trapped in incompletely degraded microspheres. This is especially true for microspheres with higher crosslink densities.

Each MXN-loaded microsphere formulation was characterized using SEM and particle size analysis. Particle morphology and topology were observed using SEM and particle-size distributions were measured using the Coulter LS 230. Particle size, as calculated by the Beckman Coulter particle characterization software, is summarized with

Table 4-9 Weight percent drug and drug-loading efficiency for the MXN loaded BSA microspheres used in the i*n vivo* studies. Drug loading was determined by enzyamtic digestion of the microspheres.

Microsphere formulation	Weight % MXN	Standard deviation	MXN loading efficiency
MXN 20-40 μm	12.8%	(1.0)	85%
MXN 5-10 μm (2% GTA)	14.3%	(0.6)	95%
MXN 5-10 μm (8% GTA)	15.7%	(0.6)	105%

data for each sample in Table 4-10. Typical SEM micrographs and particle-size distributions for each microsphere size range and crosslink density are shown in Figure 4-10 through 4-13.

Electron microscopy of the microspheres revealed differences in the topology. The 20 to 40 μm and the 5 to 10 μm MXN-loaded microspheres crosslinked with 8% (w/w) GTA were smooth and spherical in shape. The 5 to 10 μm MXN-loaded microspheres crosslinked with 2% (w/w) GTA were spherical, but had a porous structure. The development of a porous structure seems to be related to the presence of MXN within the microsphere since nonloaded microspheres produced under similar conditions had smooth surfaces (micrographs not shown). Hadba found that microsphere surface roughness and porosity was often due to a complex interaction of the CAB and GTA concentrations as well as the presence of MXN during synthesis. A more complete study and discussion of this phenomenon can be found in Hadba's dissertation.[9]

The particle-size distribution for each of the MXN-loaded microspheres was measured. The particle-size data is summarized in Table 4-10 and the distributions are shown in Figures 4-12 and 4-13. The mean diameter for each of the 5 to 10 μm

Table 4-10 Particle-size distribution statistics for the MXN-loaded BSA microsphere formulations used in the *in vivo* studies.

Microsphere formulation	Mean diameter (μm)	S. D. (μm)	Median diameter (μm)	Mean/ median ratio	90th percentile (μm)	10th percentile (μm)
MXN 20-40 μm	37.71	22.62	41.12	0.917	1.093	65.66
MXN 5-10 μm (2% GTA)	8.704	8.443	7.532	1.156	0.224	20.59
MXN 5-10 μm (8% GTA)	6.555	7.13	2.932	2.235	0.212	16.56
Blank 20-40 μm	18.96	12.21	19.84	0.956	1.311	34.85
Blank 5-10 μm (8% GTA)	6.153	4.329	6.096	1.009	0.853	12.16

BSA-microsphere formulations was found to be within the target range desired for use in the *in vivo* studies. The MXN loaded 20 to 40 μm BSA microspheres were found to be larger than expected based on previous analysis with a mean diameter closer to 40 μm than the expected 30 μm. This increase in mean diamaeter makes the MXN-loaded microspheres larger than the control microspheres used in the *in vivo* studies utilizing 20 to 40 μm microspheres. This is not expected to have made a significant difference in the results of the study.

4.1.2 In Vitro Release of MXN from Loaded Microspheres

The *in vitro* release of MXN from the loaded microspheres was evaluated in a PBS medium. The release profiles are shown in Figure 4-14. The cumulative percent of the loaded drug released was statistically compared after 24 and 120 hours. A significantly greater percent MXN was released from the 5 to 10 μm 2% GTA formulation than the other two formulations within the first 24 hours (65.8 ± 9.8% compared to 33.6 ± 0.3% for the 20 to 40 μm 8% GTA and 39.5 ± 0.8% for the 5 to 10 μm 8% GTA microspheres). The cumulative release from all of the formulations was statistically different after 120 hours of incubation (one-way ANOVA, $p<0.001$; Tukey's MCT, family error rate < 0.05).

The rate of release and the total percent of the loaded drug released from the microspheres were found to increase with decreasing crosslink density and particle size. This is in accordance with expectations based on previous studies. A decrease in crosslink density (% GTA) allows the microspheres to swell to a greater extent. This creates a more open interpenetrating network of the albumin, which makes up the matrix of the microsphere. This more open network allows for a greater diffusive flux of drug across the surface of the microsphere. A decrease in microsphere size increases the

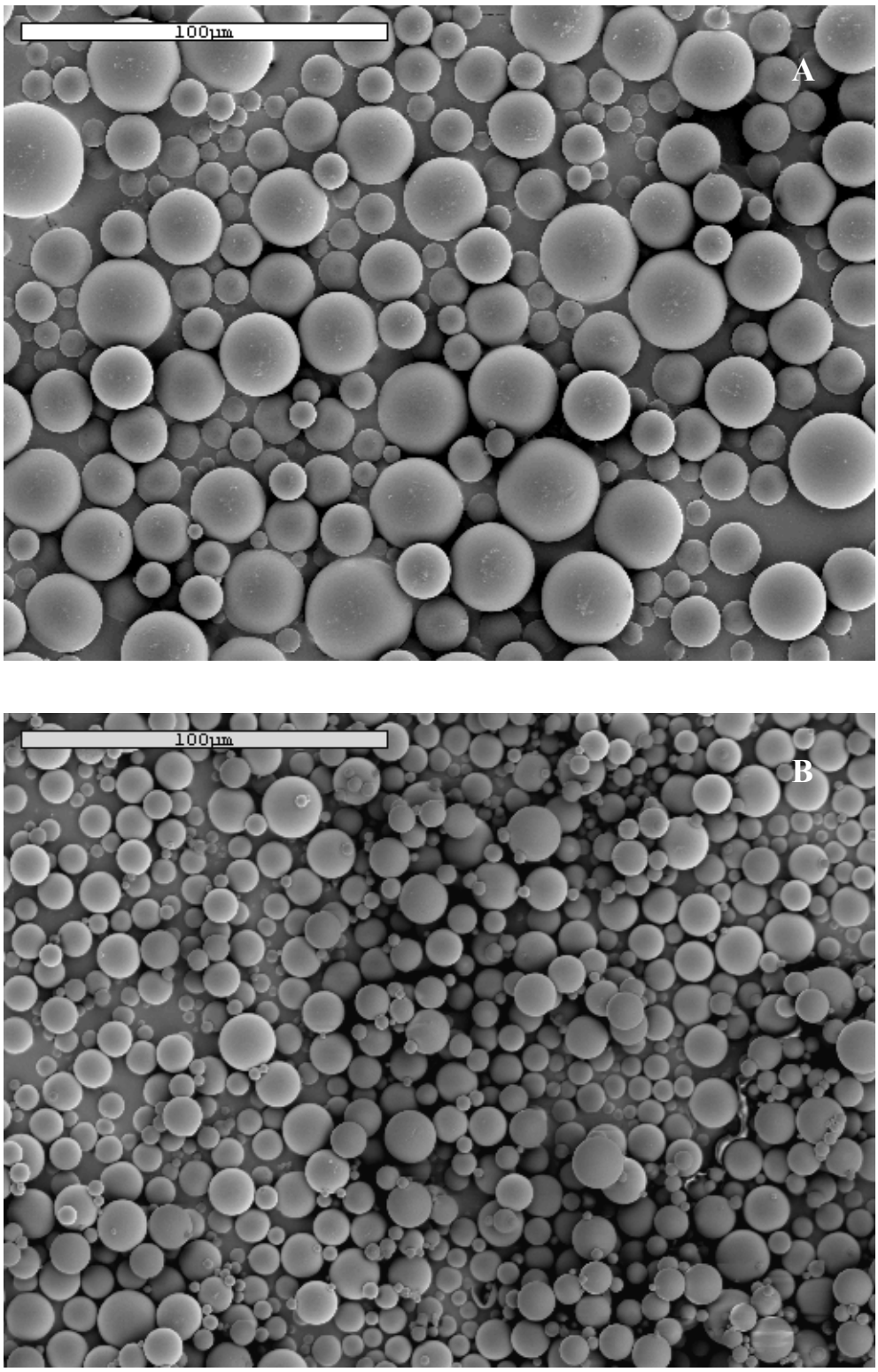

Figure 4-10 8% GTA MXN-loaded BSA microspheres SEM micrographs. A) 20 to 40 µm microspheres. B) 5 to 10 µm mesospheres. (both 500x)

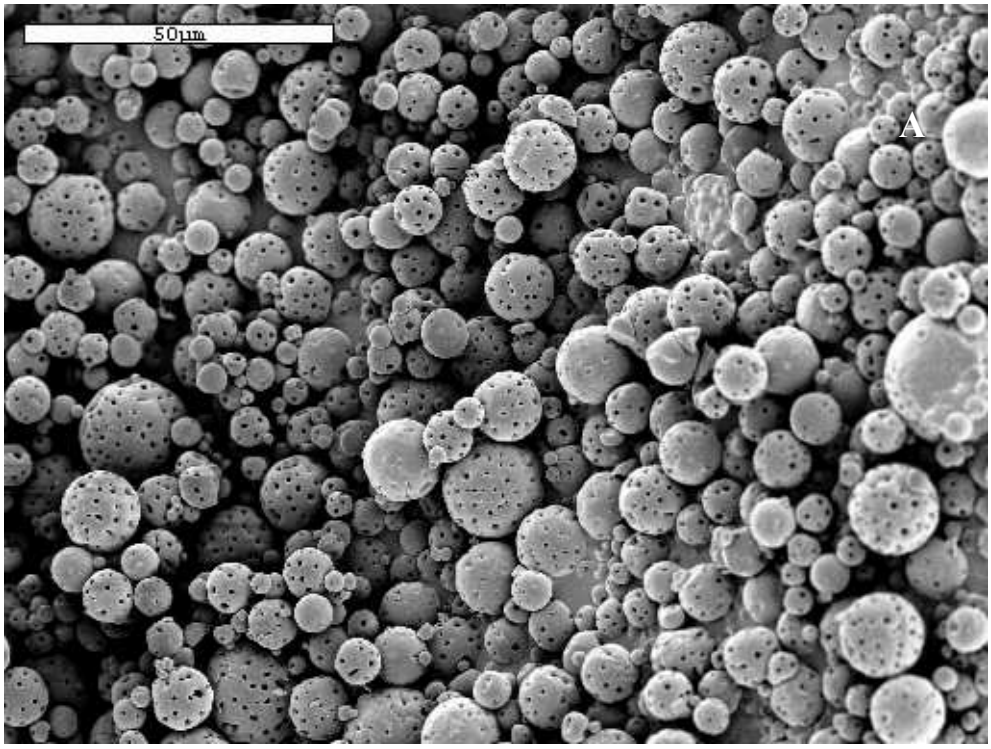

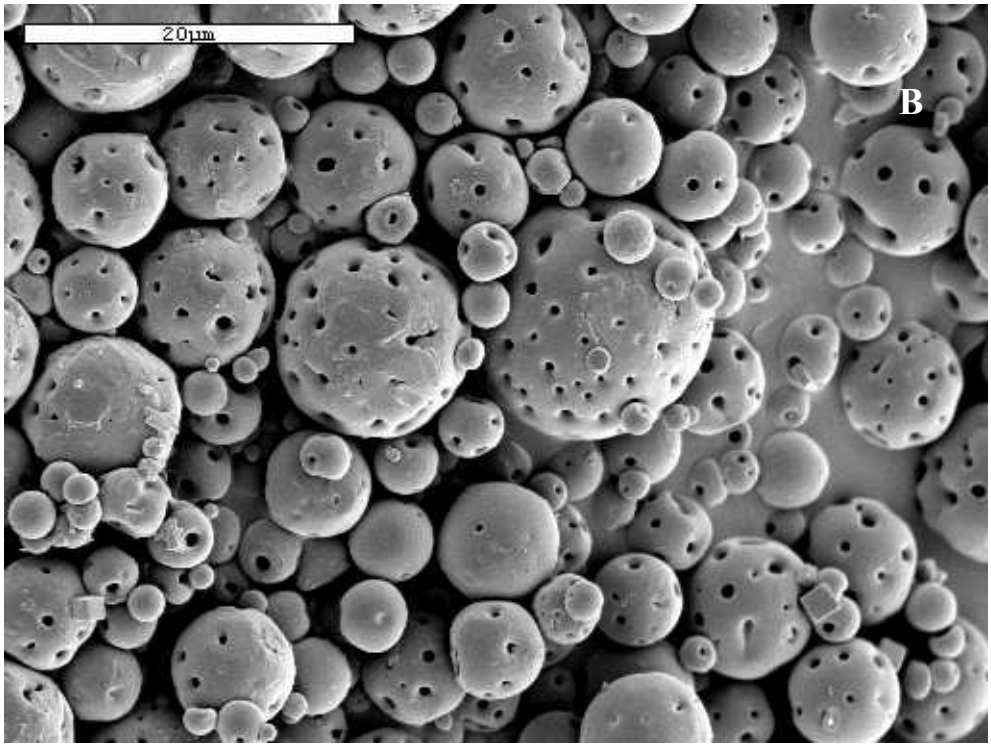

Figure 4-11 5 to 10 µm MXN-loaded BSA mesospheres with 2% GTA crosslink density SEM micrographs. A) 750X. B) 2000X.

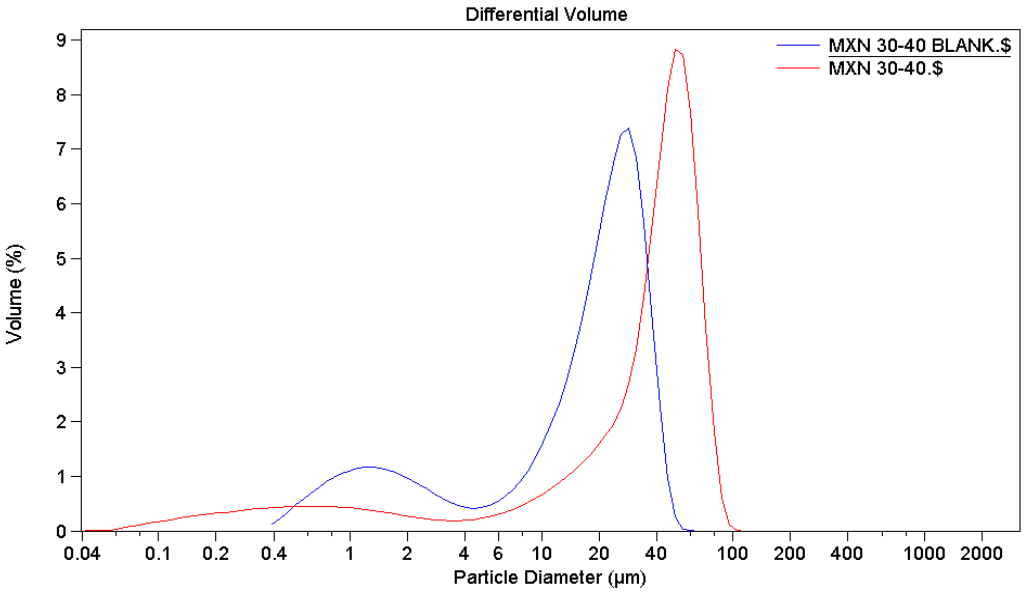

Figure 4-12 Particle-size distributions for BSA microspheres used in the 20 to 40 µm *in vivo* studies. MXN 30-40 Blank are the unloaded microspheres that were used as controls, and MXN 30-40 are the MXN loaded BSA microspheres.

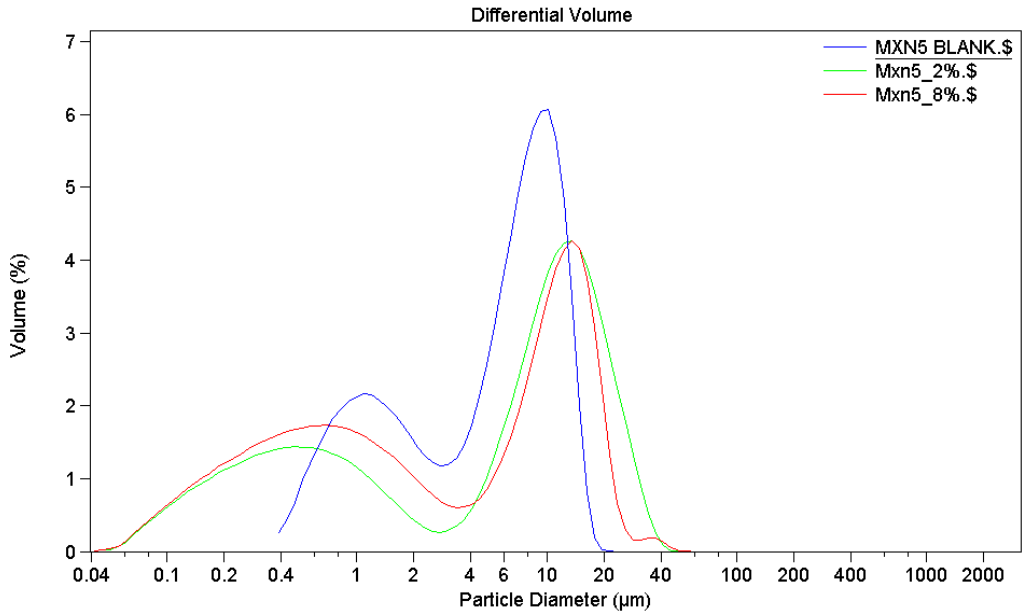

Figure 4-13 Particle size distribution for MXN-loaded BSA mesospheres used in the 5 to 10 µm *in vivo* studies. MXN Blank are nonloaded microspheres that were used as controls. MXN5_#%, the # refers to the crosslinking density in % GTA.

surface area to volume ratio, which along with the shorter diffusion path required to escape the microsphere matrix allows for a greater flux of entrapped drug out of the microsphere.

It should be noted that the release of drug into a PBS medium under "infinite sink" conditions only allows the qualitative evaluation of the release profiles and does not truly reflect the release of drug *in vivo*. For one thing, the *in vitro* release into PBS only measures release due to diffusion of drug from the microsphere with the minimal degradation of the microsphere due to hydrolysis. In an *in vivo* environment the tumor does not act as an infinite sink. Instead, the diffusion of a highly protein bound drug such as MXN from the microsphere would be influenced by the amount of drug in surrounding extracellullar fluids and bound to the surrounding tissues. In addition, there is poor venous and lymphatic drainage of the extracellular fluid from the tumor tissues. The protein matrix of the microsphere will also be subjected to enzymatic degradation *in vivo*, which will facilitate the release of additional drug that was "trapped" within the microsphere and would not be released in an *in vitro* assay. Thus, in order to obtain a valid model of the drug release from loaded microspheres, the release into the tumor environment should be measured *in vivo*. This could be done by microdialysis measurements of the tumor environment, or possibly non-invasively using labeled drugs and imaging techniques such as magnetic resonance imaging (MRI).

4.2 Synthesis and Characterization of 5-FU–Loaded BSA Microspheres

Because 5-FU is often used clinically in combination with anthracycline or anthracenedione chemotherapeutic agents for the treatment of breast cancer, it was of interest to develop 5–oaded microspheres for use alone and in combination with MXN formulations. Therefore, a feasibility study was performed to show that 5-FU could be

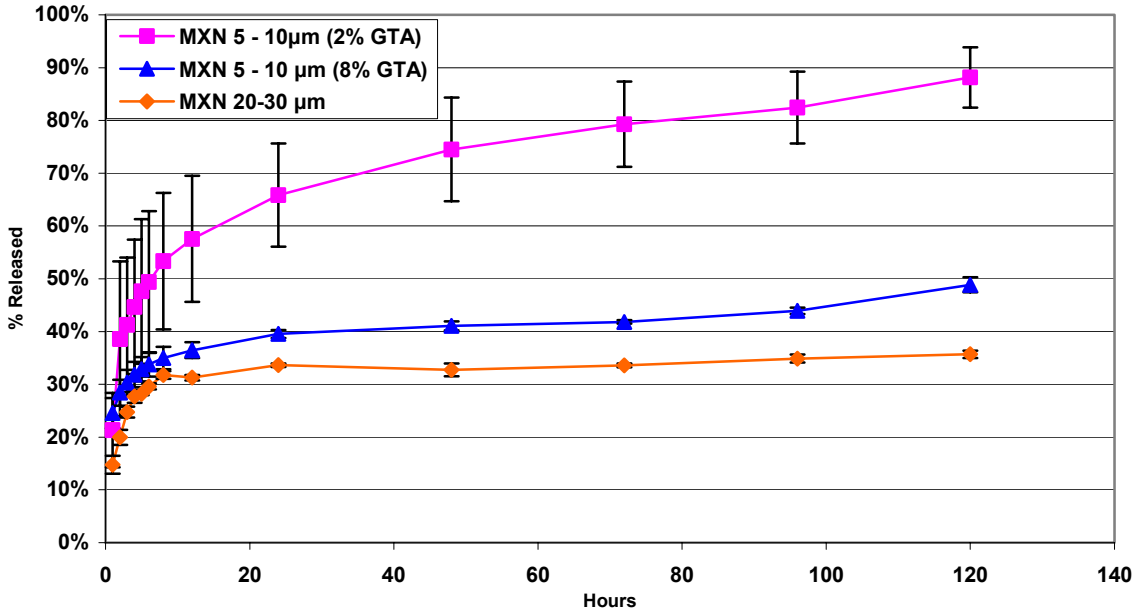

Figure 4-14 Cumulative percent of loaded MXN released from albumin microspheres over time in PBS pH 7.4 at 37ºC under infinite sink conditions.

loaded into and released from albumin microspheres using the synthesis protocol developed by Hadba. Microspheres were prepared with three different crosslink densities corresponding to 2, 4, and 8% (w/w) GTA. The processing parameters used to prepare the 5-FU–loaded BSA microspheres are found in Tables 3-3 and 3-4.

4.2.1 5-FU–Loaded Microsphere Morphology and Particle Size

Each sample of 5-FU–loaded microspheres was characterized. Particle morphology and topology were observed using SEM, and particle-size distributions were measured using the Coulter LS 230. Particle-size data, as calculated by the Beckman Coulter particle characterization software, is summarized data for each sample in Table 4-11. A typical SEM micrograph and the particle-size distributions for each crosslink density are shown in Figures 4-15 through 4-20.

SEM micrographs reveal that, in general, smooth spherical microspheres are produced using this synthesis technique. The 2% GTA lower crosslink density samples

had more debris associated with them. Additionally, the 2% GTA microspheres frequently exhibited a distorted spherical morphology. This appears to result from smaller microspheres impacting the larger microspheres during the crosslinking step of the synthesis. The relatively low crosslink density is not sufficient to prevent these impacts from distorting the shape of the resulting microsphere. Such distorted microspheres are readily seen in Figure 4-15 associated with what are presumable the smaller impacting microspheres embedded into the larger microspheres. Distorted morphology is less frequently seen in the 4 and 8% GTA microspheres, presumably due to the increased stability imparted by their higher crosslink density.

Some interesting observations were made regarding the particle-size distributions of the microspheres produced in this experiment. It was assumed prior to performing this study that the effect of the mixer used to form the emulsion would have a minimal effect on particle size and size distribution. However, it is readily apparent from examination of the particle-size distribution curves shown in Figures 4-16, 4-18, and 4-20 that this was not the case. The mean diameter and the ratio of the mean to the median diameters, which is representative of the symmetry of the distribution, were analyzed statistically. A one-way ANOVA found no statistically significant difference in either response variable between the samples.

Although it was not planned *a priori*, the data were also analyzed to test the significance of the mixer used in the microsphere preparation. A two-way ANOVA was performed, using the GLM ANOVA procedure since the data were unbalanced, on both the median diameter and the mean to median diameter ratio with percent GTA and mixer as independent factors. It was found that the mixer used to prepare the samples did

significantly affect both the median diameter and the mean to median diameter ratio of the microspheres produced ($p < 0.001$ and $p = 0.005$, respectively). The percent GTA used in the synthesis did not significantly affect either the mean diameter or the mean to median diameter ratio ($p = 0.283$ and $p = 0.364$, respectively). It was found that the Caframo mixer produced smaller microspheres with a less symmetrical particle size distribution than the Lightnin' mixer.

The distribution of all of the microsphere samples was bimodal. However, inspection of the distribution curves shows that the samples prepared using the Caframo mixer had a more pronounced bimodal distribution. These differences presumable result from the differences in the shear fields produced by the two mixers. It is unclear at this time if the differences in shear fields result from differences in the mixers themselves or subtle variations in the stir rods used with them. Further studies specifically designed to clarify these effects of miser and mixer blade should be performed in the future.

Table 4-11 Particle-size distribution statistics for the 5-FU–loaded BSA microspheres synthesized in these studies.

Sample ID	Mean diameter (μm)	S. D. (μm)	Median diameter (μm)	Mean / median ratio	90th percentile (μm)	10th percentile (μm)	Mixer used
2% - 1	15.26	13.24	15.04	1.014	1.124	27.73	Lightnin'
2% - 2	19.65	24.43	17.12	1.148	1.216	32.54	Lightnin'
2% - 3	11.10	20.17	6.548	1.695	0.837	21.09	Caframo
4% - 1	6.05	9.816	3.468	1.743	0.791	11.36	Caframo
4% - 2	5.04	4.023	4.119	1.223	0.784	10.97	Caframo
4% - 3	15.20	9.364	16.72	0.909	1.366	26.89	Lightnin'
8% - 1	14.41	9.637	15.72	0.917	1.165	26.80	Lightnin'
8% - 2	13.43	8.847	14.80	0.907	1.142	24.66	Lightnin'
8% - 3	4.05	3.339	2.842	1.426	0.747	9.129	Caframo

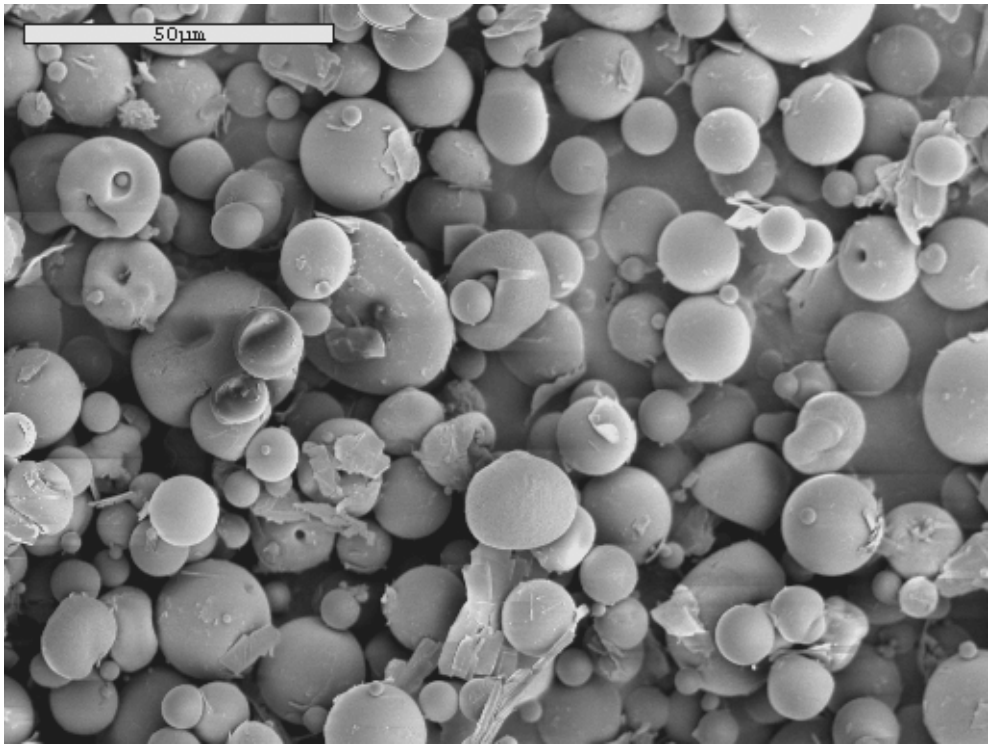

Figure 4-15 5-FU–loaded BSA microspheres crosslinked with 2% GTA SEM micrograph. (sample 2%-1, 750X)

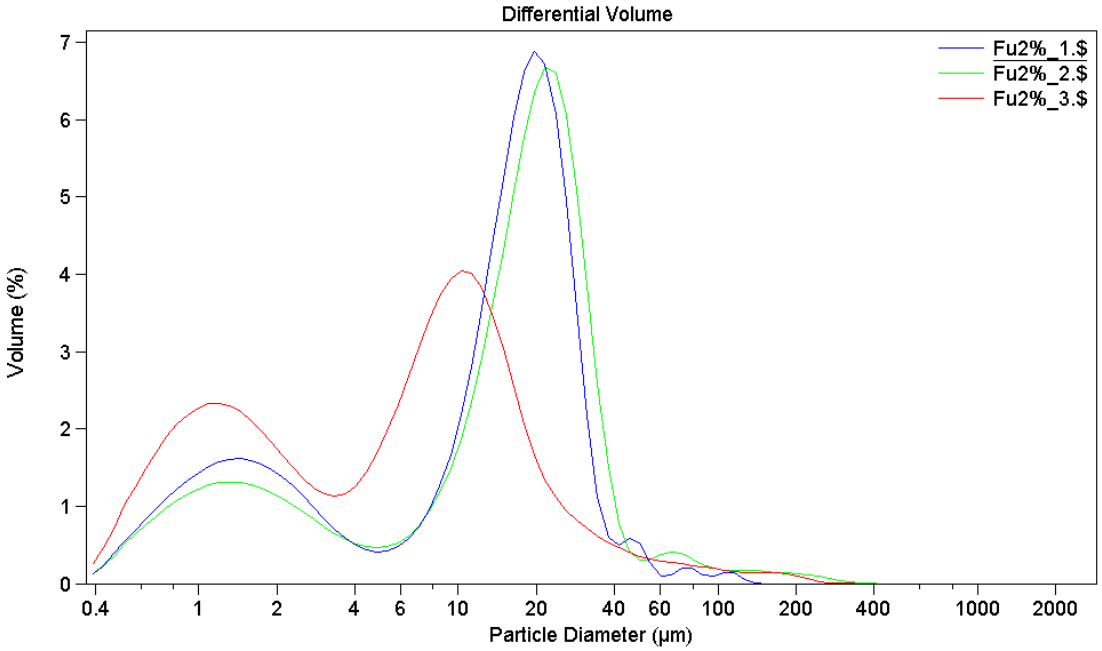

Figure 4-16 Particle-size distribution for 5-FU–loaded BSA microspheres crosslinked with 2% GTA.

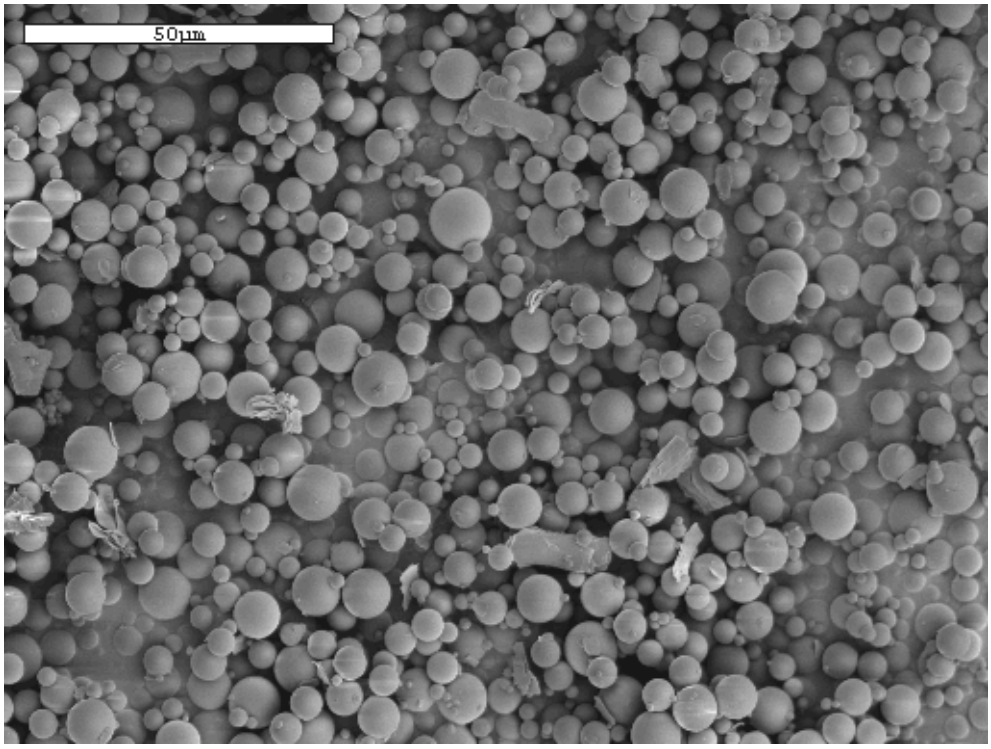

Figure 4-17 5-FU–loaded BSA microspheres crosslinked with 4% GTA SEM micrograph. (sample 4%-2, 750X).

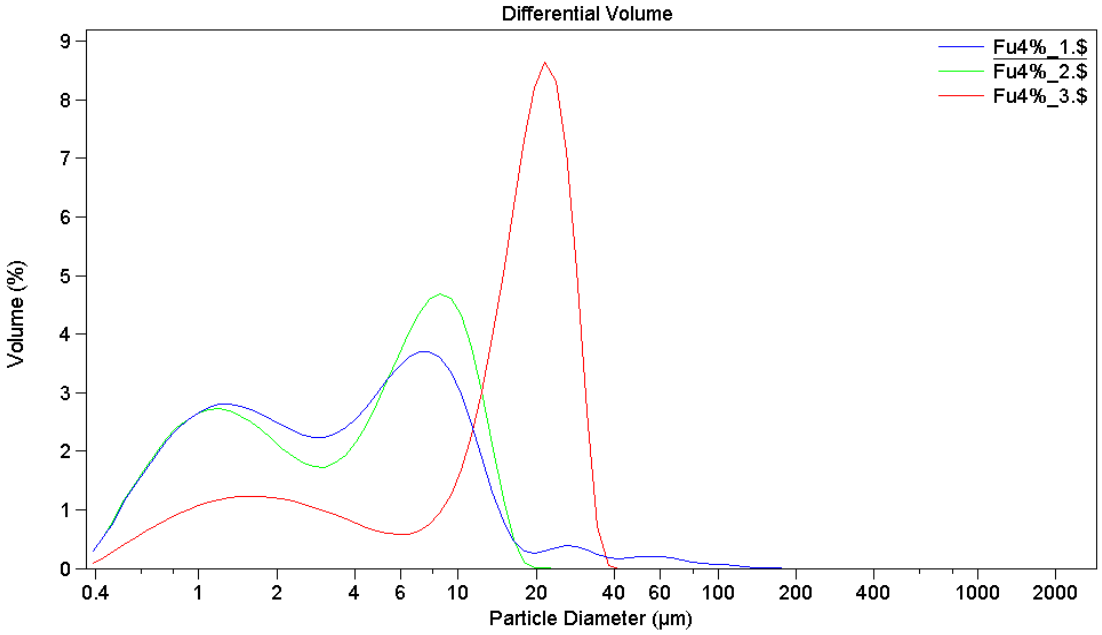

Figure 4-18 Particle-size distribution for 5-FU–loaded BSA microspheres crosslinked with 4% GTA.

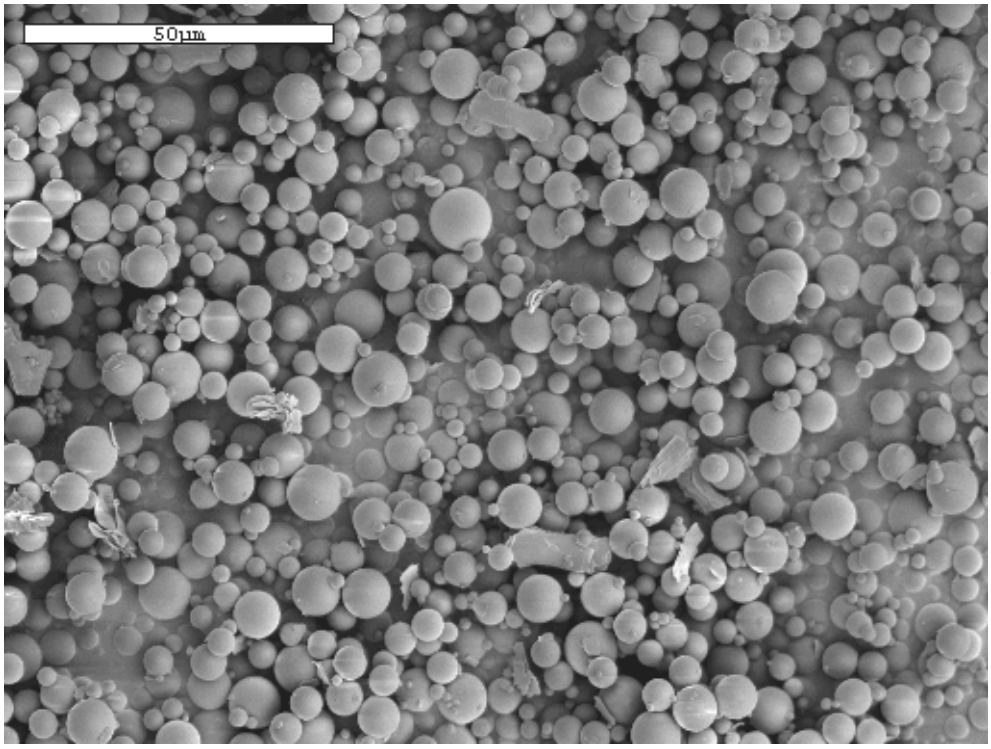

Figure 4-19 5-FU–loaded BSA microspheres crosslinked with 4% GTA SEM micrograph. (sample 8%-1, 750X)

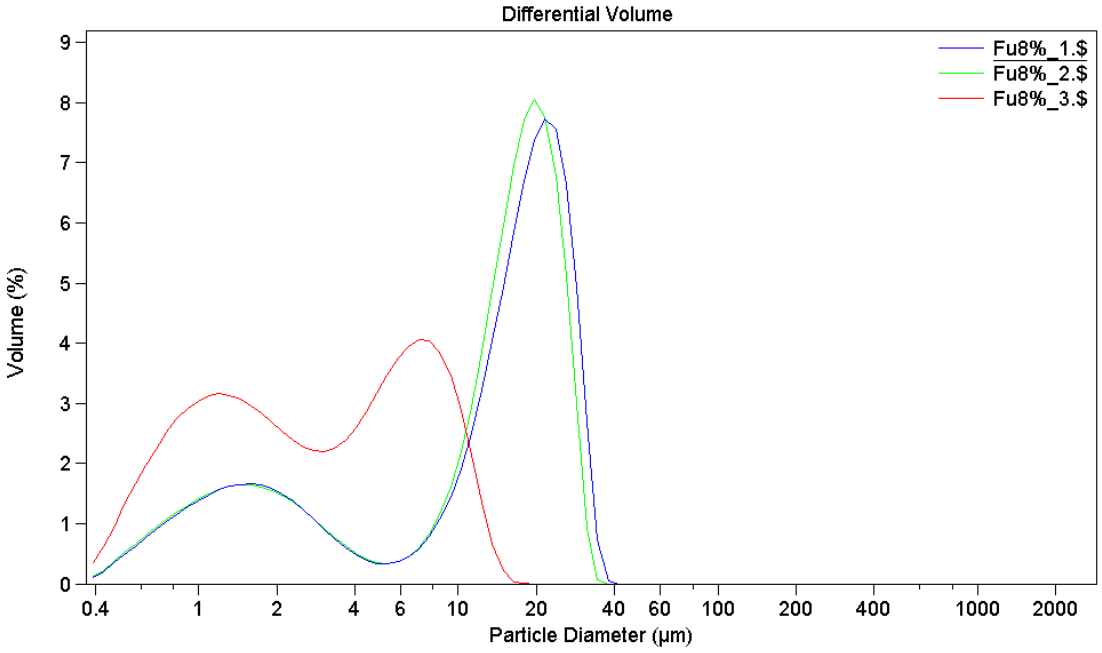

Figure 4-20 Particle-size distribution for 5-FU–loaded BSA microspheres crosslinked with 8% GTA.

4.2.2 5-FU–Loaded Microsphere *In Vitro* Release

The release of 5-FU from the loaded microspheres was also measured *in vitr*o in PBS (0.5mM, pH 7.4) at 37ºC. The release curves for each crosslink density are shown in Figure 4-22. It is readily apparent that the majority of albumin microsphere-loaded 5-FU drug is released within the first hour in this infinite sink system. The amount of additional drug released between the 24 and 120 hour time points decreased with increasing crosslink density (% GTA), although all three formulations continued to release small amounts of 5-FU.

The initial rapid release of 5-FU from the microspheres is probably due to several factors. The low molecular weight of 5-FU facilitates the diffusion through the protein matrix of the microsphere. Probably more important is the relatively low protein binding affinity of 5-FU, which is approximately 10% compared to 78% for MXN. The strong van der Waals bonding of a drug to the protein matrix may slow the release of a drug from the matrix because equilibrium is developed between the bound and free drug in the local microenvironment of the microsphere and surrounding tissues. This equilibrium will decrease the concentration of drug that is free to diffuse out of the microsphere, thereby lowering the concentration gradient of free drug between the microenvironments inside the microsphere and adjacent to it. Fick's first law of diffusion (Figure 4-21) shows the diffusive flux across a surface is directly proportional to the concentration gradient of the freely diffusing species.[71, 109, 110] Thus by decreasing the concentration of

$$J = -D \frac{\delta C_{drug}}{\delta x}$$

Figure 4-21 Fick's first law of diffusion. J = flux across a surface, C = concentration, x = distance, D = intrinsic diffusivity (or diffusion coefficient).

the free drug within the protein matrix of the microsphere, the flux of drug from the microsphere is also decreased when the drug has a high degree of protein binding. Conversely, a drug with a low degree of protein binding will have a relatively high concentration of free drug within the matrix, and therefore a high concentration gradient will exist across the surface drive the rapid flux of drug from the microsphere.

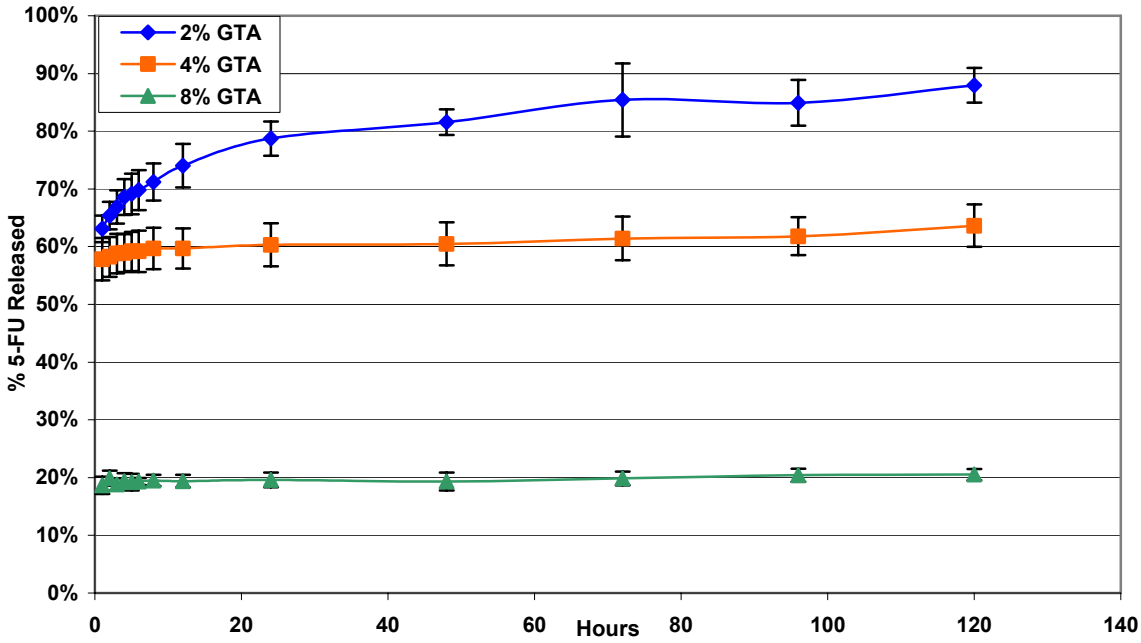

Figure 4-22 Cumulative percent of loaded 5-FU released from albumin microspheres over time in PBS pH 7.4 at 37ºC under infinite sink conditions.

CHAPTER 5
RESULTS AND DISCUSSION OF *IN VIVO* EXPERIMENTS

5.1 Tumor Growth Characteristics of 16/C MAC Model

The 16/C MAC tumor model is a fast growing tumor model. Data from 66 nontreatment, Tsaline, and microsphere control animals have been combined to determine the growth characteristics of the tumor line as used in these *in vivo* studies. The tumor weights, normalized by dividing by the tumor weight at the time of randomization (NTW), for the tumor line was determined and plotted against time measured in days after the tumor reached 10 mm in longest dimension (the day of randomization, Day 0). The tumor growth data are shown in Figure 5-23. Data beyond Day 5 are not presented because the animals with the fastest growing tumors reached a tumor weight estimated to be 10% of the body weight at that time and were sacrificed. The loss of the data from these animals would unfairly bias any attempt to continue the curve past Day 5.

An exponential equation was fitted to the tumor growth data, which produced a correlation coefficient (R^2) greater than 0.605. Based on this equation, the approximate doubling time (NTW = 2) for the tumor model is 3 days. This falls within the range of 2 to 3 days cited by Corbett in the original description of the tumor line.[106] The average tumor weight at the time of treatment, when the tumor reached 10 mm in its longest dimension, was 0.37 ± 0.07 g for these 66 mice in control treatment groups. It should be noted that a perfectly spherical tumor with a diameter of 10 mm would have an estimated weight of 0.50 g.

Histological examination of 16/C MAC specimens reveals characteristics of a high grade adenocarcinoma. Typical high and low power photomicrographs are shown in Figure 5-24. The tissue is composed of poorly organized basophilic cells (dark purple regions) with regions of coagulation necrosis (light pink regions). The viable(dark purple) cellular areas contain a high number of mitotic figures. The viable cells are arranged in a poorly defined glandular structure separated by fibrovascular stroma. On average, 115 mitotic figures are visible per 10 high power fields. This high percentage of dividing cells is characteristic of fast growing, high-grade tumors. Therefore the tumor histology corresponds with the published data on the 16/C MAC, a high grade, rapidly growing adenocarcinoma.

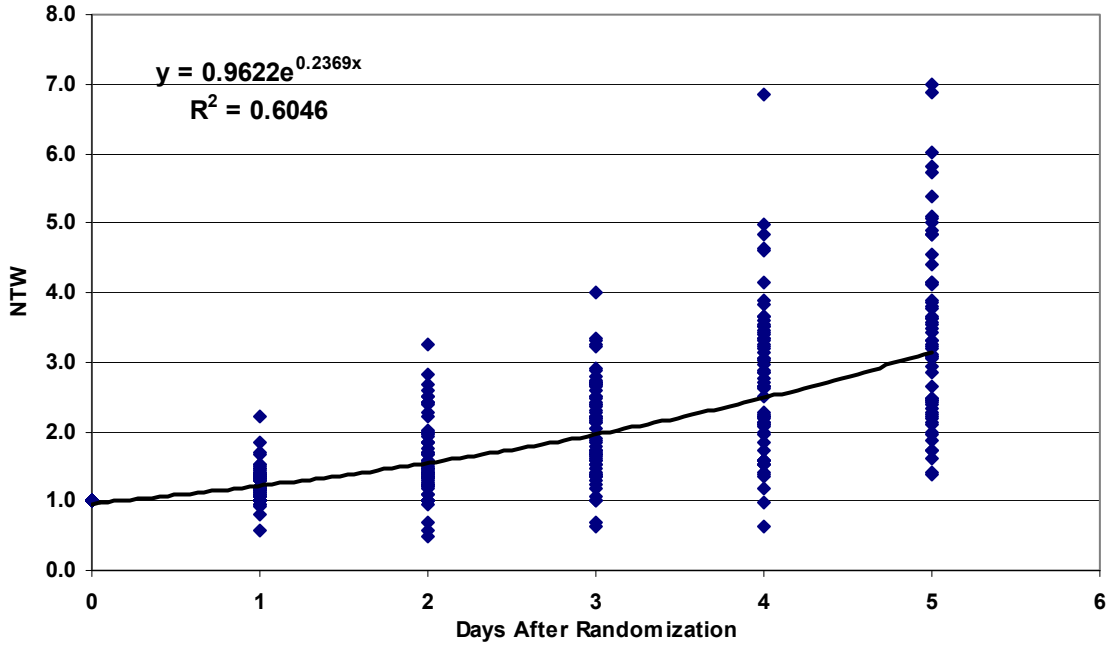

Figure 5-23 Average normalized tumor weight (NTW) for the 16/C MAC tumor model. Mice were randomized to control groups on Day 0 when their tumors reached 10 mm in the longest dimension. The line is the best-fit curve for the data, which produced a coefficient of determination (R2) = 0.6046. Each ♦ represtents a single time point for one of the 66 mice included in this analysis of nontreated tumors. The approximate doubling time for the 16/C MAC tumor model implanted subcutaneously is 3 days, based on the best-fit curve.

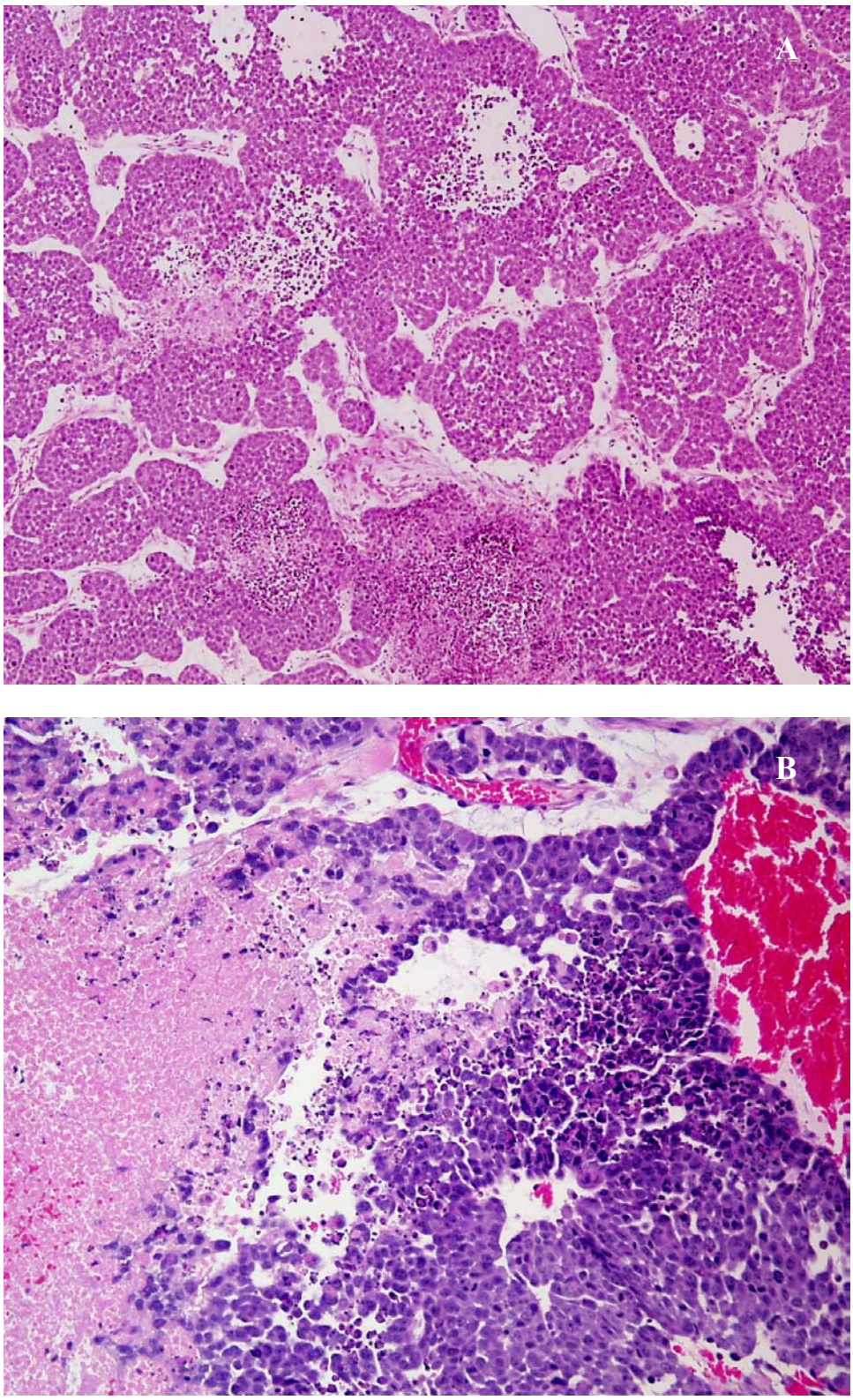

Figure 5-24 Photomicrographs of normal 16/C MAC histology at low and high power.
A) Note the poorly defined glandular structure in the low power image.
B) A large number of mitotic figures are visible in the higher power image.

5.2 IV Compared to IT Neoadjuvant Chemotherapy with F-MXN

5.2.1 Introduction

This study was performed as a baseline comparison of IT chemotherapy with systemic IV chemotherapy. Systemic chemotherapy is the clinical standard for the chemotherapeutic treatment of breast cancer and most other neoplasms. It is therefore necessary to be able to compare alternative treatments to IV chemotherapy. This study was designed with the specific aim of demonstrating the superior efficacy of IT chemotherapy using free MXN (F-MXN) to systemically administered F- MXN. Once this was established, other studies involving micro- or mesosphere delivered MXN (MS-MXN) could be compared to IT free MXN. If they had superior efficacy, then their superiority to IV free MXN could be inferred.

The comparison of IV to IT F-MXN study was designed to test the efficacy of F-MXN alone and as neoadjuvant chemotherapy (in combination with surgery after the chemotherapy treatment). The doses used in this study were 4 and 8 mg/kg of F-MXN calculated based on an average mouse weight of 20 g. A flow chart of the treatment groups and group codes for this study can be found in Figure 3-5.

5.2.2 Body Weight

The change in body weights for the mice in this study were used as an empirical measure of toxicity for the chemotherapy treatments. The normalized tumor adjusted body weight (NTABW) was used as the measure of body weight change. The NTABW for Day n was found by subtracting the weight of the tumor from the body weight (to find the tumor adjusted body weight) and dividing by the tumor adjusted body weight on the day of treatment (Day 0). This NTABW was then used for the statistical comparison of all groups on Day 5 and the IV4, IT4, and IT8 groups on Day 10. The control and IV8

groups were not included in the Day 10 analysis because an insufficient number of animals in these groups survived to Day 10 to provide unbiased data. The average NTABW for each treatment group through Day 10 is shown in Figure 5-25.

Statistical analysis of the NTABW data shows that the IV8 treatment had significantly lower NTABW's on Day 5 than all of the other treatments (one-way ANOVA, $p < 0.001$; Tukey's MCT, family error rate < 0.05). A two-way analysis of the MXN treated groups on Day 5 reveals that both the treatment dose and modality were significant independent factors in determining the NTABW (GLM ANOVA, $p < 0.001$ for dose, $p = 0.001$ for modality, $p = 0.365$ for the interaction). Analysis of the three groups with a significant number of surviving animals on Day 10 shows that the IV4 treated mice had a significantly lower NTABW than the IT4 mice (one-way ANOVA, $p = 0.029$; Tukey's MCT, family error rate < 0.05). There was not a significant difference between the two dose levels of the IT treatments on Day 10.

All of the MXN treatments except for the 8 mg/kg dose given systemically (IV) were well tolerated having on average less than 5% tumor adjusted body weight losses at all time points through Day 10. Inspection of the data reveals that the IV8 treatment was clearly toxic and the dose was above the LD_{50} for mice. It is important to note for future studies that the MXN toxicity was manifested within 10 days of treatment. Furthermore, the equivalent dose had no significant toxicity when delivered IT. This demonstrates that there is significantly less systemic toxicity associated with IT chemotherapy compared to conventional systemic chemotherapy. However, the maximum tolerated dose of MXN that can be delivered with minimal resulting toxicity cannot be determined based on this study.

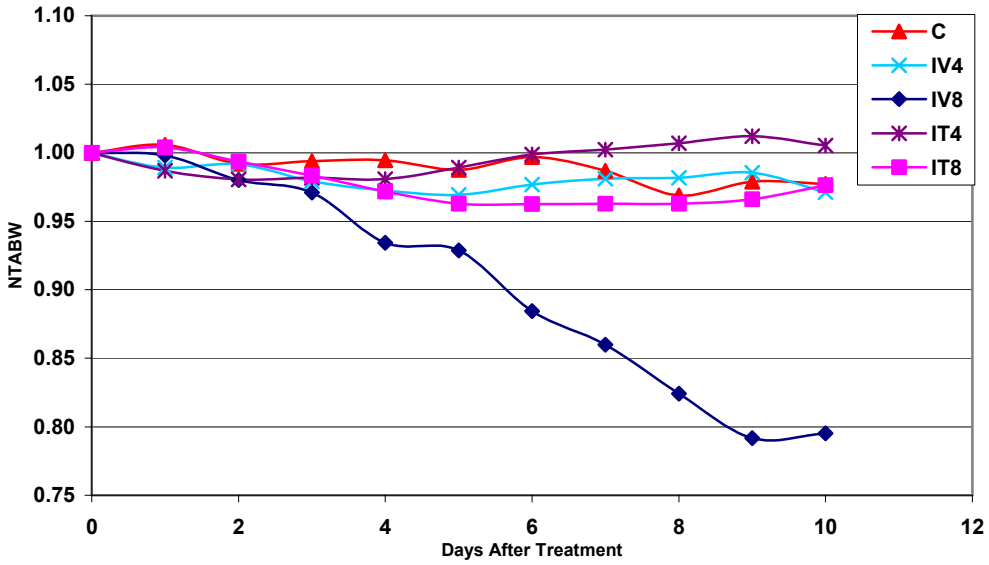

Figure 5-25 Average normalized tumor-adjusted body weight (NTABW) for the IV vs IT F-MXN study. Tumor weight is normalized to the weight at the start of treatment. (n = 19 for control; 25 for IV4, 24 for IV8, 24 for IT4; and 28 for IT8)

5.2.3 Tumor Growth

The weight of the tumors was estimated based on the tumor dimensions and monitored at least every other day. The weight of each tumor was normalized to the weight of the tumor at the initiation of treatment (normalized tumor weight (NTW) = weight on Day n /weight on Day 0). The average NTW for each treatment group five and ten days after treatment on Day 0 is shown in Figure 5-26. The NTW data for each treatment group was compared on Day 5. Additionally, the NTW data for the IV4, IT4, and IT8 treatment groups were compared on Day 10. An insufficient number of IV8 and control mice survived to Day 10 to allow an unbiased evaluation of their tumor growth. There was a statistical difference in the NTW between treatments five days after treatment (one-way ANOVA, $p < 0.001$). Multiple comparisons revealed that all MXN treatments had significantly less tumor growth than controls on Day 5 and both IT treatments were produced a greater inhibition of tumor growth than the IV4 treatment

(Tukey's MCT, family error rate < 0.05). Additional statistical analysis showed that the inhibition of tumor growth was due to an interaction of both treatment dose and modality (GLM ANOVA, p = 0.0024 for the interaction). Analysis of the NTW on Day 10 showed that the superiority of the IT treatments persisted for at least 10 days compared to the IV4 group (one-way ANOVA, p < 0.001; Tukey's MCT, family error rate < 0.05).

Several insights can be found in tumor growth data from this study. First of all the IT injection of free MXN is clearly superior at inhibiting tumor growth compared to the IV treatments. The systemic (IV) dose had to be increased to toxic levels (8 mg/kg) in order to produce a similar level of growth inhibition. Additionally, what little inhibition of tumor growth was produced by the 4 mg/kg IV dose had clearly abated by Day 10. Thus it can be seen that following a single injection, systemic chemotherapy offers limited value in inhibiting tumor growth and that local intratumoral chemotherapy is required to achieve a significant prolonged reduction in tumor mass.

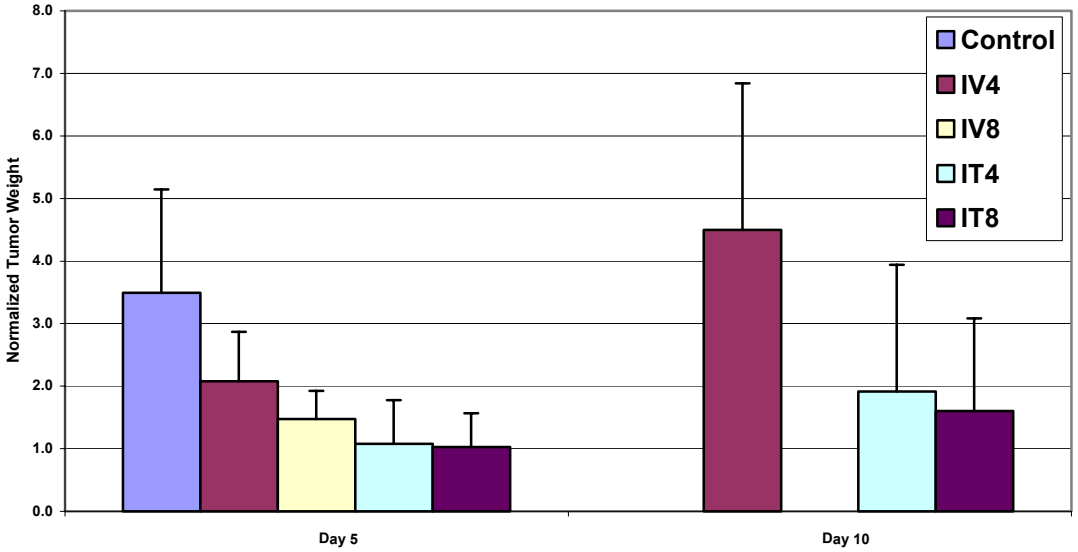

Figure 5-26 Average normalized tumor weight (NTW) for the IV vs IT F-MXN study. Doses of 4 or 8 mg/kg of F-MXN were injected either IT or IV on Day 0 and compared to nontreatment controls. (n = 19 for control; 25 for IV4, 24 for IV8, 24 for IT4; and 28 for IT8)

5.2.4 Histology

Upon necropsy samples of the tumor and liver tissues were obtained from each animal in this study for histological evaluation. Each specimen was fixed in 10% neutral buffered formalin and stained with H&E after sectioning. The tumor sections were evaluated for evidence of treatment effect of the MXN, and the liver sections for evidence of toxicity. Only a representative sample of each treatment group containing animals that experience both little and significant (> 10%) changes in the TABW were inspected.

Each of the tumor sections inspected was evaluated for degree of necrosis, number of mitotic figures per high power field (HPF), and the number of individually necrotic cells per HPF. The overall degree of necrosis present in each tumor was rated by a certified pathologist (Dr. Detrisac) on an ordinal scale from 1 to 4 (with 1 ≤ 25%, 2 = 26-50%, 3 = 51-75%, and 4 ≥75% necrosis). The median degree of necrosis and mean number of individual necrotic and mitotic cells visible per HPF for each treatment group are shown in Figure 5-27. Based on these graphs, there appears to be an increase in the amount of necrosis present in the 8 mg/kg treated animals. However, statistical significance cannot be established because the animals were euthanized at different time points (ranging from 8 to 23 days) and for different reasons (body weight loss or tumor growth).

The examination of the liver specimens revealed minimal signs of toxicity. Changes consistent with occasional foci of extramedulary hematopoesis, mononuclear minimal hepatitis, and fatty change or glycogen storage of the hepatocytes were noted in scattered animals with no apparent association to treatment group or the presence of significant body weight loss. Typical micrographs are shown in Figure 5-28.

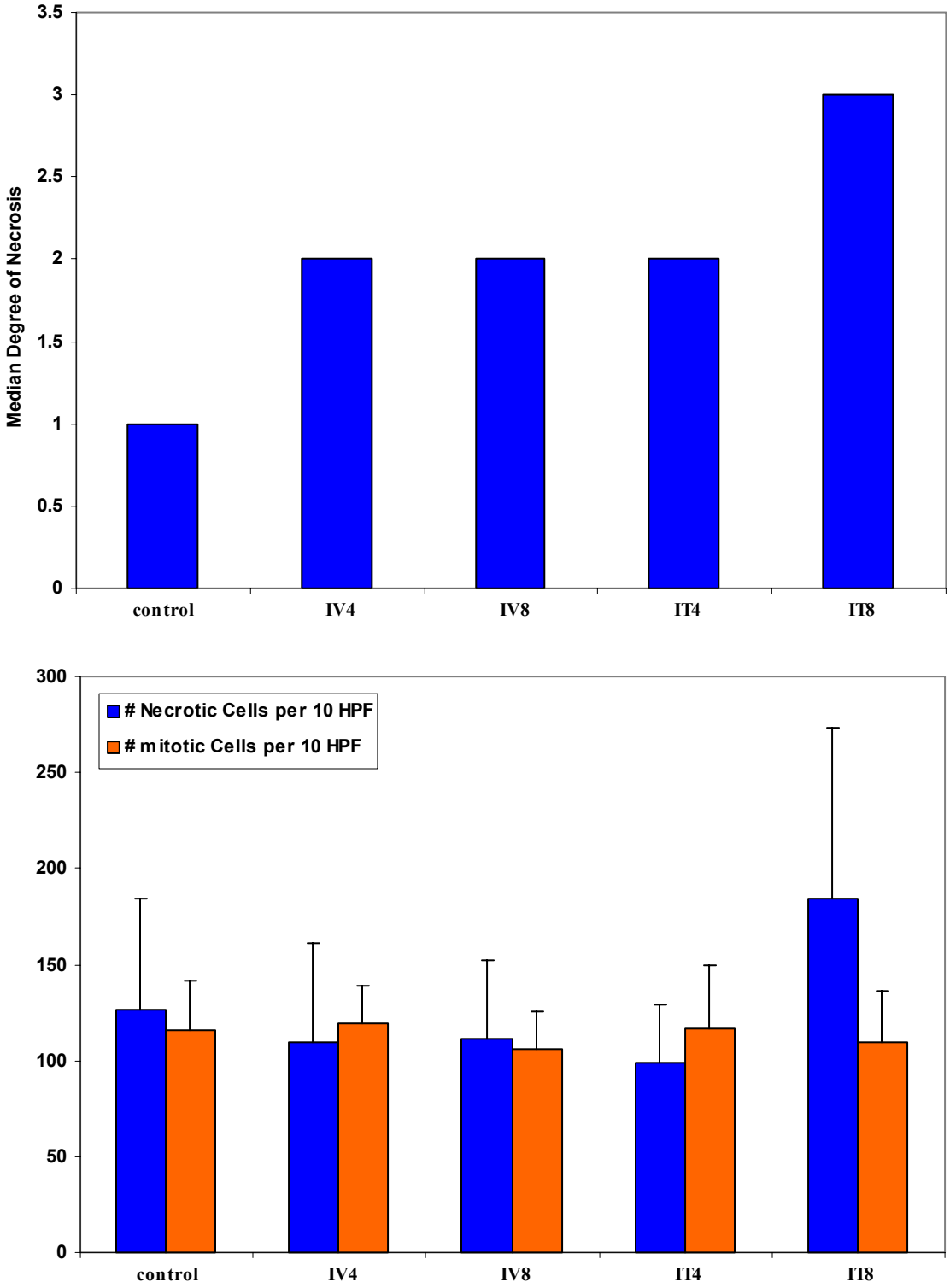

Figure 5-27 The median degree of necrosis and mean number of individual necrotic and mitotic cells visible per 10 HPF. Mice were treated with either 4 or 8 mg/kg of F-MXN delivered either IT or IV. Control animals did not receive any treatment.

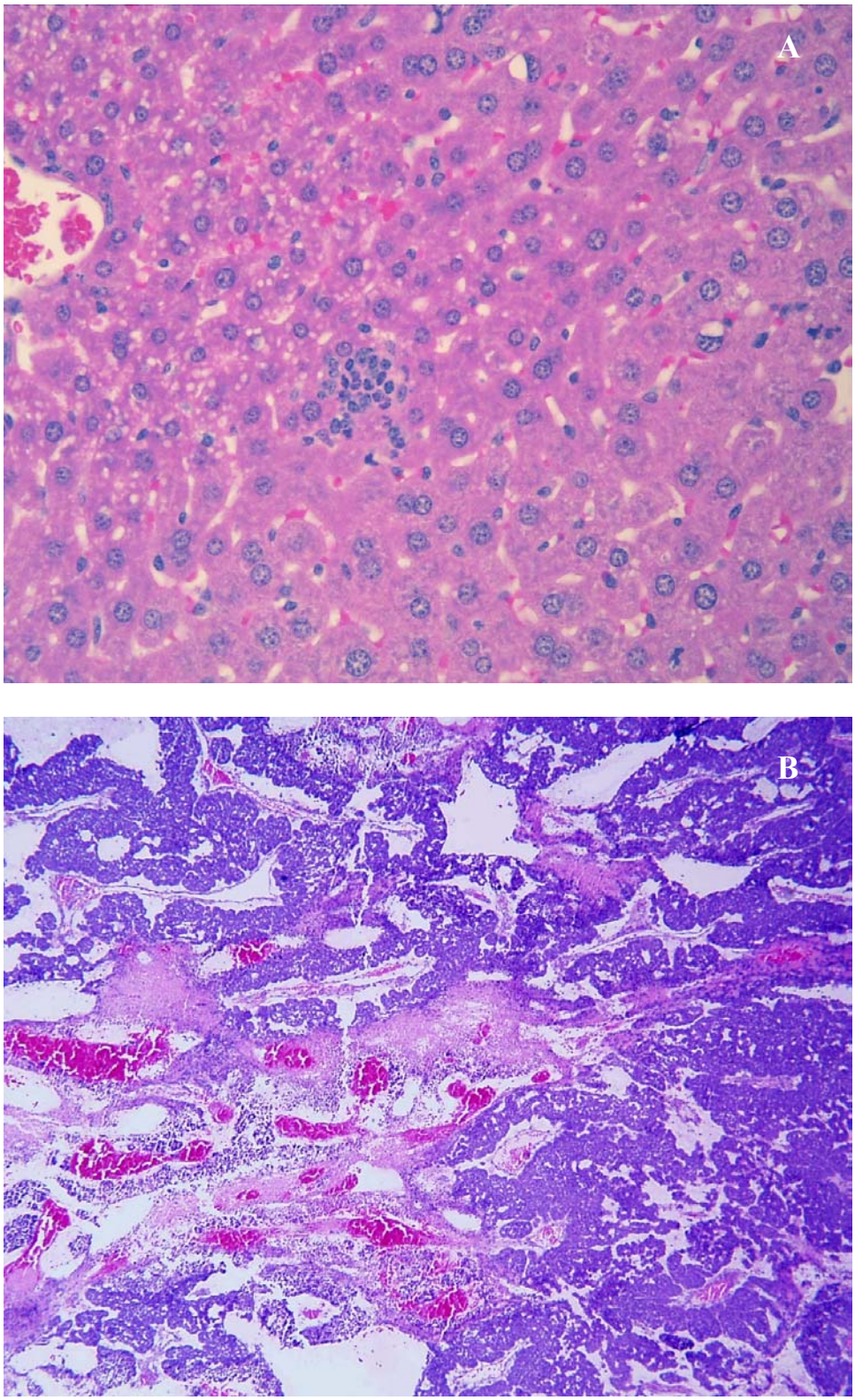

Figure 5-28 Micrographs of typical liver and tumor tissues. A) Moderate fatty change or glycogen accumulation with a small focus of extramedulary hematopoesis. B) Low power image of necrotic (pink) and viable regions (blue) of tumor.

5.2.5 Survival

Survival was deemed to be the most important response variable for this study. The unmodified survival curves for all treatment groups are shown in Figure 5-29. Survival plots were also prepared for subsets of the treatment groups in order to aid in the interpretation of the data. Figure 5-30 shows the survival curves for all nonsurgical treatment groups. Figure 5-31 shows the survival after surgery (not from the day of treatment in as in the other survival graphs) for the surgical treatment groups (modified to exclude animals that died prior to surgery on Day 10). Figures 5-32 and 5-33 show subsets of the survival curves for each treatment dose (4 or 8 mg/kg) (also modified to exclude animals randomized to receive surgery, but died prior to surgery; except for group IV8-S10 for which only 2 animals survived to receive surgery).

Nonparametric statistical analysis of the Kaplan-Meyer survival curves (right censored for survival at the end of the study, Day 60) was performed using the log-rank statistical test. Only the data for the animals surviving to receive surgery were included in the analysis of neoadjuvant treatment groups, except for those in the IV8-S10 treatment group for which only 2 animals survived to surgery. This treatment was clearly toxic and the data was included for completeness only. The comparison of all treatment groups was highly significant ($p < 0.0001$), so pairwise comparisons were performed of each combination of treatments. The significance level was set at $p < 0.05$ with no adjustment made for the performance of multiple comparisons.

The most effective treatment based on survival was IT4-S10, which was statistically superior to all treatment groups except for IT8-S10 and IT 8 (for which it almost achieved significance, $p = 0.0649$). The next most efficacious treatment was IT8-S10, which was statistically superior to all other treatments except for IT4-S10, IT8

and C-S5 (for which p = 0.0723). The IT8 treatment was superior to the IV4, IV8, IV8-S10, and control treatments. The IT4 treatment was superior to the IV8 and nontreated control treatments, and achieved a p = 0.0711 when compared to IV8-S10. The IV4-S10 treatment was superior to IV4, IV8, and nontreated control, with a p = 0.0726 when compared to IV8-S10. The IV4 group was superior only to the nontreated controls. It was interesting to note that the mice that received surgery only (C-S5) had a significantly better survival than the IV4, IV8, IV8-S10, and nontreated control groups. The survival outcomes for this study are summarized in Table 5-12.

It is readily apparent when comparing the survival curves that IT treated mice had a better survival than the mice treated with the conventional systemic (IV) chemotherapy. The median day of death for the most efficacious IV treatment group (4 mg/kg IV F-MXN) was Day 11, whereas the median survival for the least efficacious IT treatment group (4 mg/kg IT F-MXN) was 16 days. Animals treated with the most efficacious IT treatment (8 mg/kg IT F-MXN) had twice the median survival time of the most efficacious IV treatment (22 vs. 11 days), and 25% of the mice in the IT group were cured of their tumor compared to 0% of the IV treated mice.

The combination of surgery with neoadjuvant IT chemotherapy produced the best results. Cures (survival past Day 60) were achieved in 45% (9 out of 20) of the mice treated with IT chemotherapy (at either dose level) and surgical excision of their tumor mass. Of the mice receiving 4 mg/kg IT F-MXN, 55% survived. Therefore a median survival time could not be calculated for this treatment group. The increase in median life span (ILS) compared to controls was for this treatment group (IT4-S10) was greater than 650%, while the ILS for the IT8-S10 group was 400% (median survival = 40 days).

The difference between the lower dose IT4-S10 and the IT8-S10 group may represent improvement in the surgeon's skill rather than a true difference in the treatments since the IT8-S10 mice received their surgeries before the IT4-S10 mice. It should be noted that most of the "cured" mice were observed for much longer times (>100 days) with no recurrence of their tumors. It is also significant that the animals treated with surgery only five days after randomization had better outcomes than those treated with conventional systemic (IV) chemotherapy only, even disregarding the clearly toxic 8 mg/kg IV dose.

The IT treatments were also better tolerated than the IV treatments. The 8 mg/kg dose was clearly toxic when given IV. However, it was well tolerated when given as an IT injection of F-MXN into the subcutaneous tumor. This is clear evidence that higher doses can be safely delivered by local IT injection with significantly less systemic toxicity than a similar dose delivered in the conventional IV manner. Further more, it is reasonable to believe that this higher local dose of MXN leads to increased tumor cell death and therefore improved treatment outcomes, specifically survival.

Table 5-12 Survival statistics for the treatment groups included in the IV vs. IT F-MXN study. Mice were treated with either 4 or 8 mg/kg either IT or IV of F-MXN on Day 0. Mice were also randomized to surgical or nonsurgical groups, with F-MXN treated mice receiving surgery 10 days after treatment and control animals receiving surgery 5 days after randomization.

Treatment	IV4	IV8	IT4	IT8	C	C-S5	IV4-S10	IV8-S10	IT4-S10	IT8-S10
# Randomized	12	12	12	16	19	12	12	12	12	12
# Surviving to surgery						12	6	2	11	9
Median survival [a]	11	9	16	22	8	21	28	8	**	40
ILS [b]	38%	13%	100%	175%	N/A	163%	250%	0%	> 650%	400%
% Cures [c]	0%	0%	8%	25%	0%	17%	0%	8%	55%	33%

[a] Time until reaching 50% survival after treatment (in days), only animals receiving surgery are included for the surgery groups.

[b] Percent increase in median lifespan after treatment compared to untreated control.

[c] Animals alive 60 days after treatment, only animals receiving surgery are included for the surgery groups (except IV8-S10).

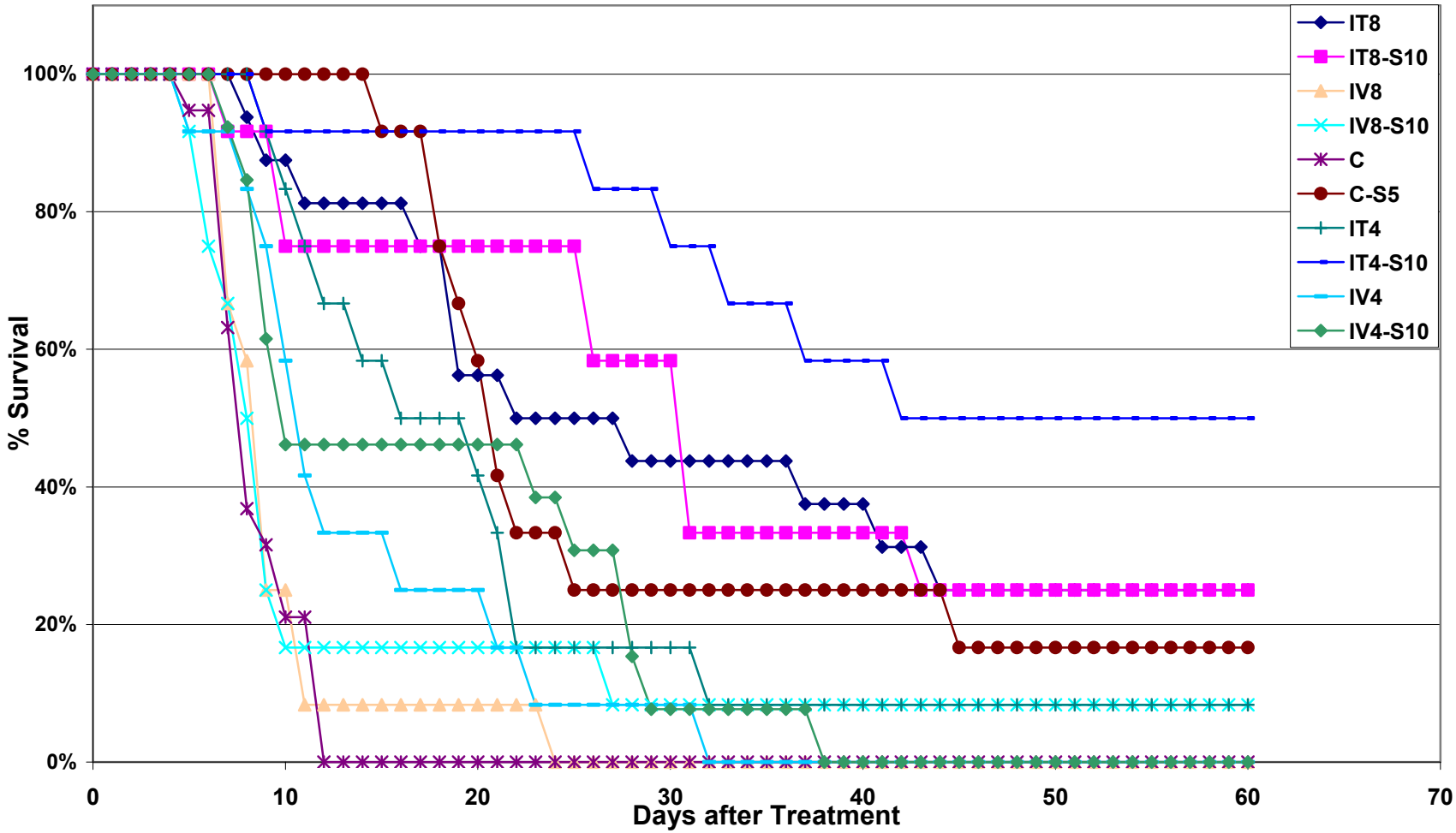

Figure 5-29 Survival graph for all treatment groups in the IV vs. IT F-MXN study. Survival time is measured from the time of treatment (injection) on Day 0.

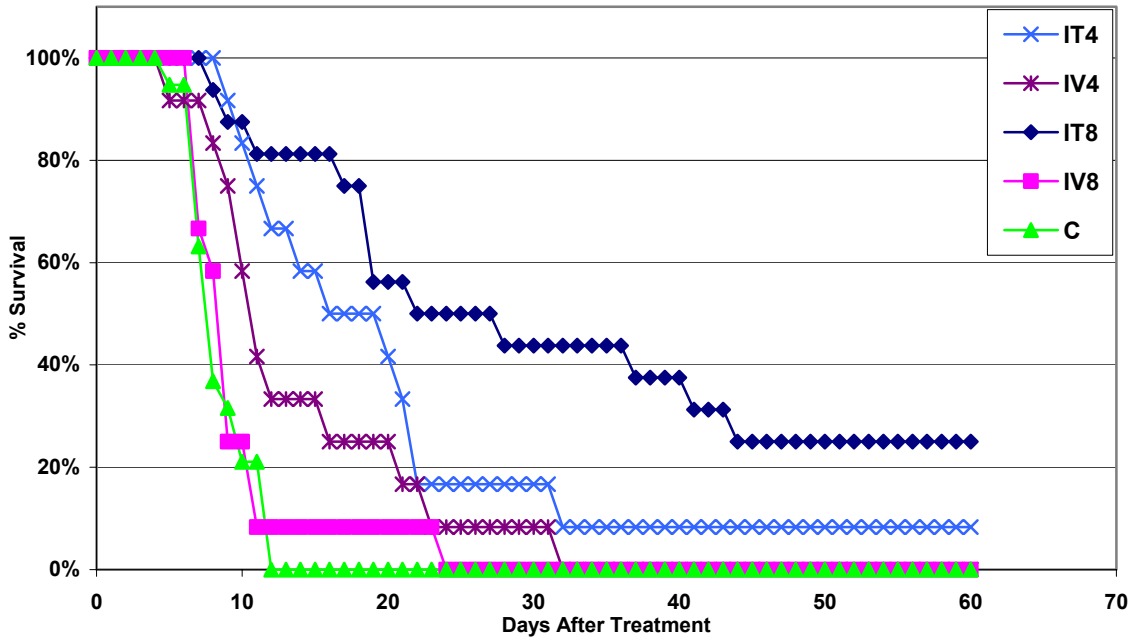

Figure 5-30 Survival graph for nonsurgical treatment groups in the IV vs. IT F-MXN study. Survival is from the time of treatment (injection) on Day 0.

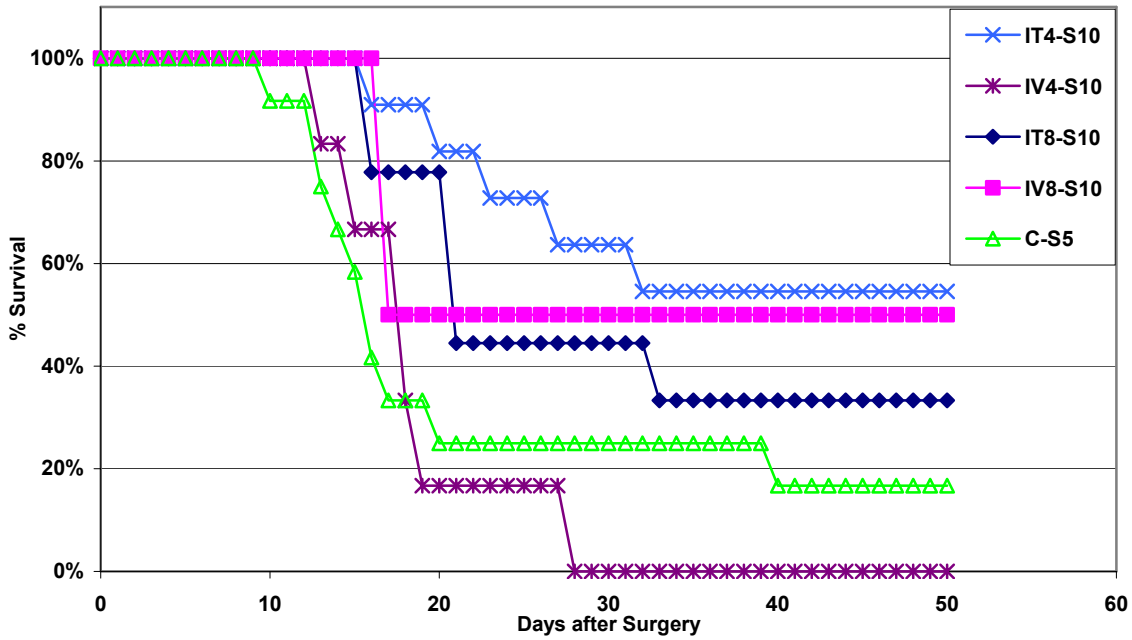

Figure 5-31 Survival graph for surgical treatment groups in the IV vs IT F-MXN study. Survival is from day of surgery. Animals that died prior to surgery have been omitted. Note only 2 animals in the IV8-S10 group survived to the day of surgery.

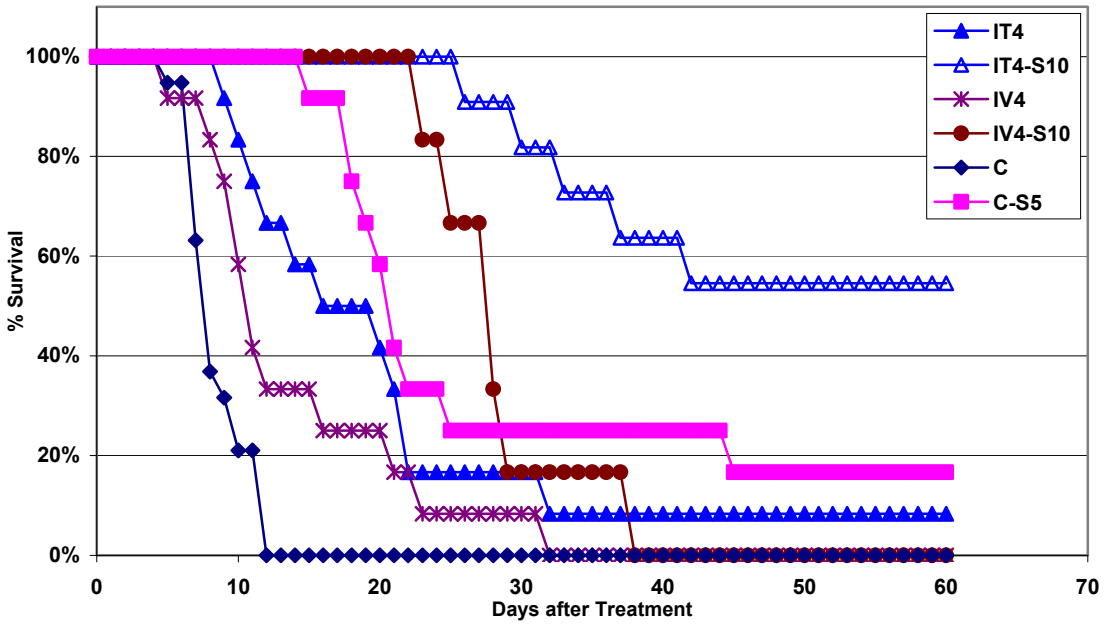

Figure 5-32 Survival graph for 4 mg/kg MXN treatment groups in the IV vs IT F-MXN study. Survival is from day of treatment (Day 0). Data for animals randomized to receive surgery that did not survive to the day of surgery have been omitted, except for IV8-S10 which has not been modified.

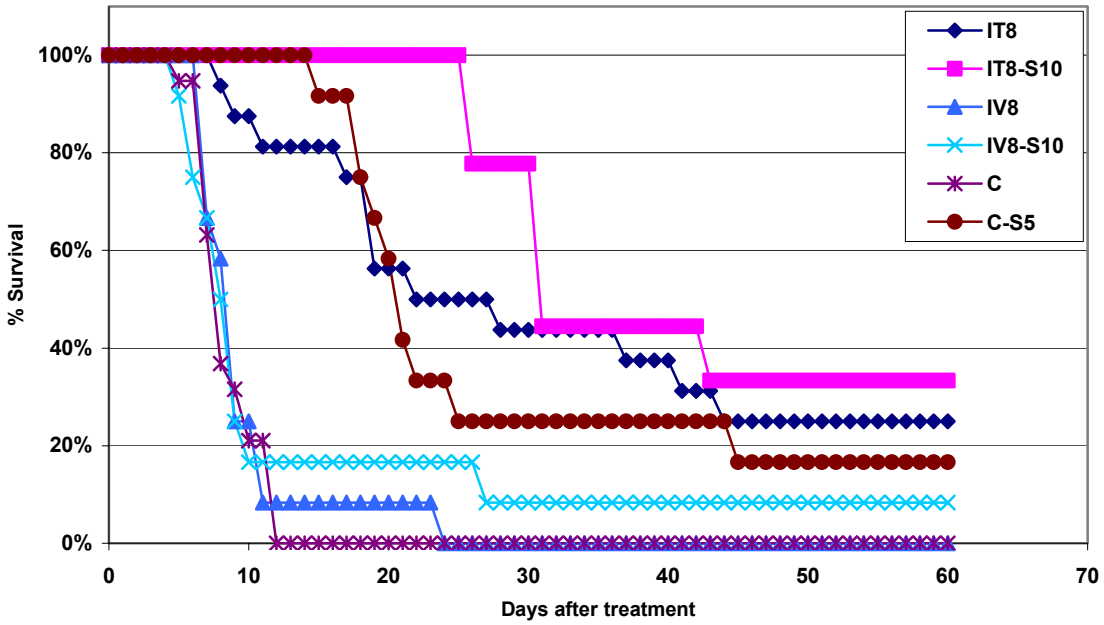

Figure 5-33 Survival graph for 8 mg/kg MXN treatment groups in the IV vs IT F-MXN study. Survival is from day of treatment (Day 0). Data for animals randomized to receive surgery that did not survive to the day of surgery have been omitted, except for IV8-S10 which has not been so modified.

5.3 Intratumoral Therapy with Free or 20 to 40 μm Microsphere-Loaded MXN

5.3.1 Introduction

This study was performed as a pilot study to determine the efficacy of MXN-loaded microspheres for the IT treatment of breast cancer and to identify suitable dose levels for future larger studies. All treatment groups consisted of a single IT treatment with either free or microsphere-loaded MXN. It was known when designing this study that the IT free MXN delivered at doses of 4 and 8 mg/kg were efficacious and produced little, if any, toxicity. However, it was not known how much the doses could be increased before significant toxicity would be clinically evident. It was also uncertain what dose levels could be safely delivered loaded into microspheres. Therefore, this study was initially conducted as a dose escalation study. Initial groups consisted of free drug delivered at 4, 8, 16, 24 mg/kg or microsphere-loaded drug delivered at 8, 16, or 24 mg/kg.

It quickly became apparent that MS-MXN was not efficacious at doses less than 24 mg/kg, and that the use of a surfactant in the microsphere delivery medium greatly enhanced the ease of administering the dose. Therefore, additional groups consisting of 24, 32, and 48 mg/kg doses of MS-MXN delivered in a 0.5% Tween 80 in normal saline solution, which was referred to as Tsaline, were added to the study. An appropriate control group receiving Tsaline was also added to the study. Data for this modified study are presented with the data for the original microsphere doses delivered in saline omitted. The complete results for these omitted groups was reported by Hadba.[9]

It requires noting that two mice were excluded from the analysis of this study. They were two control animals (one F0 and one M0) that experienced an inexplicable regression of their tumor after being enrolled in the study. In the several hundred animals

injected with the 16/C MAC tumor line in this laboratory, spontaneous regression has been observed in less than 1% of the animals. Therefore, these animals were considered outliers and unrepresentative of the normal, nontreated progression of this tumor.

5.3.2 Body Weight

Changes in body weight were used to assess the toxicity of the treatments. It was necessary to adjust the body weight for the estimated weight of the tumor. A tumor adjusted body weight loss of 20% was considered evidence of significant toxicity and the mouse was euthanized. The average tumor adjusted body weight data for each treatment group is presented in Figure 5-34.

Statistical comparisons of the NTABW data for each group were compared on Day 5. Significant differences were found between treatment groups on Day 5 (one way ANOVA, $p < 0.001$). The F24 treatment group suffered the greatest weight loss which was statistically greater than all other treatments except F16 and M48 (Tukey's MCT, family error < 0.05). The M48 had significantly lower NTABW than the control groups, F4, F8, and M32 treatments (Tukey's MCT, family error < 0.05). The F16 treatment also produced a greater weight loss than the F0 control group (Tukey's MCT, family error < 0.05). . The data was also compared on days 10 and 15 for the treatment groups that had a significant number of survivors at those time points (all except the control groups and F24). On Day 10 the F4 treatment group had significantly higher NTABW's than the F16 and M48 treatment groups (one-way ANOVA, $p = 0.025$, family error < 0.10, not significant at the family error < 0.05 level). Additionally there was a statistical difference detected by one-way ANOVA on Day 15 ($p = 0.047$), however no pairwise comparisons were statistically different (Tukey's MCT, no $p < 0.10$).

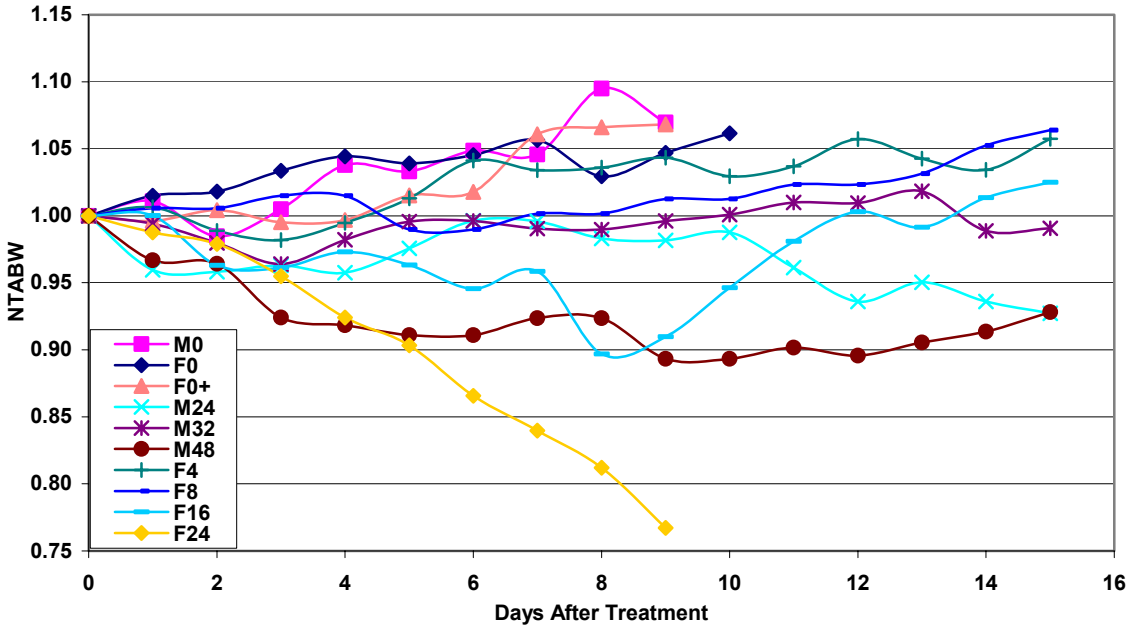

Figure 5-34 Average normalized tumor-adjusted body weight (NTABW) of mice treated with 20 to 40 μm MS-MXN or F-MXN.

Significant toxicity was seen in some of the treatment groups. All of the animals in the F24 group and 50% of the animals in the F16 group were euthanized for toxicity as evidenced by excessive body weight loss. The F8 group did not exhibit any significant weight loss. Based on this study, the maximum tolerated dose (MTD) for F-MXN was estimated to be between 8 and 16 mg/kg. The M48 treatment group experienced a statistically greater weight loss compared to the other treatment groups, except for F24. However, none of these mice were euthanized as a result of body weight loss, and all mice recovered from the short-term weight loss. This significant weight loss would suggest that 48 mg/kg of MS-MXN approaches the MTD for this formulation.

5.3.3 Tumor Growth

Data for tumor growth were examined on Days 5, 10, and 15. The tumor weight for each mouse was normalized by dividing it by each mouse's tumor weight at the time of treatment (NTW). This was done to control for variances in tumor weight at the

beginning of treatment. A NTW of 1.0 is equivalent to no tumor growth or regression. Average NTW for each treatment group on days 5, 10, and 15 is shown in Figure 5-35.

Treatment group was found to have a statistically significant effect on tumor growth (one-way ANOVA, $p < 0.001$) on Day 5. Tukey's multiple comparisons tests (family error, $p < 0.10$) of the data for Day 5 show that all of the MXN treatment groups are significantly different from the control groups, except for M24 and M0 which were not statistically different. The control groups were not included in the analysis of Days 10 and 15 since most of the control animals did not survive to these time points. There was no statistical difference found between the MXN treatment groups on Day 10 or 15 (one-way ANOVA). This was likely due to the large variance in tumor size within treatment groups with some animals' tumors having completely regressed to a non-measurable size while other "treatment failures" had begun to progress after a short treatment associated delay in growth. This heterogeneity in tumor sizes in evident in the dot plot of the data for Day 15 (Figure 5-36).

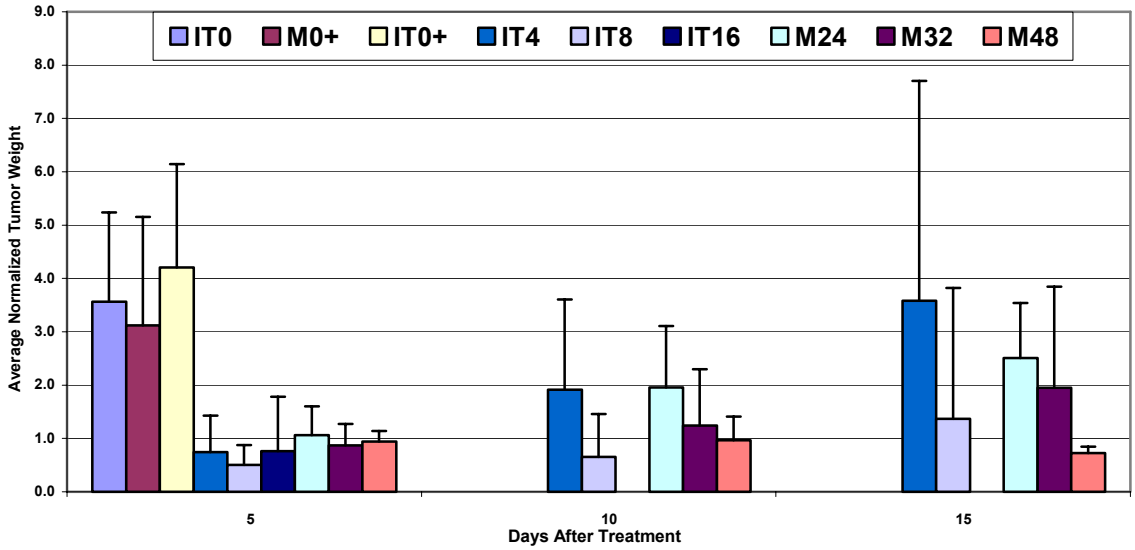

Figure 5-35 Average normalized tumor weight (NTW) of mice treated with 20 to 40 µm MS-MXN or F-MXN. A NTW = 1 represents no growth or regression.

5.3.4 Survival

It is readily apparent from examination of the nonparametric Kaplan-Meier survival graph (Figure 5-37) that the MXN treatments had a significant effect on survival (log rank, $p < 0.0001$). When multiple comparisons were performed, the MXN treatments were found to be statistically different from the control survival curves (log-rank, $p < 0.05$). However, few differences were found between the treatment groups, with only the M24 and M48 survival curves being statistically different (log-rank, $p = 0.0067$).

The survival plot suggests that MS-MXN is more efficacious than F-MXN in treating the breast adenocarcinoma tumor model by IT injection at the higher dose levels since all M48 animals survived at least 31 days after treatment compared to 16 days for the F8 treatment group. The use of microspheres allowed MXN to be delivered at dose levels at least three times higher than the MTD of F-MXN (48 mg/kg vs. 16 mg/kg).

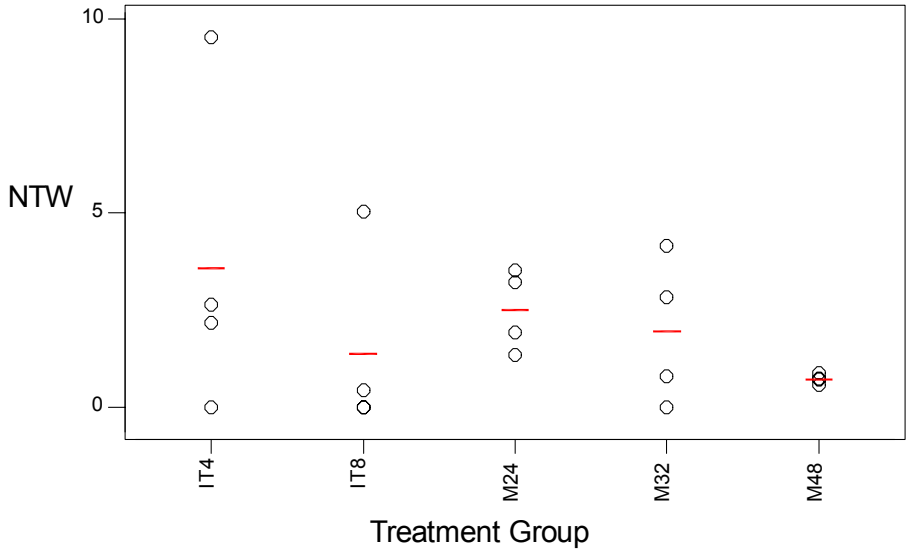

Figure 5-36 Dotplot of normalized tumor weights (NTW) for mice 15 days after IT treatment with 20 to 40 µm MS-MXN or F-MXN. Note the large variation in NTW present within most treatment groups.

Additionally, 50% of both the 8 mg/kg F-MXN and the 32 mg/kg MS-MXN groups showed complete tumor regression and were tumor free 60 days after treatment. Statistical analysis of the survival data was limited by the small group size. However, nonparametric Kaplan-Meier analysis of the data revealed that all intratumoral MXN treatment significantly improved survival compared to the control animals (log-rank test, $p < 0.05$). The small group sizes prevented the detection of a significant difference between MXN treatment groups, with only the M48 compared to M24 achieving significance ($p = 0.0067$). Most of the late-term treatment failures appeared to be due to regrowth of the tumor from peripheral regions. This observation coupled with gross examination of excised tumor (which showed dark-blue MXN-stained necrotic regions adjacent to the viable growing regions of tumor that led to the animal's euthanasia) suggested that prolonged drug residence time at the tumor site is not sufficient to result in complete tumor regression without complete perfusion of the tumor by the drug. The survival outcomes for this study are summarized in Table 5-13.

Table 5-13 Survival statistics for 16/C MAC treated with free or 20 to 40 μm microsphere-loaded MXN

Treatment	F0	F0+	M0	F4	F8	F16	F24	M24	M32	M48
# Treated	4	4	3	4	4	4	4	4	4	4
Median survival [a]	10	7	7	21	44	10	8	19	20	43
ILS [b]				200%	529%	43%	14%	171%	186%	514%
% Cures [c]	0%	0%	0%	25%	50%	25%	0%	0%	25%	50%

[a] Time until reaching 50% survival after treatment (in days)
[b] Percent increase in median lifespan after treatment compared to controls (median for combined control groups = 7 days)
[c] Animals alive 60 days after treatment

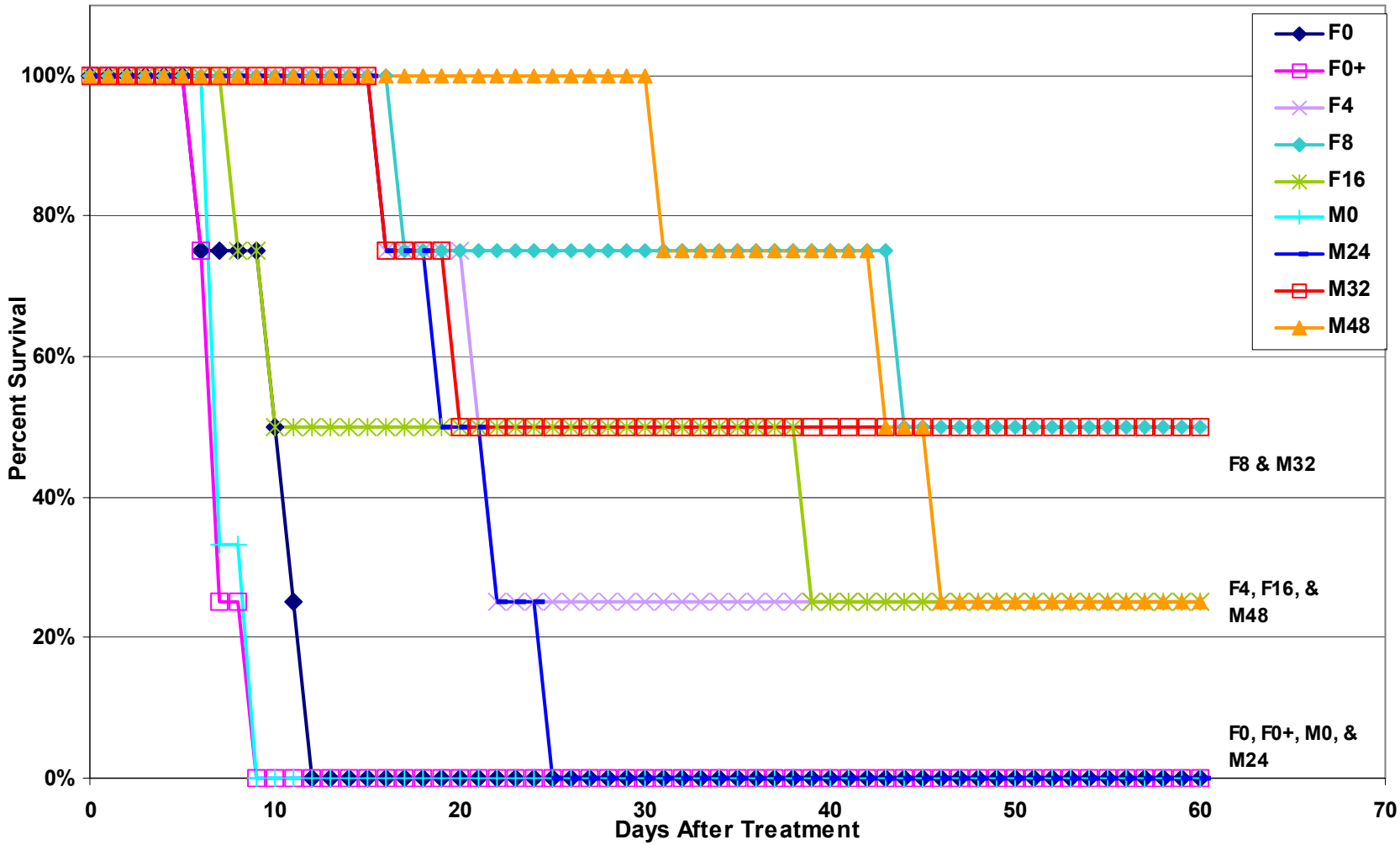

Figure 5-37 Survival graph for mice treated with 20 to 40 μm MXN-loaded albumin microspheres. Mice were treated on Day 0.

5.4 Intratumoral Therapy with 20 to 40 μm Microspheres Combined with Free MXN

5.4.1 Introduction

The object of this study was the *in vivo* evaluation of the safety and efficacy of intratumoral injection of MXN both as a combination of free drug and drug-loaded albumin microspheres. Treatment groups consisted of intratumoral MS-MXN delivered in combination with free drug or in a control vehicle. It was felt that this combination of free drug with the microsphere-loaded drug would provide an initial loading dose of MXN to the tumor mass followed by prolonged exposure as MXN was released from the microspheres. The appropriate control groups were included in the study: nontreated (F0), intratumorally injected Tsaline (F0+), and unloaded albumin microspheres (M0). These evaluations were performed in the 16/C murine mammary carcinoma model. The dose levels for the treatment groups were chosen based on the results of the previous study of 20 to 40 μm MS-MXN and F-MXN. The two most efficacious doses from each of the MS-MXN and F-MXN groups were combined for this study. The 24 and 32 mg/kg MS-MXN doses were chosen, as apposed to including the 48 mg/kg dose, because 48 mg/kg was estimated to already be the maximum tolerated dose. It was believed that the addition of free drug to this formulation would result in significant toxicity. The free drug delivery vehicle consisted of 4 or 8 mg/kg of MXN in Tsaline. The study design is shown in Figure 3-6.

It requires noting that one mouse was excluded from the analysis of this study. It was a F0 control animal that experienced an inexplicable regression of its tumor after being enrolled in the study. In the several hundred animals this group has injected with the 16/C MAC tumor line, spontaneous regression has been observed in less than 1% of

the animals. Therefore, this animal was considered an outlier and was therefore excluded from the analysis of this study.

5.4.2 Body Weight

All of the treatments in this study appeared to be relatively well tolerated. The average normalized body weight data for each of the treatment groups is shown in Figure 5-38. Statistical analysis of this data reveals that there is a difference between treatment groups (ANOVA of all groups, $p = 0.013$). Multiple comparison tests reveal that the M24+F8 treatment group has a significantly lower body weight five days after treatment compared to the F0 and F0+ treatment groups (Tukey's MCT, family error rate < 0.10). The reduction in average TABW for the M24+F8 treatment group resulted from a significant TABW loss present in one mouse in the treatment group. This mouse reached a maximum loss of 18% of its TABW before recovering. Although this mouse

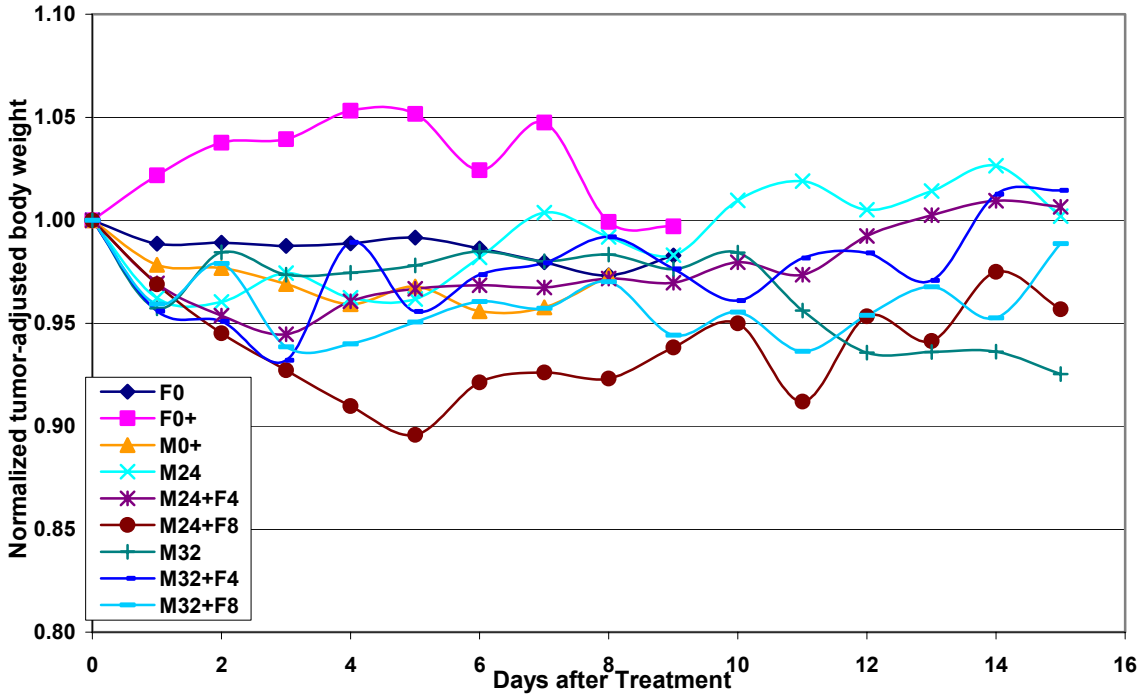

Figure 5-38 Average NTABW for mice treated with 20 to 40 µm MS-MXN combined with F-MXN in a single treatment delivered on Day 0.

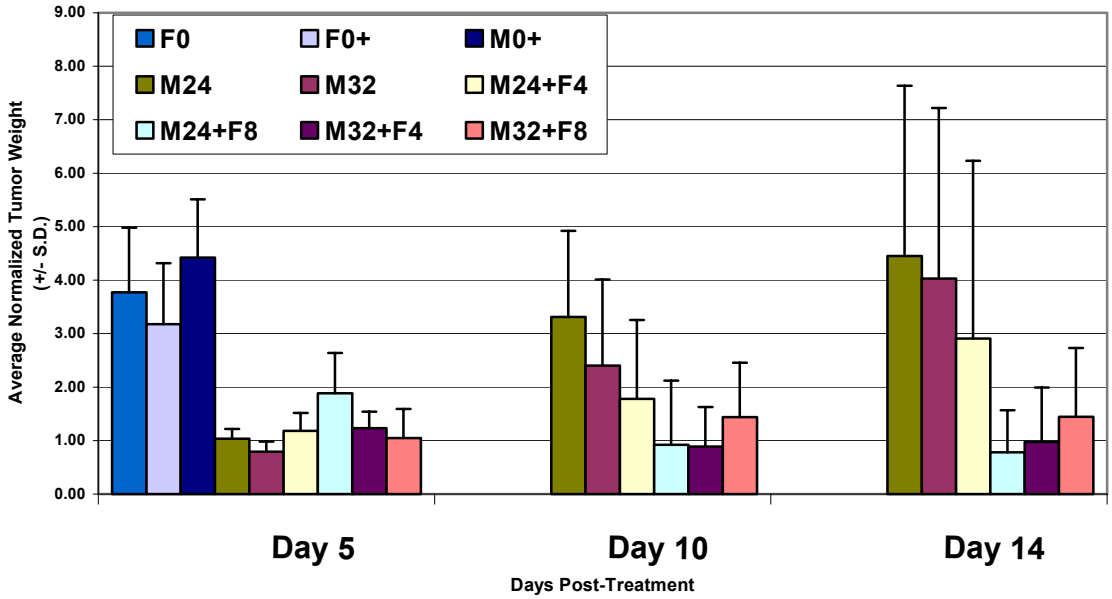

Figure 5-39 Average normalized tumor weight (NTW) for mice treated with 20 to 40 μm MXN-loaded BSA microspheres combined with F-MXN on Day 0.

suffered from significant toxicity, the mouse was "cured" with a complete regression of its tumor and survival greater than 60 days after treatment. The treatment was well tolerated by the other mice in the group. Also the higher dose M32+F4 and M32+F8 treatmented mice did not demonstrate significant a body weight loss.

5.4.3 Tumor Growth

Data for tumor growth were examined on Days 5, 10, and 15. Tumor growth was measured as NTW, as in previous studies. Average NTW for each treatment group on Days 5, 10, and 14 is shown in Figure 5-39. Statistical analysis of the NTW data shows that there is a significant difference in tumor growth between treatment groups on Day 5 (one-way ANOVA, $p < 0.001$). All intratumoral MXN treatments, MS-MXN alone or combined with F-MXN, had significantly less tumor growth than the control groups, except for the M24+F8 and F0+ groups which were not statistically different (Tukey's MCT, family error rate < 0.10). None of the MXN treatments had statistically different tumor growth on days 10 or 14 (one-way ANOVA, $p = 0.175$ and $p = 0.085$ respectivel).

5.4.4 Survival

The survival curves for each of the treatment groups are shown in Figure 5-40. Statistical analysis of the survival data once again reveals that there is a statistically significant difference in survival between treatment groups (log-rank test, $p < 0.0001$). All intratumoral MXN treatments were found to be superior to the control groups (log-rank test, $p < 0.05$). In general, mice receiving the combined treatments survived longer than those receiving MS-MXN alone (log-rank test, $p < 0.05$). The exceptions to this are that the M24+F4 group did not have better outcomes than MS-MXN alone and the M32+F8 group was not statistically superior to the M32 treatment. No statistical difference could be detected between the various combined treatment groups. It should be noted that the MS-MXN treatments did not perform as well in this second study as in the first, with neither treatment producing any "cured" animals. However, there was significant overlap in the 95% confidence intervals for the mean time to failure for both groups in both studies. The study outcomes are summarized in Table 5-14.

Table 5-14 Survival statistics for 16/C MAC treated with 20 to 40 μm microsphere-loaded MXN delivered in Tsaline or free MXN solution

Treatment	F0	F0+	M0	M24	M32	M24 + F4	M24 + F8	M32 + F4	M32 + F8
# Treated	7	4	4	4	4	4	4	4	4
Median survival [a]	9	8	7	16	13	19	27	34	31
ILS [b]				78%	44%	111%	200%	278%	244%
% Cures [c]	0%	0%	0%	0%	0%	25%	50%	50%	25%

[a] Time until reaching 50% survival after treatment (in days)
[b] Percent increase in median lifespan after treatment compared to controls (median for combined control groups = 9 days)
[c] Animals alive 60 days after treatment

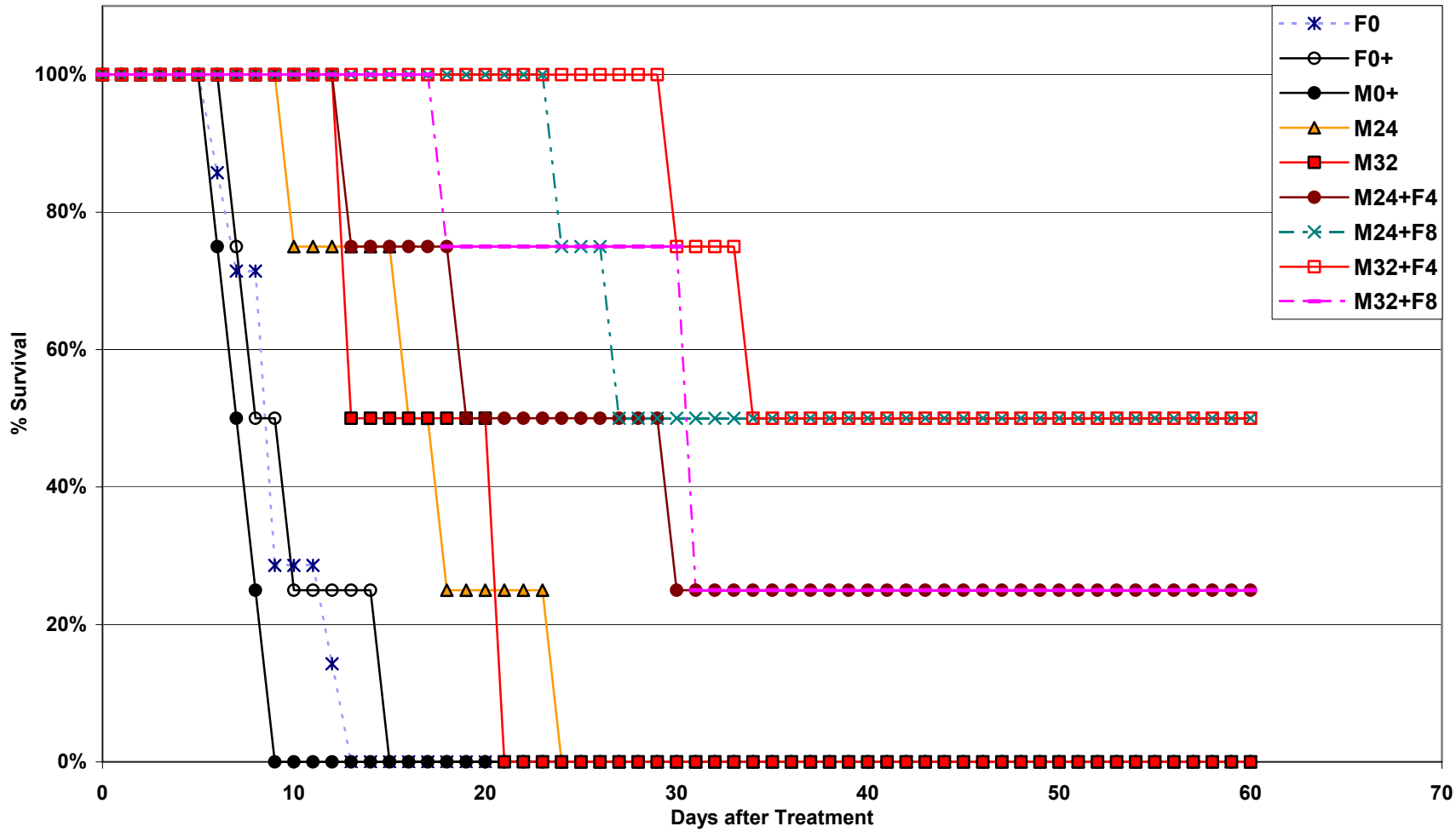

Figure 5-40 Survival graph for mice treated with 20 to 40 µm MXN-loaded albumin microspheres combined with F-MXN. Mice were treated on Day 0.

5.5 Intratumoral Therapy with Free or 5 to 10 μm Mesosphere-Loaded MXN

5.5.1 Introduction

This study was conducted in order to determine the efficacy of MXN-loaded BSA mesospheres with a smaller size distribution than the 20 to 40 μm microspheres used in previous studies. It was hypothesized that smaller mesospheres would release loaded drugs more rapidly because of shorter diffusion paths out of the mesosphere matrix and as a result of increased surface area to volume ratio. Both of these factors increase the flux of loaded drug across the mesosphere surface into the surrounding tumor tissue. It was also hypothesized that smaller mesospheres would be easier to inject through syringe needles as well as diffuse through the tissues farther from the injection site than the larger microspheres. Therefore, studies were performed with albumin mesospheres with an average diameter of 5 to 10 μm.

The mesosphere study designs were analogous to those used for the microspheres studies. The design for this study is shown in Figure 3-7. Intratumoral MXN treatment groups consisted of F-MXN delivered at 4, 8, and 12 mg/kg doses and MS-MXN delivered at 24, 32, and 40 mg/kg doses. The 4 and 8 mg/kg F-MXN and the 24 and 32 mg/kg MS-MXN doses were chosen for this study based on their efficacy in previous studies. It was known that the MTD for F-MXN was between 8 and 16 mg/kg, so the 12 mg/kg dose was incorporated into this study to better determine the MTD. The 40 mg/kg dose of MS-MXN was incorporated into this study for similar reasons. Control groups consisted of unloaded BSA microspheres with a similar size distribution (M0) or nontreated mice (F0).

Treatments consisted of a single injection of the appropriate treatment on Day 0. The study was performed using the standard protocol for tumor inoculation, treatment

initiation, injection procedure, and study endpoints described in the standard *in vivo* study protocol.

5.5.2 Body Weight

There is little difference in the NTABW data among treatment groups of mice receiving IT treatments with 5 to 10 µm MS-MXN or F-MXN. The average NTABW for each treatment group is graphed in Figure 5-41. Statistical analysis of the NTABW data on days 5, 10, and 15 shows that there is a statistical difference between groups on Day 5 (one-way ANOVA, $p = 0.027$), but not on days 10 and 15 (GLM ANOVA, $p = 0.482$ and $p = 0.328$ respectively). The difference on Day 5 was between the M40 treatment and the F0 and M0 control groups (Tukey's MCT, family error < 0.10). It is evident from inspection of the NTABW graph that although the M40 group had the lowest NTABW on Day 5, it was not the lowest on Days 4 or 6. Therefore, although the difference on Day 5 is statistically significant, it is probably not clinically significant but rather an artifact of the choice of treatment day used for analysis.

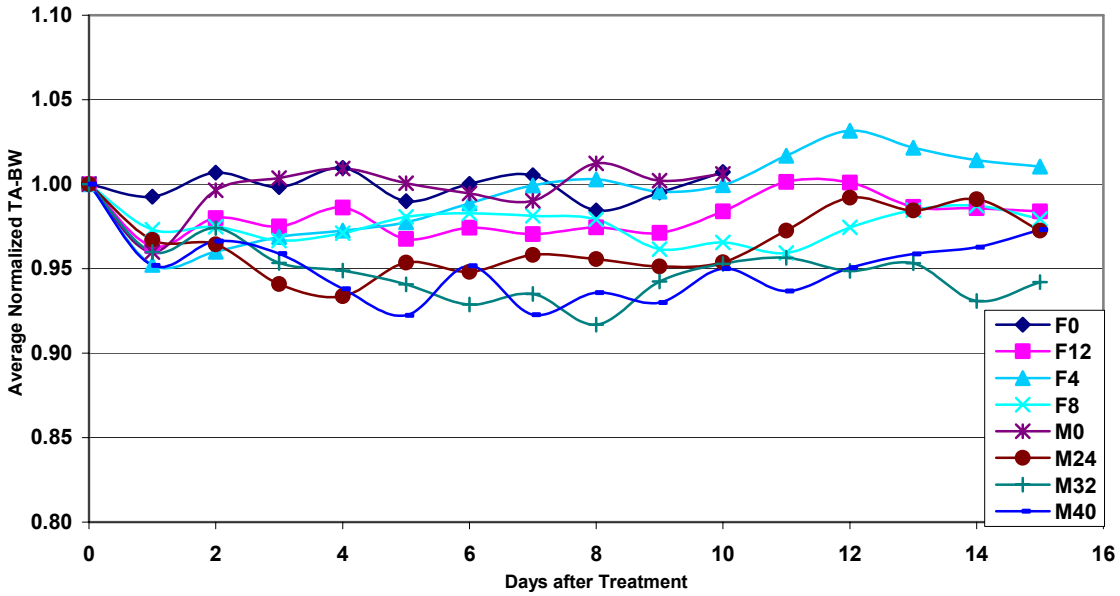

Figure 5-41 Average NTABW for mice treated with 5 to 10 µm MS-MXN or F-MXN.

Two animals enrolled in this study were euthanized for TABW loss greater than 20% or overt toxicity. One out of the five mice treated with 32 mg/kg of MS-MXN (M32) suffered an excessive TABW loss. It was euthanized when it reached a 20% weight loss 8 days after treatment. Another mouse treated with 24 mg/kg MS-MXN was euthanized 30 days after treatment. This mouse never reached 20% weight loss, but instead developed a profound lethargy after it's tumor ulcerated (TABW of 0.91, 0.97, and 0.87 on days 10, 15, and 30 respectively). This mouse most likely developed an infection secondary to the ulceration of its tumor since most animals developing significant toxicity, as measured by weight loss, require euthanasia 8 to 10 days after treatment.

5.5.3 Tumor Growth

All of the MXN treatments tested were effective in reducing tumor growth. The majority of the control animals did not survive to Day 10 or 14; so only the MXN treatment groups are analyzed at these time points. Statistical analysis of the NTW data (Figure 5-42) showed a significant difference between groups five days after treatment (one-away ANOVA, $p < 0.001$), whereas no statistical difference was found between the MXN treatments on Days 10 or 14 (one-way ANOVA, $p = 0.176$ and $p = 0.717$ respectively). Multiple pairwise comparisons of the treatment groups on Day 5 show that all MXN treatments had a significantly lower NTW than the microsphere control group and all F-MXN groups were significantly lower than the nontreated control group as well (Tukey's MCT, family error < 0.10). The M40 treatment group appears particularly effective for regressing, or delaying, tumor growth with an average NTW of 0.40 g on Day 14. However, it failed to achieve statistical significance because of the number of

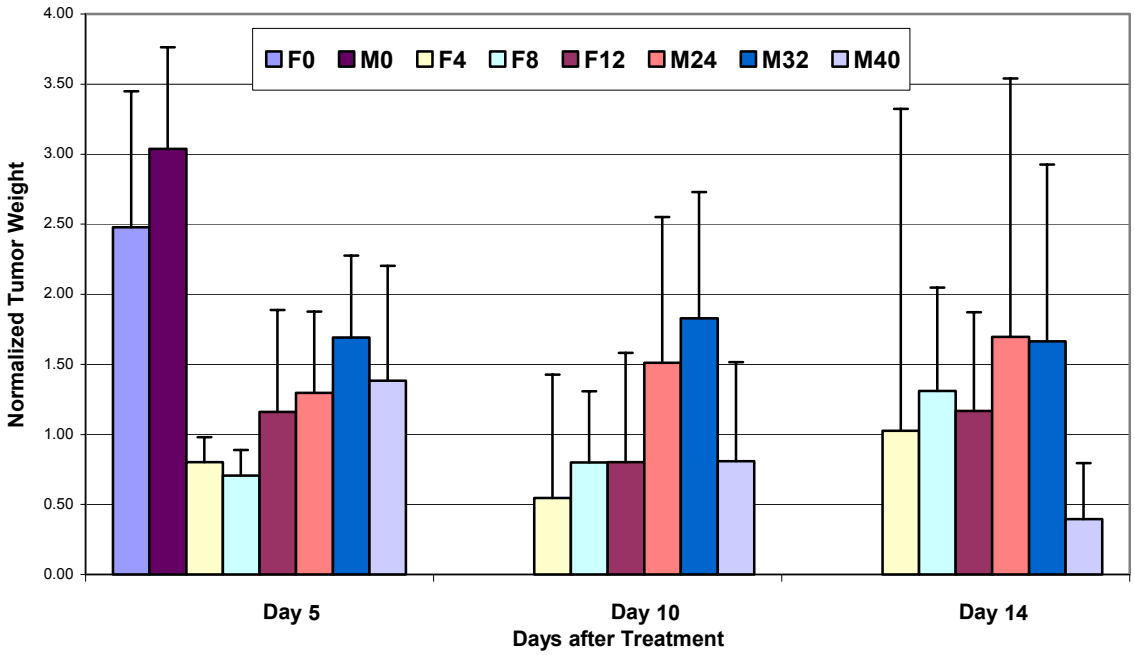

Figure 5-42 Average NTW for mice treated with 5 to 10 μm MXN-loaded BSA mesospheres.

complete regressions (NTW = 0) in the other treatment groups, which produces the high standard deviations seen in Figure 5-42.

5.5.4 Survival

The Kaplan-Meier survival curves for the treatment groups in this study are shown in Figure 5-43 and the treatment outcomes are summarized in Table 5-15. The survival curves were compared using the nonparametric log-rank test. The survival curves were found to be statistically different ($p < 0.0001$). The F0 and M0 control groups were not found to be statistically different ($p = 0.8361$), so the data for these two groups were combined and used to evaluate the ILS of the MXN treatments and for pairwise comparisons of the survival curves.

The comparison of the survival curves shows that all MXN treatments (F-MXN or MS-MXN) had statistically superior survival curves than the control group ($p < 0.05$). The 40 mg/kg dose of MXN delivered loaded in microspheres produced the best survival

results with 80% of the treated animals being cured. This M40 treatment group was statistically superior to the F12 treatment ($p = 0.0330$) and almost achieved the 5% significance level when compared to the F4 and F8 treatment groups ($p = 0.0797$ and $p = 0.0554$, respectively).

The MS-MXN treatments appeared to improve survival compared to the F-MXN treatment groups, although only the M40 group achieved a statistically significant difference. This was probably due to the small number of animals (5 per group) receiving each treatment. All of the MS-MXN treatments produced 40% or more survivors compared to the 20% of the F-MXN treated mice that were cured of their tumor. Plus, the highest dose of MS-MXN, 40 mg/kg, cured 4 out of the 5 mice treated with a single IT injection, and the one treatment failure survived for 35 days after treatment compared to a median of 11 days for the control animals. This treatment is clearly promising, although it is probably close to the MTD for this microsphere formulation.

Table 5-15 Survival statistics for 16/C MAC treated with 5 to 10 μm mesosphere-loaded MXN delivered in Tsaline or free MXN solution.

Treatment	F0	M0	F4	F8	F12	M24	M32	M40
# Treated	5	5	5	5	5	5	5	5
Median survival [a]	11	12	43	31	26	30	29	**
ILS [b]			291%	182%	136%	173%	164%	**
% Cures [c]	0%	0%	20%	20%	20%	40%	40%	80%

[a] Time until reaching 50% survival after treatment (in days)
[b] Percent increase in median lifespan after treatment compared to controls (median for combined control groups = 11 days)
[c] Animals alive 60 days after treatment

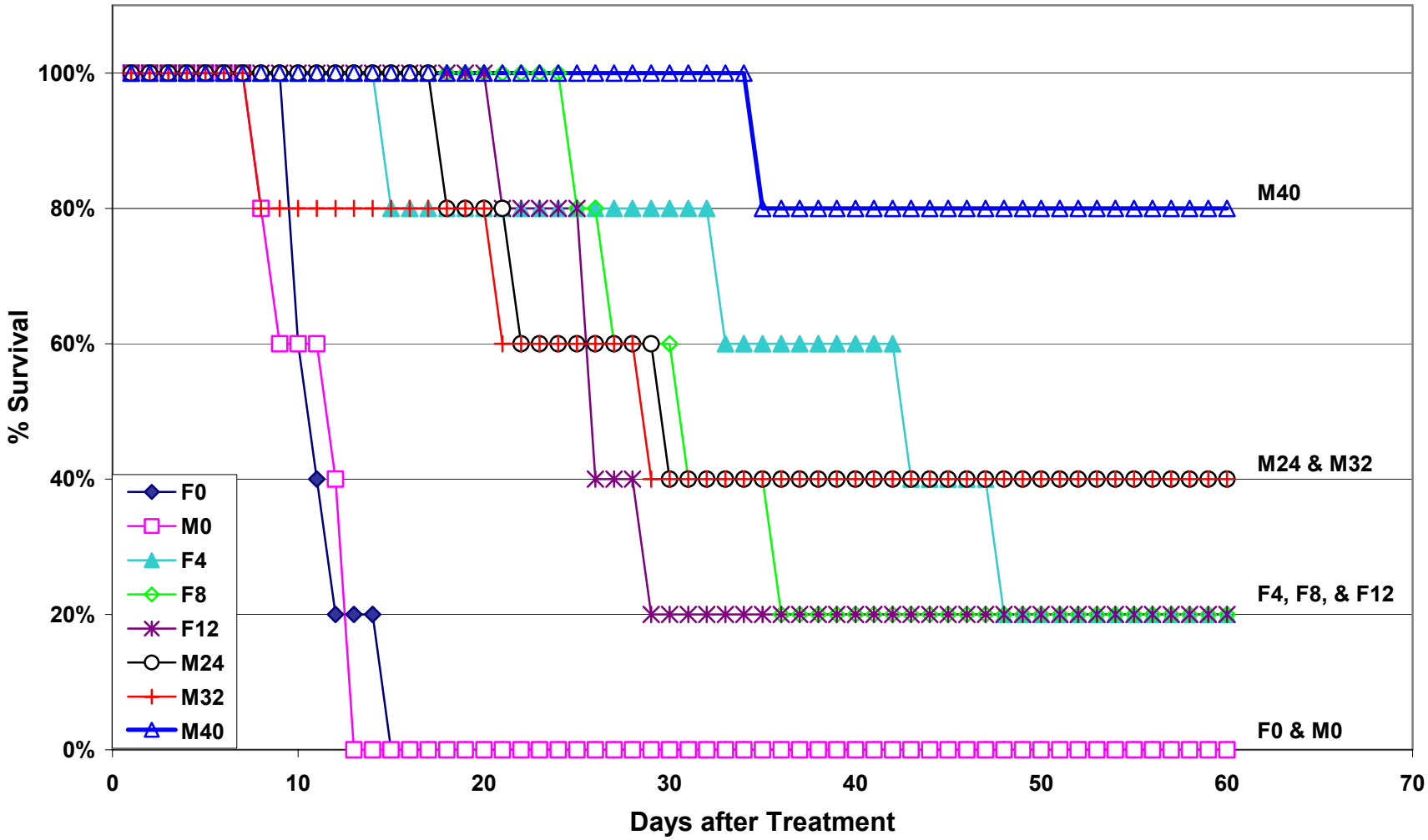

Figure 5-43 Survival graph for mice treated with 5 to10 µm MXN-loaded BSA microspheres. Mice were treated on Day 0.

5.6 Intratumoral Therapy with 5 to 10 μm Mesospheres Combined with Free MXN

5.6.1 Introduction

This study was conducted in order to evaluate the efficacy and toxicity of small 5 to 10 μm mean diameter MXN-loaded albumin mesospheres delivered in a F-MXN solution. This study was conducted in an analogous fashion to the similar study with 20 to 40 μm microspheres combined with F-MXN. The study was originally designed to test the M32+F4, M32+F8, M40+F4, and M40+F8 dose combinations. These dose combinations were chosen based on the results of the previous study of 5 to 10 μm MS-MXN delivered in Tsaline. The significant toxicity associated with the 32 and 40 mg/kg MS-MXN containing doses prompted the addition of two lower dose combinations based on a 24 mg/kg MS-MXN component, M24+F4 and M24+F8. Since these latter two groups were added only after the initial results of the other treatment groups were known, there was less follow-up and in the case of M24+F8 incomplete enrollment in these two treatment groups at the time of this analysis.

Each animal received a single treatment of MS-MXN combined with F-MXN delivered on Day 0, or no treatment if randomized to the control group. The study was performed using the standard *in vivo* study protocol for tumor inoculation, treatment initiation, injection procedure, study endpoints and statistical analysis described in section 3.2.6.

5.6.2 Body Weight

The body weight of each mouse was measured daily after treatment. Graphs of the normalized NTABW for each treatment group are shown in Figure 5-44. The NTABW for each treatment group was statistically compared on Day 5 of the study. Only groups M24+F4, M24+F8, and M32+F4 were statistically analyzed at Day 10 and

15, due to the small number of survivors in each of the other groups. On Day 5, the M32+F4, M32+F8, M40+F4, and M40+F8 treatments were found to have a significantly decreased NTABW compared to the nontreated control group (GLM ANOVA, $p = 0.002$; Tukey's MCT, adjusted $p < 0.10$). Additionally, the M32+F8 treatment was found to result in statistically smaller NTABW's than the M24+F4 treatment on Day 5 (Tukey's MCT, adjusted $p < 0.0576$). No statistically significant differences between the other treatment groups were detected on Day 5, or between the M24+F4, M24+F8, and M32+F4 groups on Day 10 or 15.

There was a significant amount of toxicity associated with the higher dose treatments used in this study (those based on 32 or 40 mg/kg of MS-MXN). This was not expected based on the results of the previous study delivering 20 to 40 µm MS-MXN combined with F-MXN in which a 32 mg/kg dose of MS-MXN delivered in combination with F-MXN was well tolerated. The M32+F8, M40+F4, and M40+F8 were all too toxic

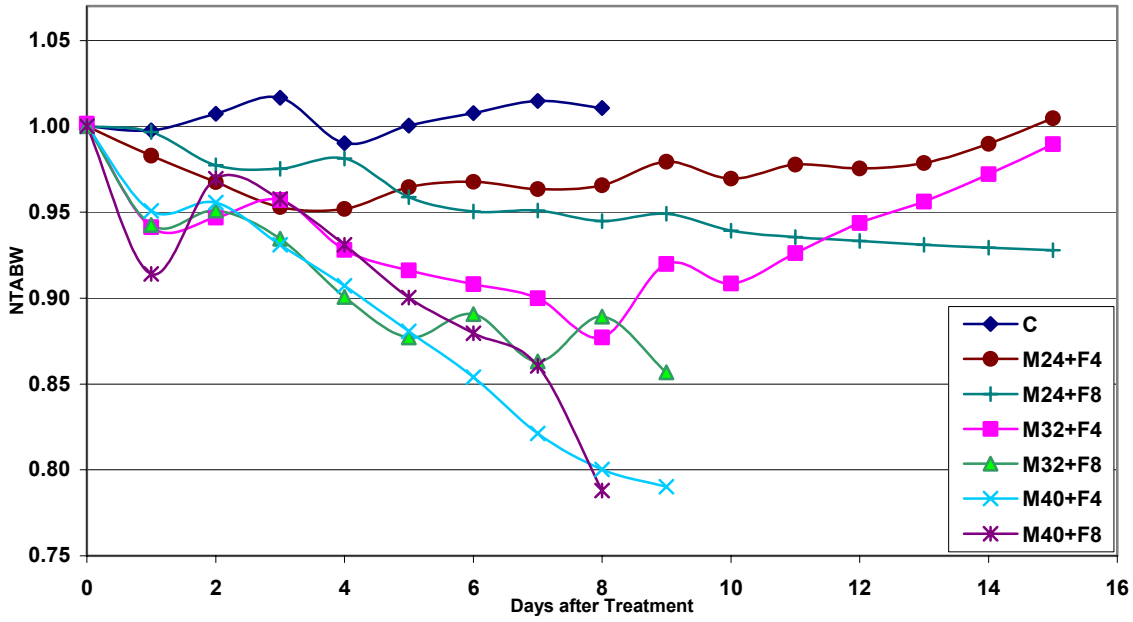

Figure 5-44 Average normalized tumor-adjusted body weight (NTABW) for mice treated with 5 to 10 µm MS-MXN combined with F-MXN.

for future use in this animal model. Although only one animal in the M32+F4 treatment group reached 20% TABW loss and required euthanasia, three out of the five animals treated with this dose lost 15% or more of their TABW within ten days of treatment. This was judged to represent an unacceptable level of toxicity, and therefore this treatment also is deemed too toxic for use in this animal model. However, little toxicity was noted in the M24+F4 and M24+F8 treatments, and the efficacy of these doses deserves further study.

The high amount of toxicity seen in these animals relative to the mice treated with similar doses of the 20 to 40 µm MS-MXN was most likely due to the higher rate of drug release from the smaller mesospheres. This would cause higher concentrations of MXN to reach the systemic circulation in a short amount. This more intense exposure of the bone marrow and other toxicity target organs to the drug would result in an increase in the MXN-associated toxicity.

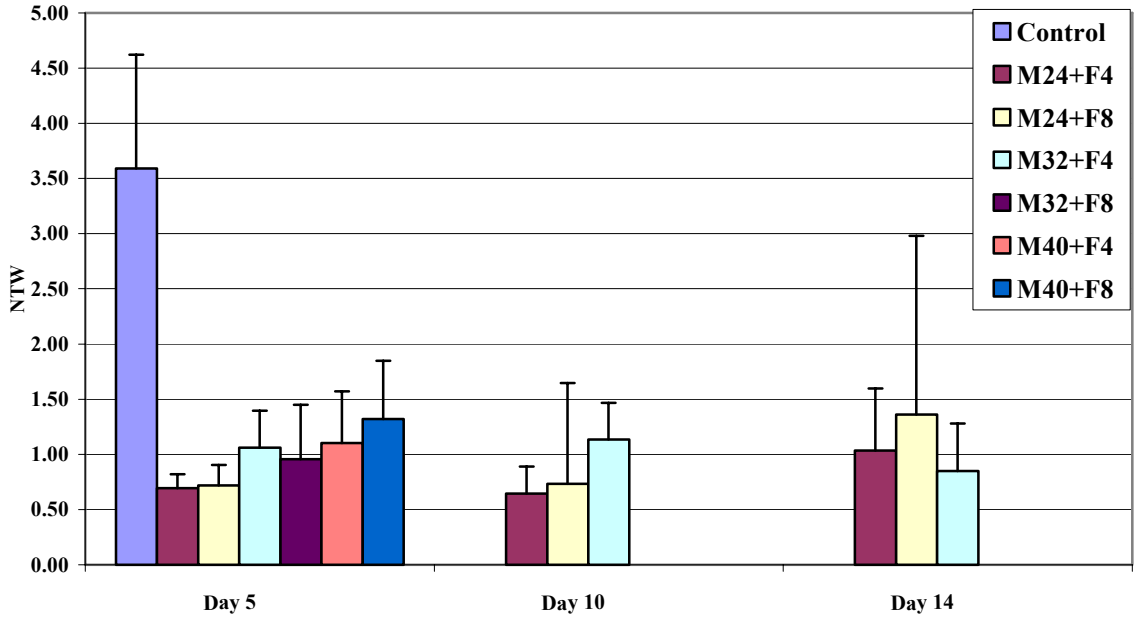

Figure 5-45 Average normalized tumor weights (NTW) for mice treated with 5 to 10 µm MS-MXN combined with F-MXN.

5.6.3 Tumor Growth

The tumor growth for each animal was monitored daily after treatment on Day 0. The average NTW for each treatment group on days 5, 10, and 14 are shown in Figure 5-47. Only the data for the M24+F4, M24+F8, and M32+F4 treatment groups are shown on Days 10 and 14 because an insufficient number of animals survived to these time points in the other treatment groups. The NTW data for all groups was compared statistically on Day 5, and the NTW data for the M24+F4, M24+F8, and M32+F4 treatment groups were analyzed on Days 10 and 14. All IT MXN treatments resulted in significantly smaller NTWs than the nontreatment control group on Day 5 (GLM ANOVA, $p < 0.001$; Tukey's MCT, adjusted $p < 0.05$). No statistically significant differences were found between the six combined MS-MXN and F-MXN treatment groups on Day 5, or between the M24+F4, M24+F8, and M32+F4 treatment groups on Days 10 or 14 of the study.

Once again the IT injection of MXN has been shown to decrease the rate of tumor growth in the 16/C MAC tumor model when compared to the growth of nontreated control tumors.

5.6.4 Survival

A significant number of MXN treated animals suffered from an unexpectedly severe degree of toxicity. The high degree of toxicity observed with the higher doses of combined intratumoral chemotherapy prompted the addition of two lower dose levels to this study. Unfortunately, the late inclusion of these animals limits the amount of follow-up time available to observe for tumor recurrence after treatment. The Kaplan-Meier survival curves for the treatment groups included in this study are shown in Figure 5-46. The statistical analysis of the survival curves was performed using the

log-rank test, with the survival times right-censored at the day of minimum follow-up for each treatment group. The survival analysis showed that there was a statistical difference within the set of survival curves ($p < 0.05$). The M24+F4, M24+F8, and M32+F4 treatment groups were found to be result in significantly better survival than the control group ($p < 0.02$ for each comparison). No other statistical differences were found between the various treatments.

Both the M24+F4 and the M32+F4 treatments produced a promising percentage of cured animals. The M24+F8 treatment also produced promising results, although the minimum follow-up time was only 25 days at the time of this analysis. Therefore, no firm conclusions can yet be made regarding the efficacy of this treatment. However, both 24 mg/kg MS-MXN containing treatments produced impressive improvements in median survival compared to the controls (ILS was known to be 263% and greater than 213% for the M24+F4 and M24+F8 treatments, respectively) The survival outcomes for this study are summarized in Table 5-16.

Table 5-16 Survival statistics for 16/C MAC treated with 5 to 10 μm MS-MXN combined with F-MXN compared to nontreated control mice. The follow-up time for the M24+F4 and M24+F8 treatment groups was less than 60 days because these groups were added to the study design only after the significant toxicity of the M32 and M40 containing treatments was realized.

	Control	M24+F4	M24+F8	M32+F4	M32+F8	M40+F4	M40+F8
# Randomized	5	5	3	5	5	4	3
# Deaths due to BWL > 20%	0	0	0	1	3	3	3
Minimum time of follow-up	N/A	40	25	> 60	> 60	> 60	N/A
Median survival [a]	8	29	> 25	54	9	8	8
ILS [b]		263%	> 213%	575%	13%	0%	0%
% Cures [c]	0%	40%	67%	40%	20%	25%	0%

[a] Time until reaching 50% survival after treatment (in days).

[b] Percent increase in median lifespan after surgery compared to median for controls.

[c] Animals alive at the time of minimum follow-up after treatment.

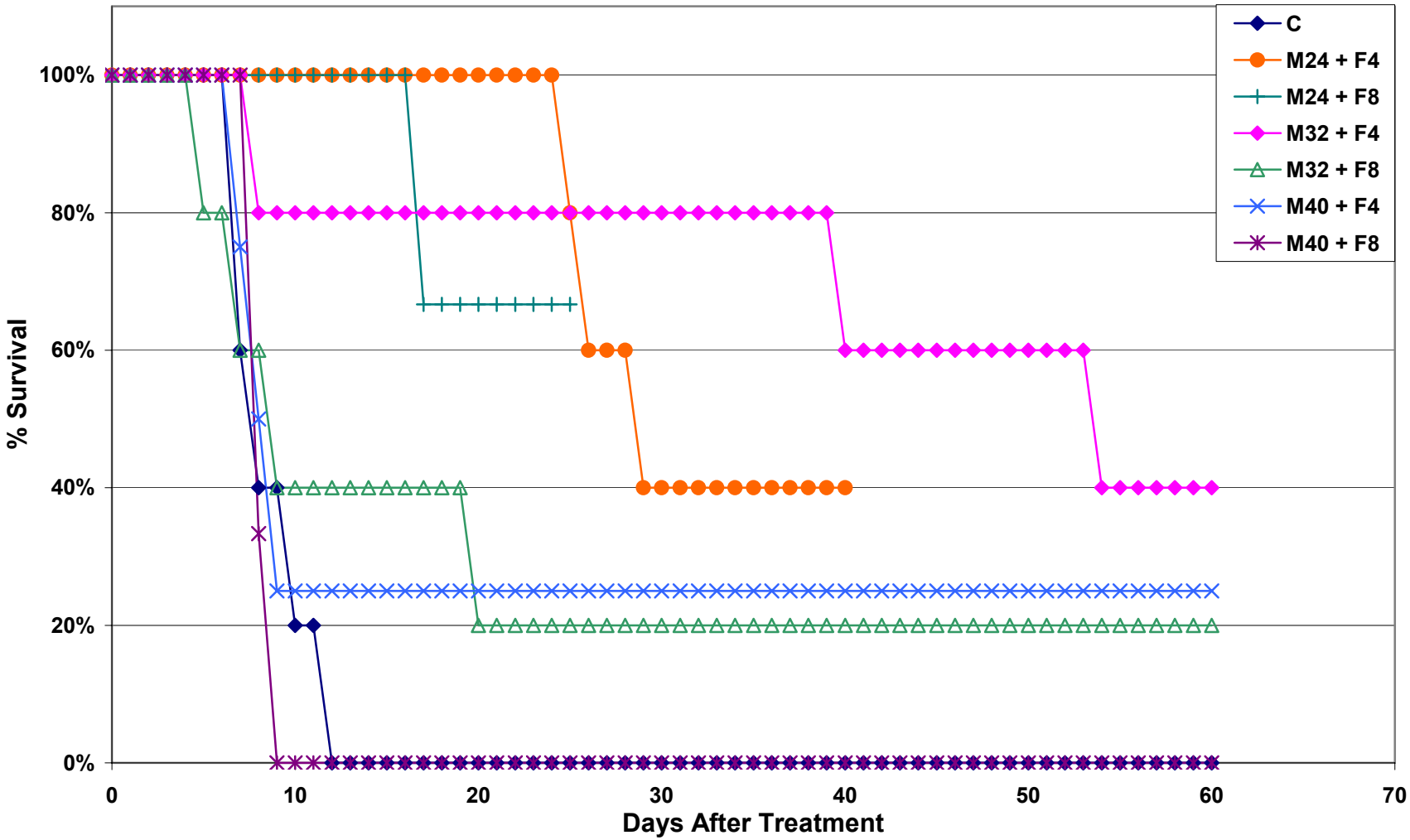

Figure 5-46 Survival graph for mice treated with 5 to 10 µm MS-MXN combined with F-MXN. Mice were treated on Day 0

5.7 Histology and Efficacy of Neoadjuvant Chemotherapy

5.7.1 Introduction

This study was designed to examine the histological effects of intratumoral chemotherapy using MXN with or without mesospheres and additionally to explore the mechanisms of toxicity of IT chemotherapy. Also of interest was the optimal timing for the surgical excision of the tumor following neoadjuvant intratumoral chemotherapy. To this end, a study was designed to compare mice treated intratumorally with F-MXN (8 mg/kg), MXN-loaded albumin mesospheres of two different crosslink densities delivered in a free MXN vehicle (24 mg/kg MS-MXN + 4 mg/kg F-MXN), or no treatment as a control. Mesospheres prepared with the lower crosslink density corresponding to 2% GTA (MS-Low) were expected to degrade at a higher rate, resulting in a more rapid release of loaded MXN into the surrounding tumor tissues than the higher crosslink density 8% GTA mesospheres (MS-High).

Surgical excision of the tumor mass was planned for 1, 7, or 14 days after the initial treatment. Nontreated control groups received surgery on Days 1 or 7 only since they were not expected to survive to Day 14. The excised tumors were fixed in 10% neutral buffered formalin prior to embedding and sectioning to prepare H&E stained

Table 5-17 Histology and neoadjuvant chemotherapy study design. MS-MXN treatments were delivered in an 8 mg/kg F-MXN vehicle. (n = 3 per treatment per time point)

Treatment (Day 0)	Day 1	Day 7	Day 14
MS-MXN (2% GTA)	T, CBC	T	T, CBC
MS-MXN (8% GTA)	T, CBC	T	T, CBC
F-MXN	T, CBC	T	T, CBC
Control	T, CBC	T	N/A

T= H&E stained slide of tumor tissue, CBC= Complete Blood Cell Count w/ differential

slides for histological examination. Tumor histology was examined to determine the effect of the intratumoral treatment on the surrounding tumor tissue as well as the distribution and degradation of the injected MXN-loaded mesospheres. Blood was drawn from the tail of the mice receiving surgery on Days 1 or 14 in order to perform CBCs with differential cell counts. This was done to determine if there was any evidence of leukopenia, which is the dose limiting toxicity for MXN given intravenously. The study design is shown in Table 5-17.

Four mice in this study died during the surgery to remove the tumor either due to anesthesia or hyperthermia. Not all of these data points were repeated. Thus, the ML-7Day treatment group consists of 2 animals, and the F-MXN-1Day group included one animal. Additionally, one mouse randomized to the F-MXN-14Day treatment group died on Day 10 prior to receiving surgery. This data point was repeated.

Table 5-18 Normal CBC values for female C3H/HeJ mice as reported by the Mouse Phenome Database Project. Values are based on measurements on ten 105 day-old female mice. The range is calculated as the mean ± 2 SD.

	units	Mean	Range
WBC	k/uL	2.073	(1.007 – 3.139)
RBC	m/uL	7.487	(6.655 – 8.319)
Platelet	k/uL	667.6	(463.6 – 871.6)
HCT	%	36.79	(33.21 – 40.37)
% Neutrophils		31.38	(17.48 – 45.28)
% Lymphocytes		61.09	(45.57 – 76.61)

5.7.2 Differential Blood Cell Counts

CBCs were performed for the MXN treated animals on Days 1 and 14 after treatment. CBCs were also performed on nontreated tumor-bearing mice one day after randomization to treatment group (C-1Day) and on normal C3H/HeJ mice with no tumor (NC). Table 5-18 shows the normal CBC values for female C3H/HeJ mice as reported by

Jackson Laboratory.[111] Summarized CBC data from this study are presented in Table 5-19 (along with the results of a one-way ANOVA of the treatment groups) and Figures 5-47 through 5-49. No significant differences in leukocyte (WBC) or erythrocyte (RBC) cell counts were found between the treatments groups. There was a difference in the spun hematocrit at the 10% significance level, but not at the 5% level. Mice treated with the MS-Low formulation had a significantly lower hematocrit than the normal, nontumor-bearing, controls at both one and fourteen days after intratumoral treatment (Tukey's MCT; family error < 0.10). A significant difference in the platelet count between groups was also found with the MS-Low treated mice having a lower platelet count on Day 1 than the NC and F-MXN-14Day groups, while the platelet count for MS-Low on Day 14 was higher than the C-1Day and F-MXN-1Day groups. These differences were further explored *post-hoc* by performing a two-way ANOVA of the MXN group data at both time points using treatment and day after treatment as the two independent variables. It was found that time after treatment had a significant effect on the platelet count, while the MXN treatment formulation did not ($p = 0.001$ and $p = 0.875$, respectively). The two control groups had significantly lower numbers of neutrophils than the F-MXN-1Day and the MS-Low-14Day groups (Tukey's MCT, family error < 0.10). No significant difference in the number of lymphocytes between groups was found. There was a significant shift in leukocyte cell populations. The two control groups both had a significantly lower percentage of neutrophils than all of the IT MXN groups except for F-MXN-14Day and MS-High-1Day (Tukey's MCT, family error < 0.10). Comparison of the percentage lymphocytes revealed the C-1Day group had a significantly greater percentage of lymphocytes than all but the MS-High-1Day group,

Table 5-19 CBC data for mice treated with intratumoral MXN. F groups received 8 mg/kg of F-MXN, MH and ML groups received 24 mg/kg MS-MXN (crosslinked with 8% or 2% GTA, respectively) + 4 mg/kg F-MXN(n = 3 per treatment per time point).

	WBC		RBC		Spun HCT		Platelets		Neutrophils		Lymphocytes	
Group	Mean	(S.D.)	Mean	(S.D.)	Mean	(S.D.)	Mean	(S.D.)	Mean	(S.D.)	Mean	(S.D.)
Normal Con.	4,867	(681)	8.80	(0.22)	49.4	(1.1)	806,333	(99,771)	1161	(260)	3577	(421)
Control 1d	4,967	(1,457)	8.88	(0.53)	47.3	(2.2)	688,333	(9,074)	1151	(208)	3584	(1,000)
F 1d	5,000	(436)	8.41	(0.22)	44.8	(2.4)	683,000	(21,656)	2374	(488)	3561	(2,361)
F 14d	5,231	(2,134)	8.29	(0.78)	46.9	(3.4)	826,000	(10,817)	2135	(326)	2678	(1,287)
MH 1d	4,967	(1,518)	8.24	(0.36)	45.7	(1.6)	738,000	(87,230)	2136	(198)	2771	(1,450)
MH 14d	3,533	(473)	8.12	(0.66)	45.1	(1.3)	820,333	(210,965)	1723	(601)	1633	(299)
ML 1d	3,567	(451)	8.26	(0.52)	43.2	(1.1)	560,667	(53,910)	2193	(371)	1280	(362)
ML 14d	4,200	(1,300)	7.68	(0.53)	43.0	(3.8)	939,667	(97,910)	2467	(919)	1507	(488)
ANOVA p=	0.501		0.194		0.060		0.008		0.018		0.102	

error < 0.10). There was not a significant increase in the number of band cells observed in any treatment group, with all animals tested having less than 3%, and on average 1%, band cells relative to the total WBC count. There were no statistically significant differences observed in the total protein, fibrinogen, icterus index, or mean corpuscular volume.

It was hypothesized that the toxicity of intratumoral MXN would be manifest as a leukopenia. However, there is no evidence of leukopenia or anemia based on these experiments. Instead what is revealed are characteristics of acute inflammation, as evidenced by the increases in number and percentage of neutrophils in the blood. At this point, it is not understood why intratumoral chemotherapy would increase the number of circulating platelets two weeks after treatment. It is possible that the differences detected here are not truly associated with the intratumoral injection of MXN. This is supported by the fact that the high average platelet count observed for the 2% GTA crosslinked microspheres is largely due to an abnormally count greater than 1,000,000 platelets/μL in one animal that was also observed to have an abnormal platelet morphology. At this

time, there is insufficient data to support the conclusion that this is, or is not, associated with the MXN chemotherapy. Grade 1 and 2 anisocytosis and polychromasia were noted in a number of the tested animals, including control animals. Although the 14 Day MS-MXN treatments had a greater incidence of grade 2 anisocytosis and polychromasia, there is insufficient evidence at this time to conclude that these observations are related to IT MXN treatments.

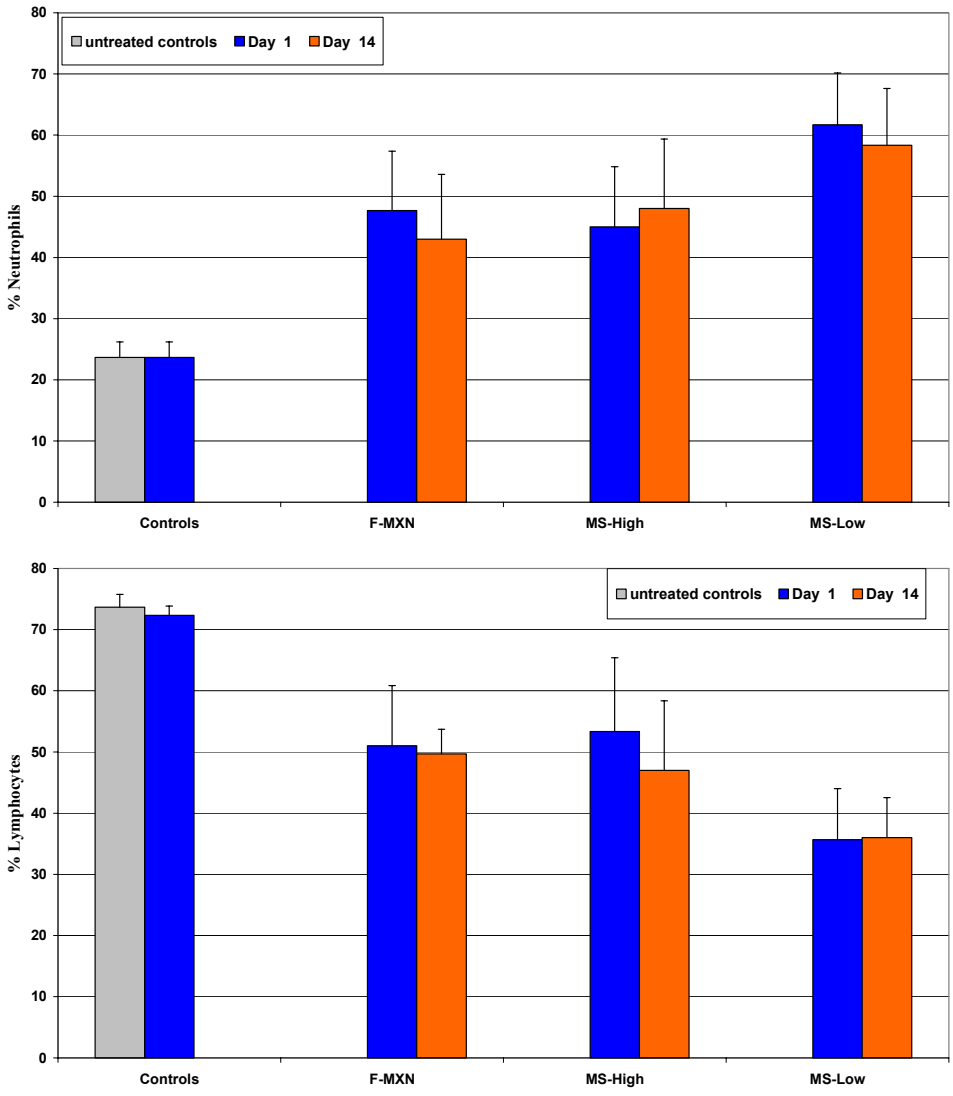

Figure 5-47 The % neutrophil and % lymphocyte count relative to the total WBC count for mice treated with 8 mg/kg F-MXN, or a combination of 24 mg/kg MS-MXN and 4 mg/kg F-MXN. MS-High are microspheres crosslinked with 8% GTA, and MS-Low were crosslinked with 2% GTA.

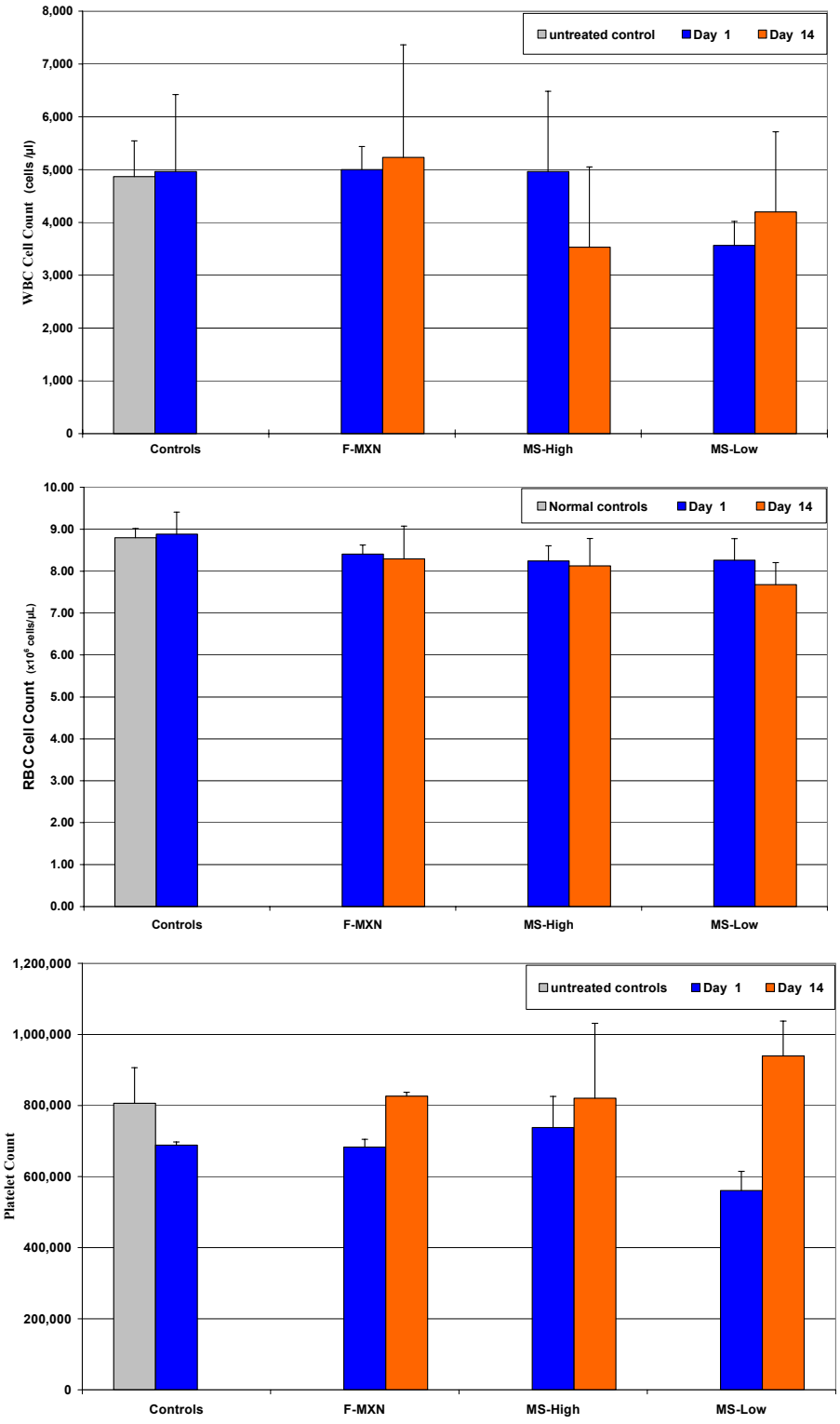

Figure 5-48 Leukocyte (WBC), erythrocyte (RBC), and platelet counts for mice treated with 8 mg/kg F-MXN, or a combination of 24 mg/kg MS-MXN and 4 mg/kg F-MXN. MS-High are microspheres crosslinked with 8% GTA, and MS-Low were crosslinked with 2% GTA.

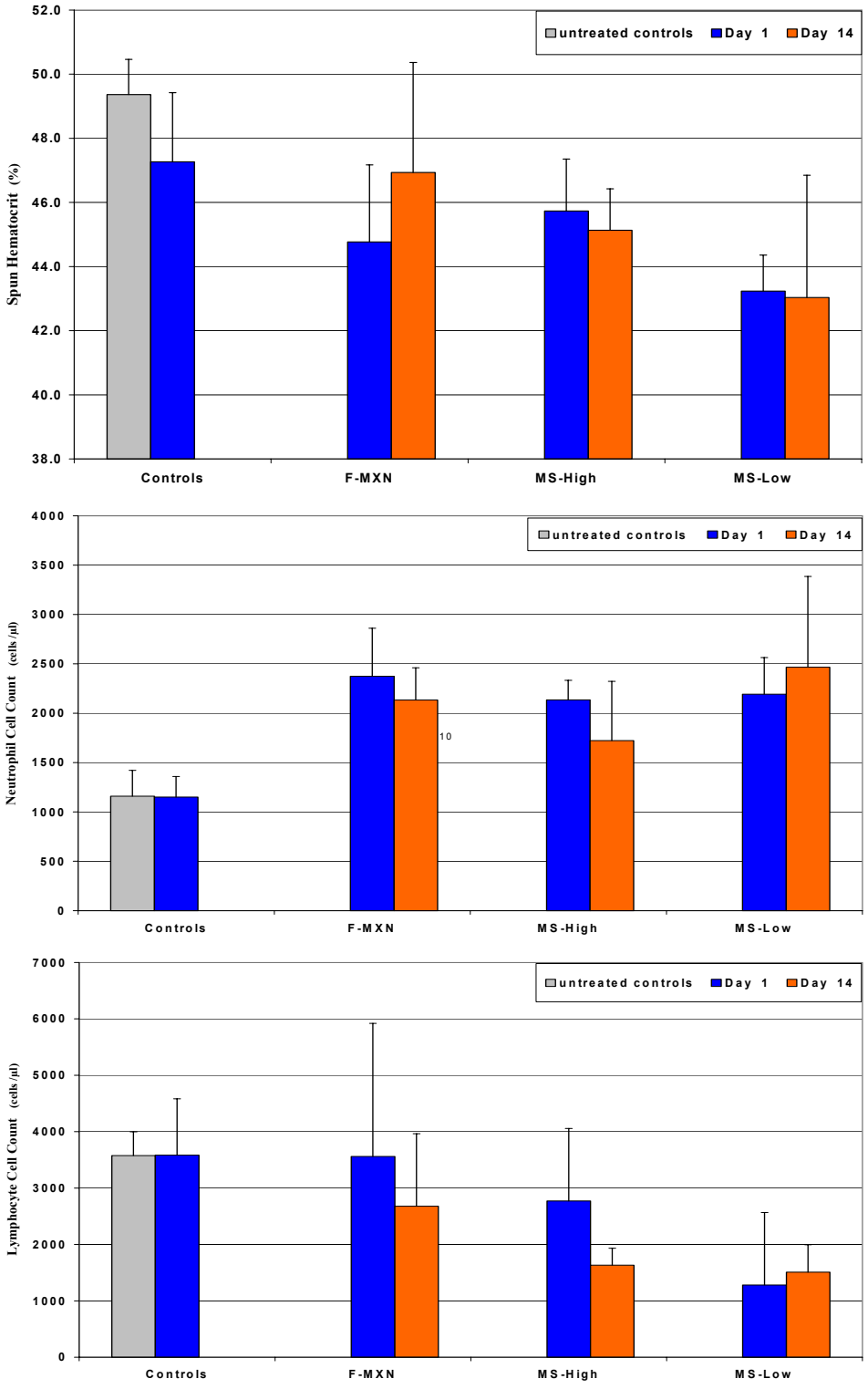

Figure 5-49 Spun hematocrits, and neutrophil and lymphocyte cell counts for mice treated with 8 mg/kg F-MXN, or a combination of 24 mg/kg MS-MXN and 4 mg/kg F-MXN. MS-High are microspheres crosslinked with 8% GTA, and MS-Low were crosslinked with 2% GTA.

5.7.3 Surgical Observations

Surgical notes were taken during the surgical excision of the tumors. In general, the extent and ease of the surgical operation was dependant upon the size of the tumors at the time of excision, with smaller tumors being much simpler to excise. The lack of any substantial subcutaneous tissue in mice prevents the excision of the tumor with large surgical margins. Instead the tumor must be dissected from the overlying skin and subcutaneous fascia and the underlying abdominal muscle tissues along the natural fascial planes. The excision of the control tumors occurring 7 days after randomization typically involved the largest tumors with indeterminate tumor margins. Figure 5-50 shows a typical nontreated tumor excised one week after randomization (the image on the left). Not surprisingly these nontreated control tumors with later excisions have the highest rate of, and shortest time to the first signs of, tumor recurrence. The tumors receiving intratumoral neoadjuvant injections of free or microsphere-loaded MXN were typically much smaller at the time of surgery than the nontreated control tumors. Tumors that were excised one day after IT injection with any of the MXN formulations were typically were observed to be very friable, and what appeared to be inflammation of the surrounding tissues was noted. The small size and dark blue staining of the tumor treated with 8% GTA mesospheres two weeks before surgery, shown in Figure 5-50 (on the right), was typical of most of the IT MXN treated tumors excised at later time points (on Days 7 and 14).

It was generally felt in the previous studies of a single intratumoral injection of free and mesosphere-loaded MXN that treatment failures due to tumor growth usually resulted from incomplete perfusion of the tumor mass with the drug rather than lack of treatment efficacy in the injected regions. This was supported by observations made

during the surgical resection of the MXN injected tumors in this study. Figure 5-51 shows examples of incompletely perfused tumors that had viable growing regions of neoplastic tissue adjacent to dark blue MXN-stained regions that appeared necrotic which presumably marked the site of IT treatment. The tumor shown on the left in Figure 5-51 was treated with low crosslink-density mesospheres injected seven days before surgery. The tumor recurred in this animal, eventually growing to 10% of the animal's body weight 34 days after surgery. This was the only microsphere treated animal that developed a tumor recurrence within 40 days of the surgical excision of the tumor (the follow up time of the study).

Blue MXN staining of the skin overlying the tumor mass was often observed when preparing the mice for surgery. The infiltration of MXN into the skin probably caused the poor wound healing observed after surgery in some of the MXN-treated animals. At least four of the animals treated with intratumoral MXN exhibited signs of impaired wound healing, such as dehiscence of the surgical wound to an extent that required the trimming of surrounding tissues and resuturing of the incision. It cannot be definitively stated that this was specifically an effect of the intratumoral treatment rather than other surgical factors such as infection or poor wound approximation during the initial wound closure. However, there were no signs of infection (such as erythema or exudates) observed in any of the wounds with impaired healing at the time of resuturing, and none of the nontreated control animals required resuturing. Regardless, this is not anticipated to represent a significant problem if intratumoral neoadjuvant chemotherapy is used in women since they would have adequate subcutaneous tissue to allow the excision of more conservative surgical margins than is possible in this mouse model.

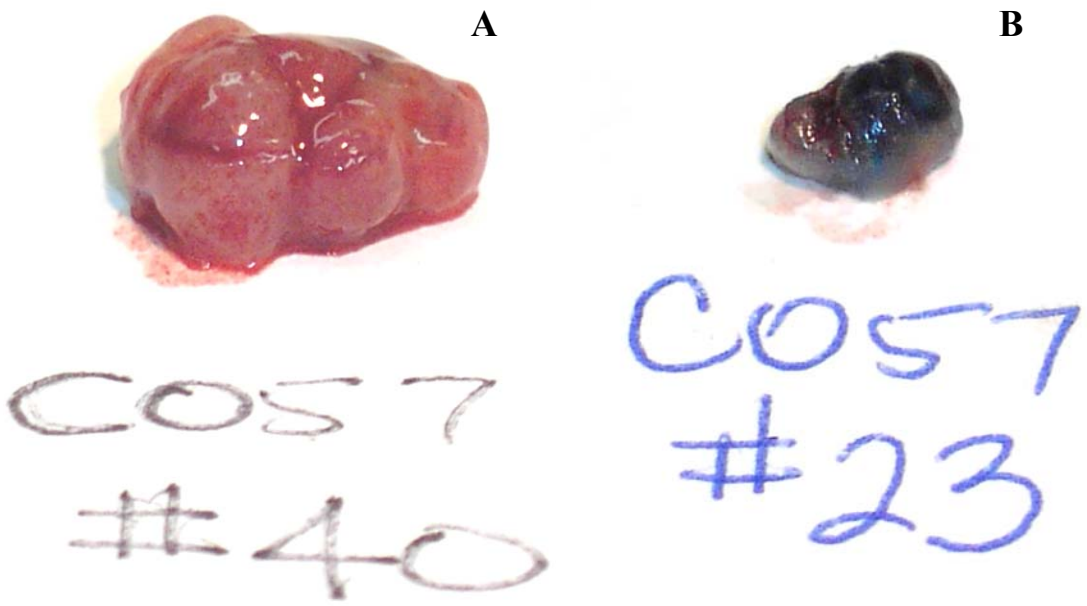

Figure 5-50 Photographs of typical tumors after surgical excision. A) A nontreated control excised 7 days after randomization. B) Tumor injected with 8% GTA high crosslink density microspheres 14 days before excision.

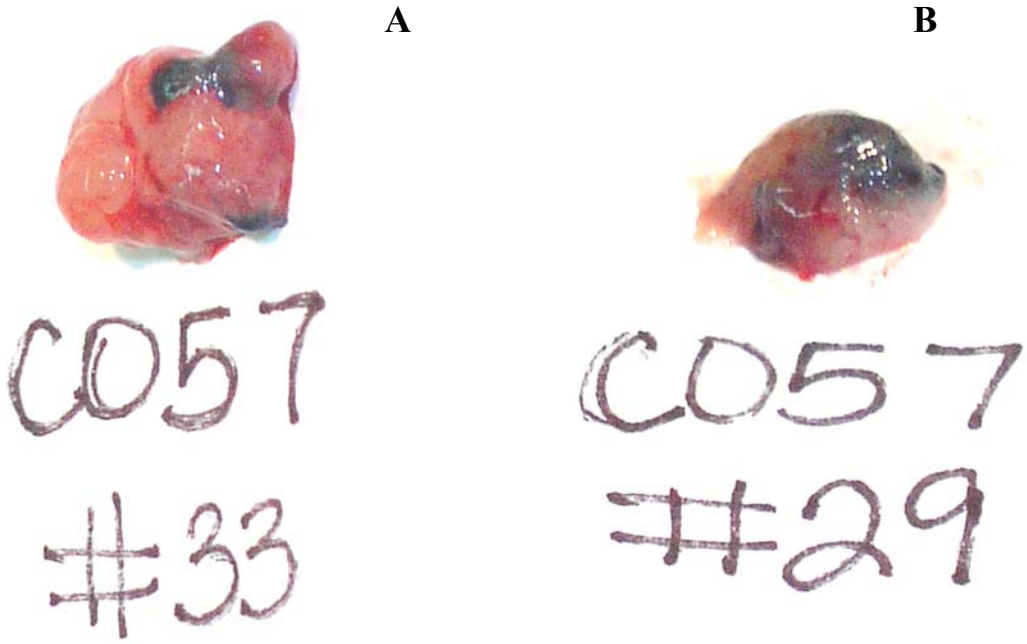

Figure 5-51 Photographs of excised tumors demonstrating incomplete perfusion of MXN throughout the tumor mass. A) Tumor injected with low crosslink density microspheres 7 days before excision. B) Tumor injected with F-MXN one day before excision.

5.7.4 Histological Evaluation

After excision each tumor was evaluated histologically. Characteristic micrographs of the tumor histology are shown in Figures 5-52 to 5-58. Necrosis was present in all tumors (treated and nontreated). There did not appear to be a relationship between the tumor treatment and the distribution of necrosis, however mesosphere associated necrosis was observed in all tumor sections in which microspheres were visible. Of the 19 tumors injected with mesospheres (10 with 2% GTA microspheres and 9 with 8% GTA mesospheres), mesospheres were visible in all of the tumor sections (Figure 5-52). However, mesospheres were only noticeable on close examination of the periphery of two tumor sections. This may have been due to a poor distribution of microspheres within the tumor, or simply that the histological sections were not cut from deep enough within the tumor mass. In at least one of these cases it was probably the former since the tumor appeared incompletely perfused and was the only microsphere treated animal that had a tumor recurrence after surgery (excised tumor is shown on the left in Figure 5-51).

In the tumor sections with readily visible microspheres, the mesospheres had either a multifocal or diffuse distribution 88% of the time. The MXN drug was visible as a blue substance in 100% of the mesospheres treated tumors excised on Day 14 and 67% of those excised on Day 7 (Figure 5-54, lower image). MXN was visible in only one of the tumors treated with free drug and none of the mesosphere treated tumors excised on Day 1 or the control tumors.

Examination of the mesosphere injected tumors revealed differences between the low and high crosslink density microspheres. Visible signs of mesosphere degradation were much more subtle in the high crosslink density (8% GTA) mesospheres. These

signs are visible in the high power micrograph show in Figure 5-53 and include small lighter colored or yellow foci, a “fuzzy outline” or halo in the lower power images. Degradation was much more prominent in the low crosslink density (2% GTA) mesospheres, as can be seen in the upper image in Figure 5-54. These degrading mesospheres stain lightly eosinophilic and have a pronounced porous structure. The porous structure apparent in the SEM of these low crosslink-density mesospheres is probably contributing to a higher rate of degradation of the protein matrix in these mesospheres.

Examination of the nontreated control tumors yields a picture of the “normal” tumor histology. Typical micrographs are shown in Figure 5-55. The 16/C MAC tumors are organized in lobules separated by a fine fibrovascular stroma. Each lobule is composed of a nest of epithelial cells with frequently indistinct cell borders and small amounts of eosinophilic cytoplasm. The neoplastic cells have large oval to indented nuclei with one to three prominent nucleoli. A high number of mitotic (dividing) cells are visible within the lobules with the median mitotic index for the tumors being 5 and 2 on Days 1 and 7 after randomization respectively. The lower mitotic index seen in the later stages of tumor growth is probably due to the overgrowth of the tumor relative to it’s vascular supply.

A significant amount of inflammation was visible associated with both MXN treated and control tumors. Typical images of tumor-associated inflammation are shown in Figure5-56. The inflammation was characterized by the presence of necrotic debris and cellular infiltration of primarily neutrophils, macrophages, and lymphocytes, which is typical of the body’s response to necrosis regardless of cause. Additionally, most tumors

were surrounded by a layer of loose connective tissue with a diffuse mild to moderated infiltrate of macrophages, lymphocytes, and neutrophils shown in the upper image of Figure 5-57.

The intratumoral treatment of the tumors with MXN was associated with some interesting changes in the cellular morphology of the tumor. These changes were not specific to one treatment, rather they were associated with both free and microsphere loaded intratumoral injections of MXN. Instead of being organized into lobules, the MXN-exposed cells frequently were arranged in chords or tendrils, which occasionally were found to interlace (lower image in Figure 5-57). The cellular chords were typically one to five cells thick and composed of cells with indistinct cellular borders and scant to abundant eosinophilic cytoplasm. The nuclei were pleomorphic having a frequently varying and atypical size and shape. Occasionally, the injected MXN was evident as a blue-staining material within vacuoles in these cells. Figure 5-58 shows typical micrographs of cells with low pleomorphism from a control tumor and of cells with a high degree of pleomorphism seen in a tumor one week after intratumoral injection of 8% GTA microspheres.

The number of mitotic figures and the degree of pleomorphism within each tumor sample were scored on an ordinal scale. The mitotic index ranged from zero to 6, with corresponding to the highest number of mitotic figures. The degree of pleomorphism score ranged from 1 to 4, with 4 corresponding to the highest degree of pleomorphism. Each sample was scored by a certified veterinary pathologist (Dr. Detrisac). The ordinal scores were statistically analyzed using the nonparametric Kruskal-Wallis test and a significance level of 10% because of the small number of samples in each group. A

significant difference in the mitotic index was found between groups ($p = 0.072$), with treatment also being a significant factor ($p = 0.011$). The MXN treated animals were further analyzed to determine if the number of days after treatment was a significant factor. It was not ($p = 0.945$).

A significant difference was also found in the degree of pleomorphism between tumors based on the group and treatment ($p = 0.096$ and $p = 0.066$, respectively). The number of days after intratumoral treatment also significantly affected the pleomorphism in the groups treated with MXN ($p = 0.098$), with the pleomorphism being higher at later time points. Based on these results the intratumoral injection of MXN decreases the mitotic index of the tumor which is representative of a slowing, or cessation, of tumor growth. However, it also increases the degree of pleomorphism observed in the tumor which is usually associated with an increase in the histological grade of neoplasm. Since the intratumoral injection of MXN has been shown in the previous studies to increase the survival of mice bearing the 16/C MAC, the significance of the higher degree of pleomorphism observed in this is uncertain in this case.

5.7.5 Survival

A secondary goal of this study was to examine the effect of the elapsed time between neoadjuvant intratumoral chemotherapy and the surgical excision of the remaining tumor mass. The Kaplan-Meier survival curves for each group are shown in Figure 5-59, and the survival outcomes are summarized in Table 5-20. The number of animals included in each treatment group is insufficient to detect a statistically significant difference in the survival curves, except for the comparison of the treatments with 100% survival (excluding F-MXN–7Day which only had one animal) and the control groups (log-rank, $p < 0.05$).

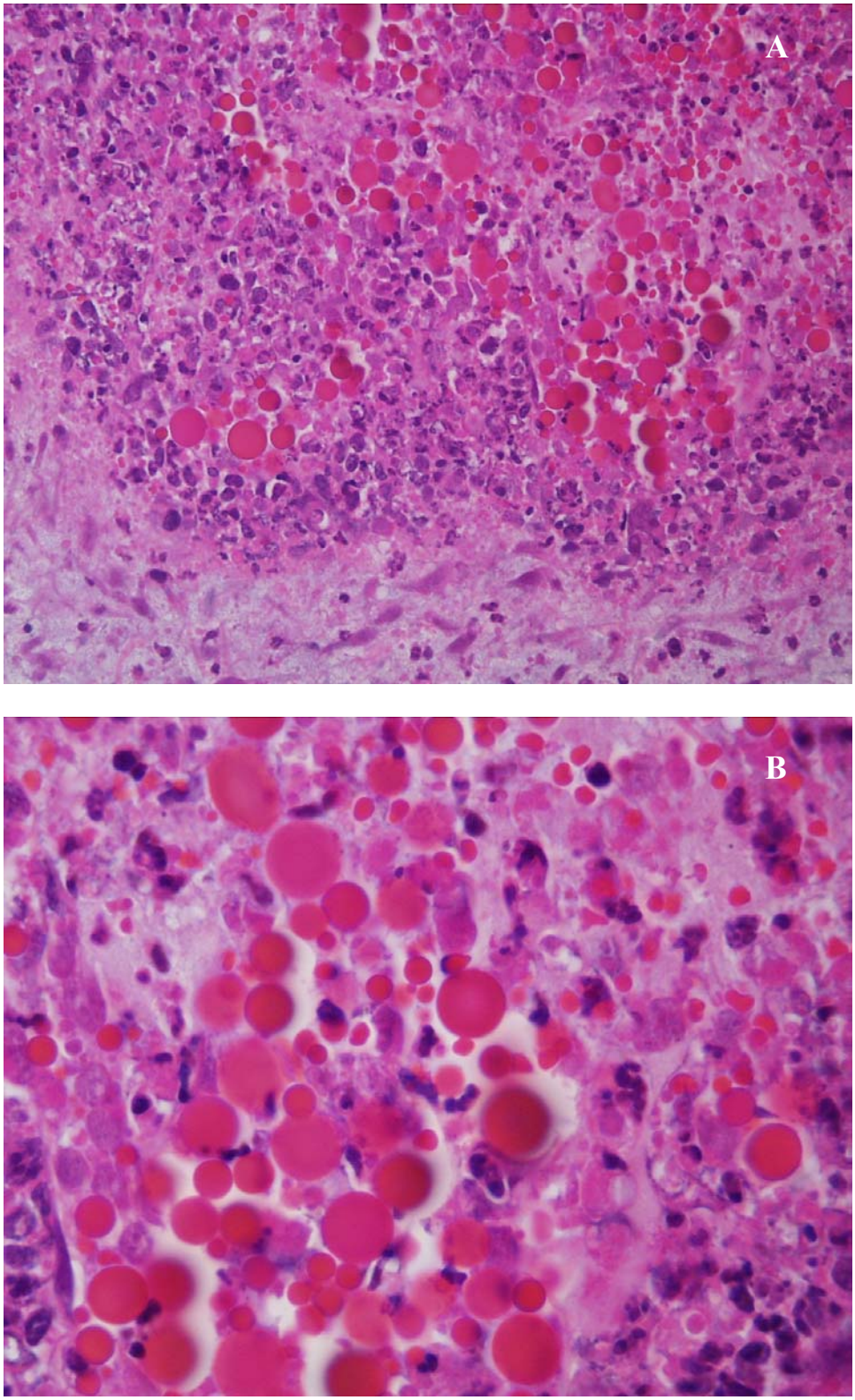

Figure 5-52 Intact microspheres (8% GTA) seen staining eosinophilic within tumor tissue one day after injection. A) 40X. B) 100X.

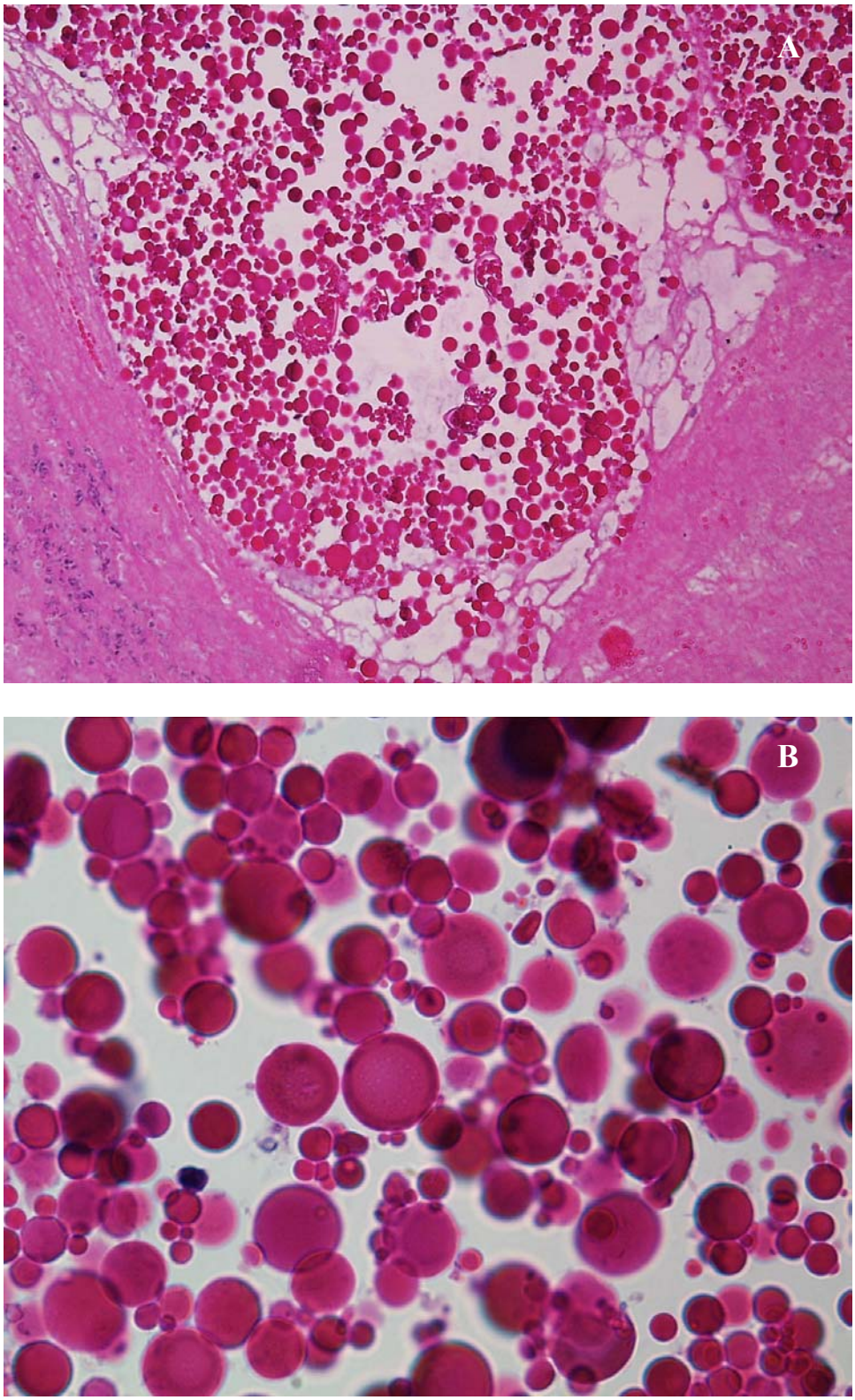

Figure 5-53 Low and high power micrographs of 8% GTA MS's with signs of microsphere degradation. A) 20X. B) 100X.

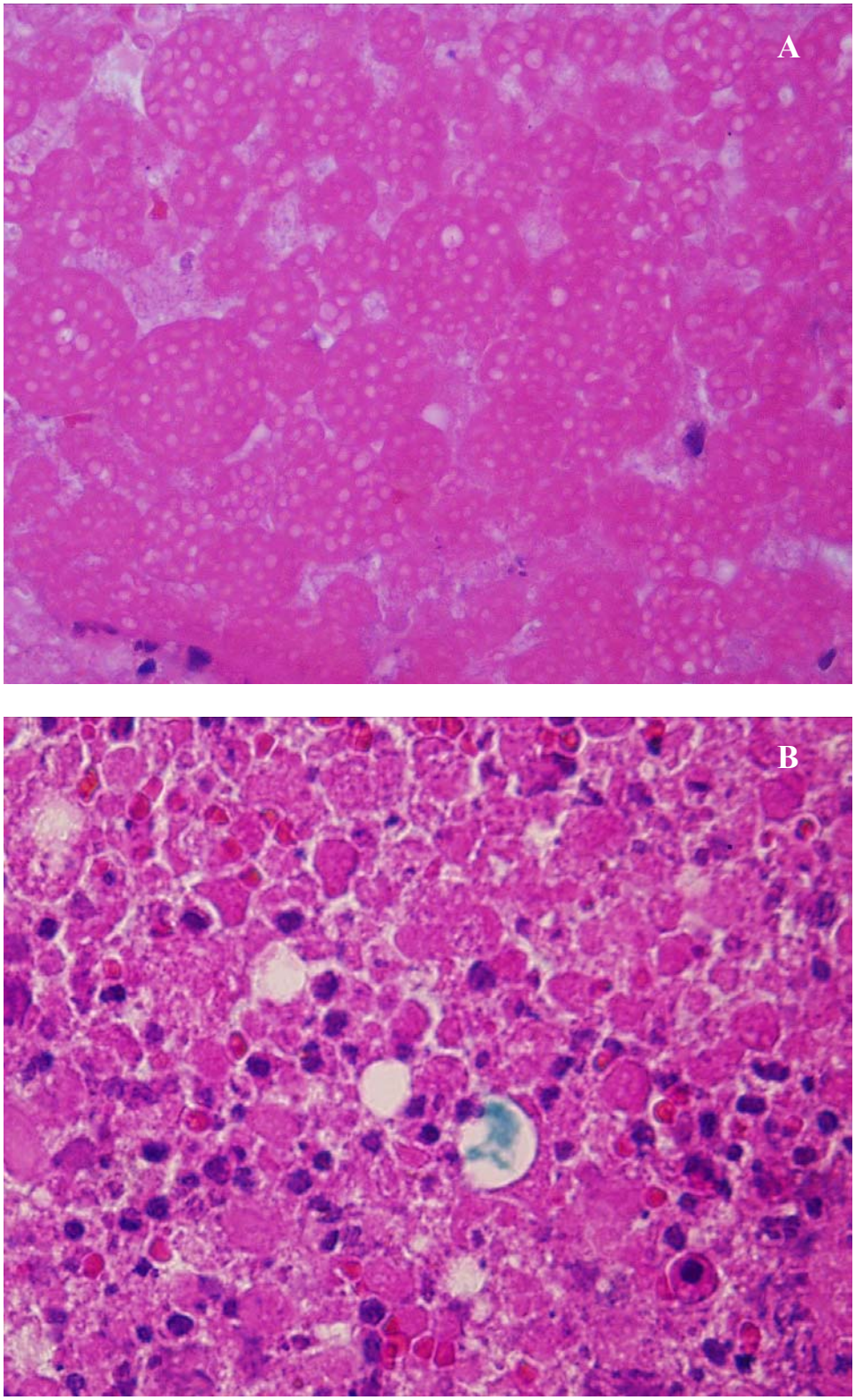

Figure 5-54 Micrographs from the same 2% GTA MS-MXN–treated tumor. A) Remnants of microspheres seen 14 days after injection. B) What appears to be MXN left in one of several holes left by microspheres. (both 100X)

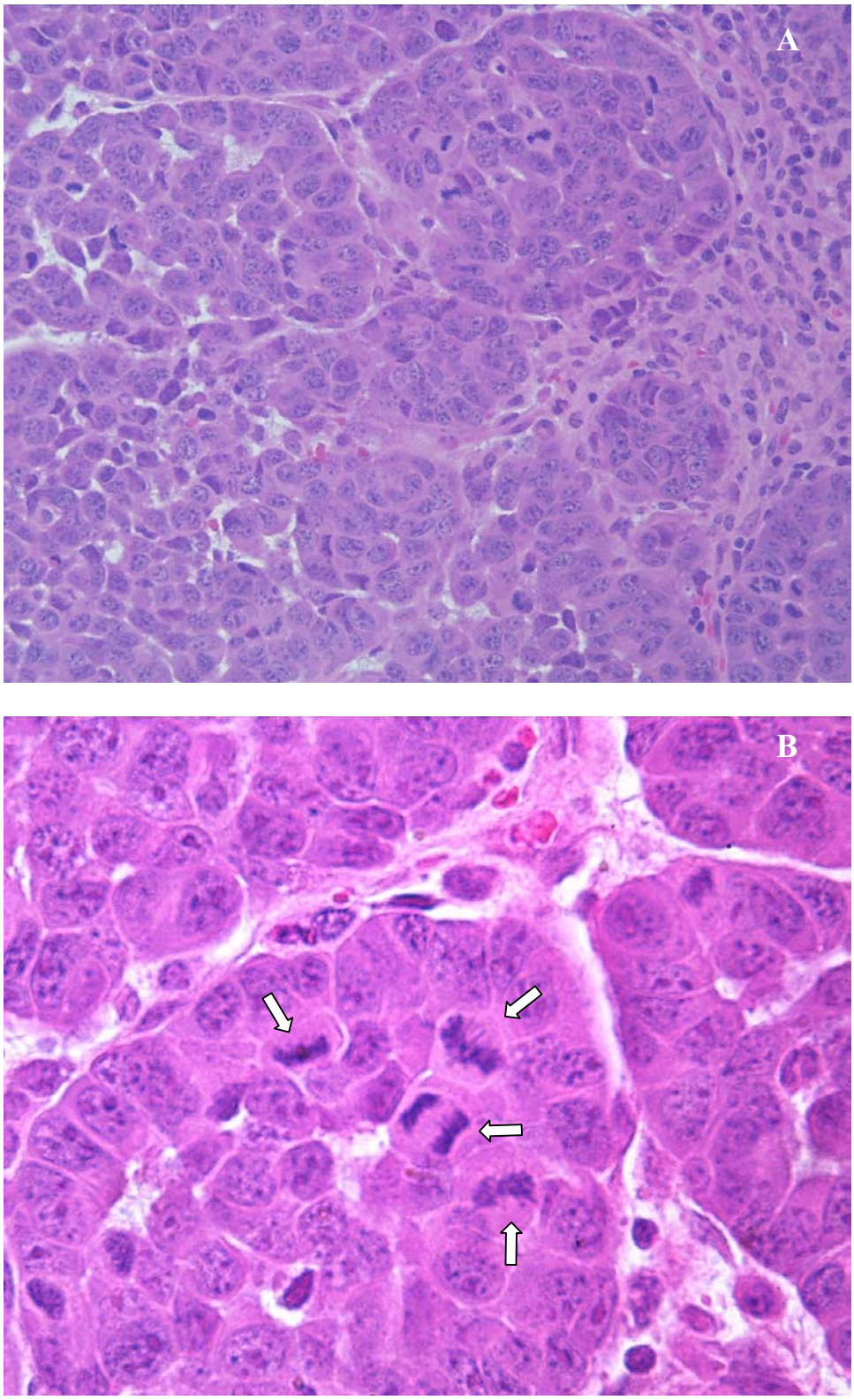

Figure 5-55 Micrographs of viable tumor tissue in an nontreated control tumor excised one day after randomization showing the lobular tissue structure and a large number of mitotic cells (arrows). A) 40X. B) 100X.

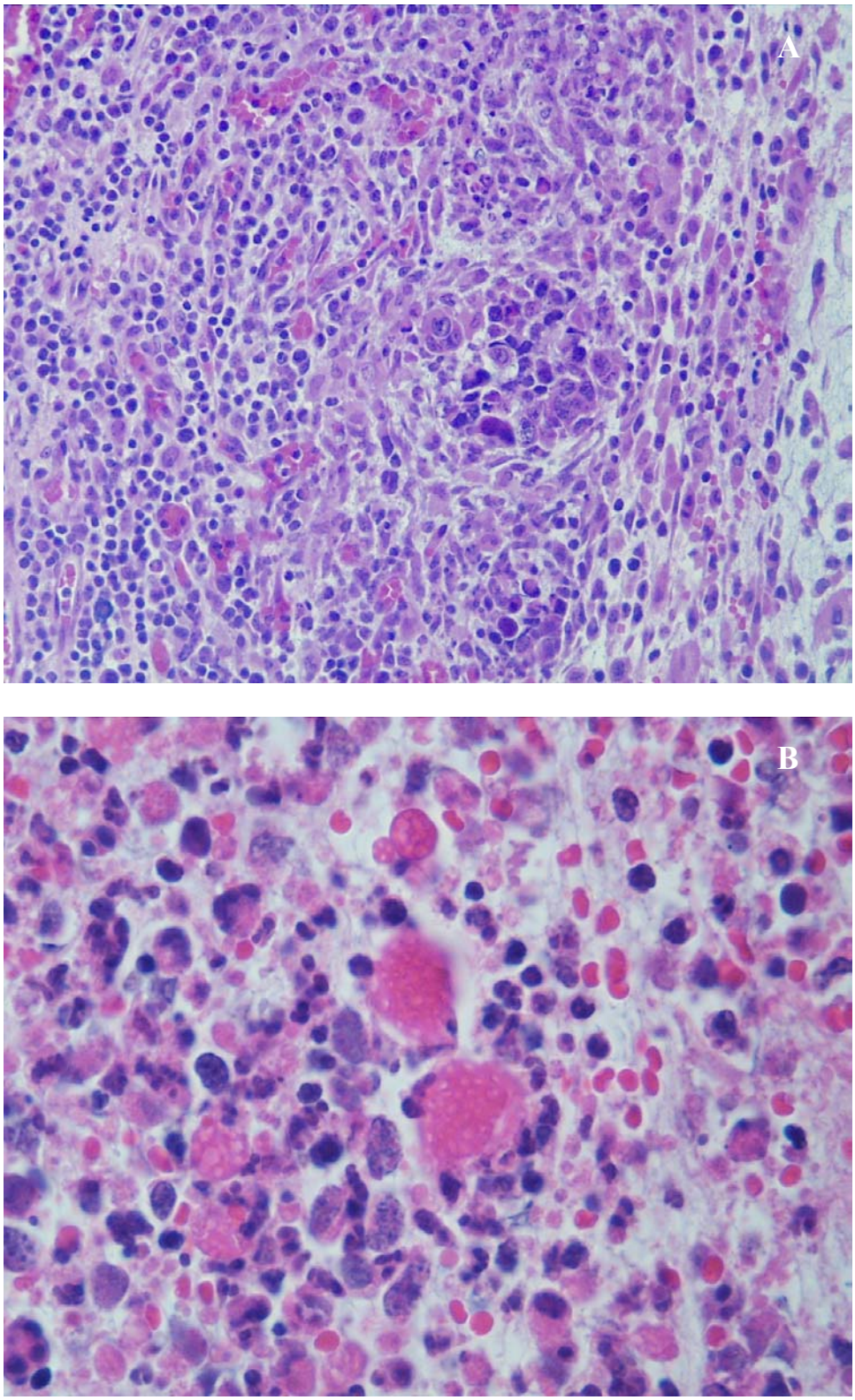

Figure 5-56 Micrographs of typical inflammation with neutrophil, macrophage, and lymphocyte infiltration. A) 20X of a nontreated control. B) 100X of a 2% GTA mesosphere [visible] treated mice.

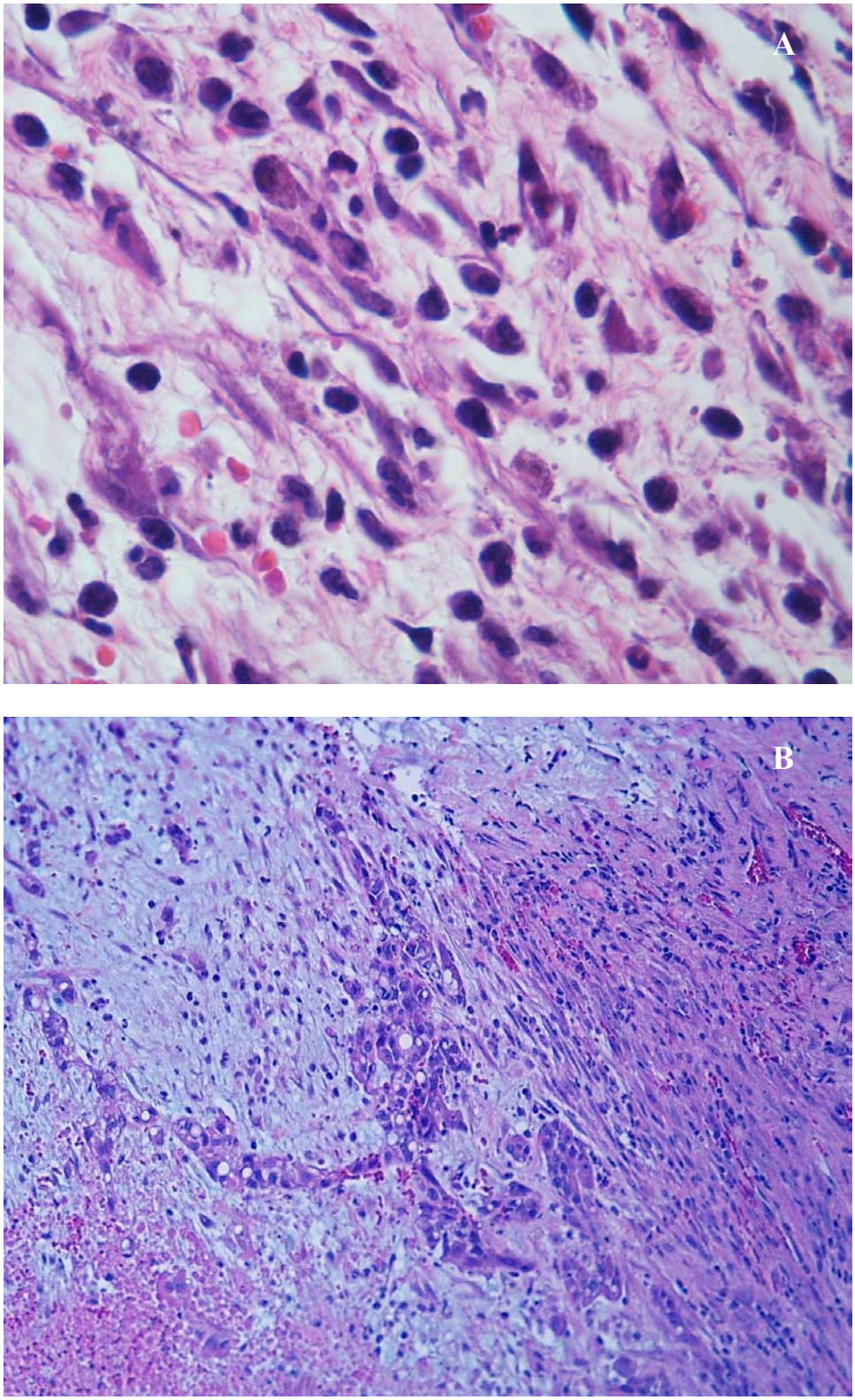

Figure 5-57 Micrographs of loose fibrous capsule typical of all tumors and tendril organization of MXN treated tumors. A) 100X. B) 20X.

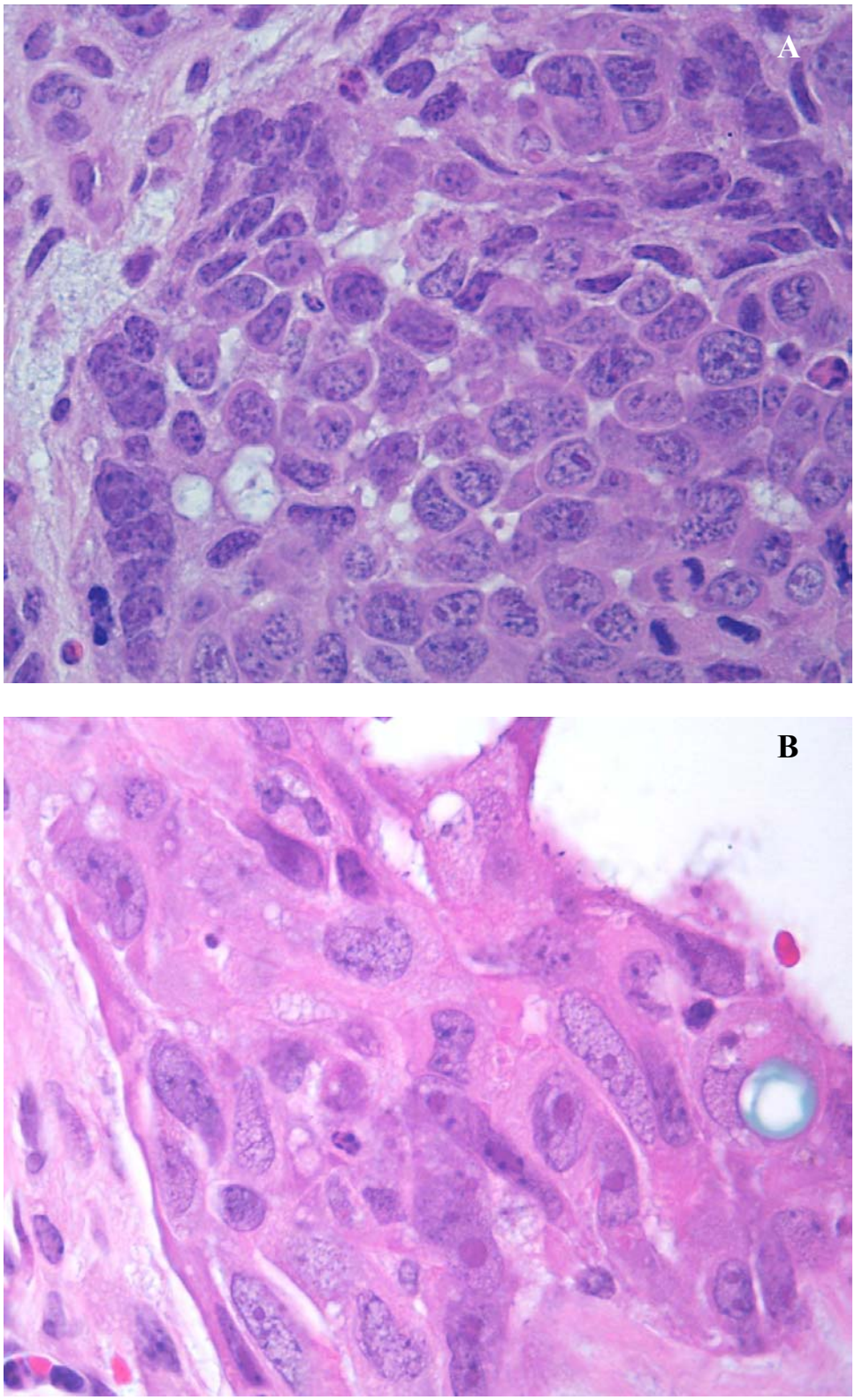

Figure 5-58 Micrographs demonstrating low and high degrees of pleomorphism. A) A nontreated tumor. B) A tumor treated with 8% GTA mesospheres with MXN visible in a cell on the right side of the image. (both 100X)

The comparison of the survival curves once again demonstrates that neoadjuvant intratumoral chemotherapy with MXN, either as free drug or mesosphere-loaded drug, is an effective treatment in this model of breast adenocarcinoma. Qualitatively, the timing of the surgical resection of the tumor mass also seemed to affect the survival at least in the control animals. The control animals that received surgery one day after randomization to treatment survived 5 days longer than those receiving surgery on Day 7. Additionally, only one of the three mice whose tumors were excised two weeks after the intratumoral injection of F-MXN survived to Day 40. This was probably due to the late timing of surgery allowing nonperfused regions of the tumor to grow to a significant size. An increase in size of the viable tumor mass seems to increase the chances that small foci of tumor cells are left after surgery. These small foci of neoplastic cells then divide eventually leading to clinical observation of a tumor recurrence and eventually death (euthanasia). This observation that the efficacy of the tumor excision is dependant upon the size of the tumor at surgery correlates well with the human clinical evidence that the tumor size (which along with lymph node involvement and distant metastasis are used to determine the stage of the cancer) is predictive of the patient's prognosis.

Table 5-20 Survival statistics for 16/C MAC for the histology and neoadjuvant intratumoral chemotherapy study.

	Controls		F-MXN			MS-High			MS-Low		
Day of surgery	Day 1	Day 7	Day 1	Day 7	Day 14	Day 1	Day 7	Day 14	Day 1	Day 7	Day 14
# Surviving sugery	3	3	3	1	3	3	3	3	3	2	3
Median survival [a]	21	16	**	**	33	**	**	**	**	34	**
ILS [b]			> 150%	> 150%	106%	> 150%	> 150%	> 150%	> 150%	113%	> 150%
%Cures [c]	0%	0%	100%	100%	33%	100%	100%	100%	100%	50%	100%

[a] Time until reaching 50% survival after treatment (in days).

[b] Percent increase in median lifespan after surgery compared to median for all controls (16 days).

[c] Animals alive 40 days after the surgical excision of the tumor mass.

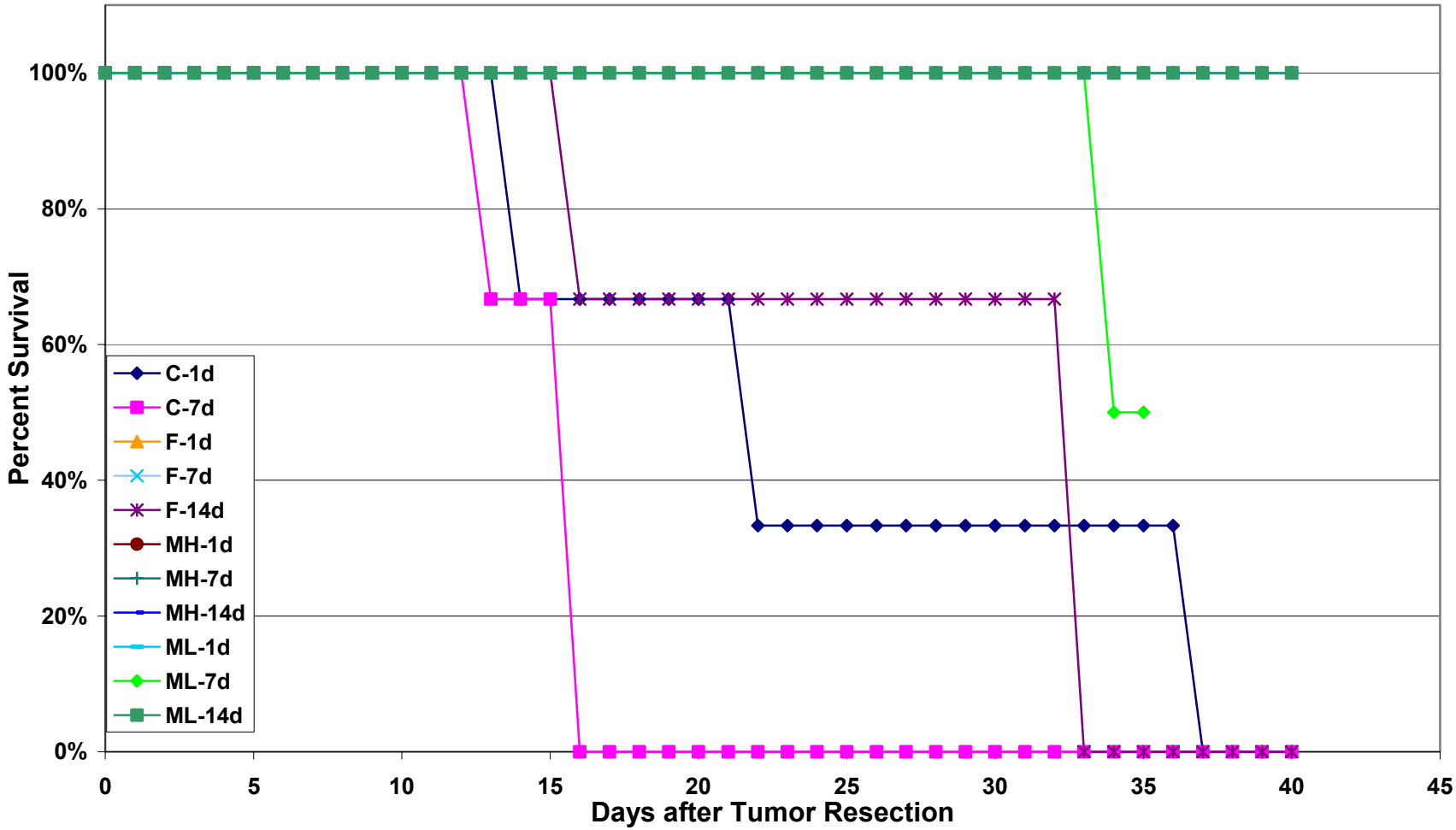

Figure 5-59 Survival graph for mice treated with neoadjuvant IT MXN either as F-MXN or as a combination of 5 to 10 μm MS-MXN (24 mg/kg) and F-MXN (4 mg/kg). Mice were treated on Day 0.

5.8 Scheduled Injections of Intratumoral Chemotherapy

5.8.1 Introduction

Multiple scheduled courses of treatment are routinely used in the clinical treatment of human breast and other cancers. Thus, it was of interest to evaluate the efficacy of intratumoral MXN delivered in a multiple injection regimen. The most common chemotherapy regimen used to treat human breast cancer consists of 4 to 6 courses of chemotherapy delivered at 3 to 4 week intervals.[112] The chemotherapy treatments are spaced 3 to 4 weeks apart to allow the patient to recover from any treatment-associated toxicity before the next course is given.[15] It was hypothesized based on the previous studies of the efficacy of single IT injections of MXN that the use of multiple injections might allow growing nonperfused regions of the tumor, which led to treatment failure in the previous studies, to be detected and adequately treated.

It was hypothesized that the opportunity to re-inject the tumor would lead to significant increases in survival time and the number of cured animals. It was also known that inadequately treated animals usually reached a tumor size equal to 10% of their body weight between three to four weeks after treatment. Since it takes on average a week to 10 days for a growing tumor to reach this mass, based on the measurements of control animals, it was decided that animals would need to be treated on a shorter interval than the three week one used clinically. An interval of one week between three IT injections was therefore chosen despite the knowledge that this short interval might lead to increased toxicity. Treatments in this study consisted of either F-MXN, MS-MXN (using 8% GTA, 5 to 10 μm mean diameter mesospheres), or nontreated control animals. The MXN treatments were repeated at one-week intervals for a total of three injections. The doses used were 8mg/kg, 4 mg/kg, and 4 mg/kg of F-MXN for each injection

respectively or 24 mg/kg of MS-MXN combined with 4 mg/kg F-MXN for all three injections. The study design is shown in Table 3-6.

All of the mice received their first two intratumoral treatments. One mouse randomized to the F-MXN treatment group received a 4 mg/kg dose of F-MXN for its first injection instead of the appropriate 8 mg/kg dose. Ten out of the twenty MXN treatment animals did not receive the third intratumoral injection. Four animals did not receive their third injection because there was no measurable tumor mass left fourteen days after the initial treatment (3 F-MXN and 1 MS-MXN), and the small palpable nodules were felt to represent scar tissue rather than a viable tumor mass. Three more animals did not receive the third injection because they had a body weight loss greater than 15% on Day 14 (all 3 were MS-MXN). The other three animals that did not receive their third injection were dead on Day 14 (1 F-MXN due to tumor progression and 2 MS-MXN due to body weight loss greater than 20%). All response variables were analyzed on an intent-to-treat basis.

One control animal was omitted from the analysis of survival time. This mouse developed a spontaneous regression of the tumor mass. The body weight and tumor size data were not anomalous for at the time points studied. Therefore, data for this mouse were included in these analyses. In the several hundred animals injected with the 16/C MAC tumor line by this research group, spontaneous regression has been observed in less than 1% of the animals. Therefore, this animal was considered an outlier and unrepresentative of the normal course of nontreated tumor progression.

5.8.2 Body Weight

Analysis of the NTABW data for this study clearly showed that the MS-MXN dose was rather high and produced significant toxicity. Average NTABW data for each

group are shown in Figure 5-60. Statistical analysis of the NTABW data for Day 5 after treatment showed that the MS-MXN treatment group had significantly lower body weights (one-way ANOVA, $p = 0.002$; followed by Tukey's MCT, family error rate < 0.05). There was no statistical difference in the NTABW of the F-MXN treatment group compared to the nontreated controls. Comparisons of the NTABW for the two MXN treatment groups were also performed at the time of the second and third injections (Days 7 and 14). The MS-MXN treatment group was found to have significantly lower NTABW at both time points (two-sample T-test, $p = 0.001$ and $p = 0.013$ respectively). The NTABW of the MXN treated mice was also compared 3 and 4 weeks after the initiation of treatment. The F-MXN treated mice had significantly higher NTABW's at 3 weeks, but not 4 weeks, after the initial treatment (two-sample T-test, $p = 0.045$ and $p = 0.206$ respectively). Six out of the ten mice treated with MS-MXN suffered a weight loss greater than 15% at some time point, with three animals missing their third injection and two requiring euthanasia before their third injection due to excessive weight loss.

The significantly increased toxicity of the MS-MXN treatment was most likely due to both the high level of MXN delivered in the formulation and the prolonged release of MXN, which did not allow for recovery prior to the second and third injections. The five animals that did receive the third MS-MXN dose tolerated it quite well. Theses five animals maintained a stable weight or actually gained weight relative to Day 14 after the last injection. The maximum toxicity for the MS-MXN treatment occurred between Days 10 and 13, between the second and third injections. This coincides relatively well with leukocyte nadirs, which are reported to occur 7 to 10 days after a single injection of MXN.[33] It is uncertain why no additional toxicity was observed after the third injection.

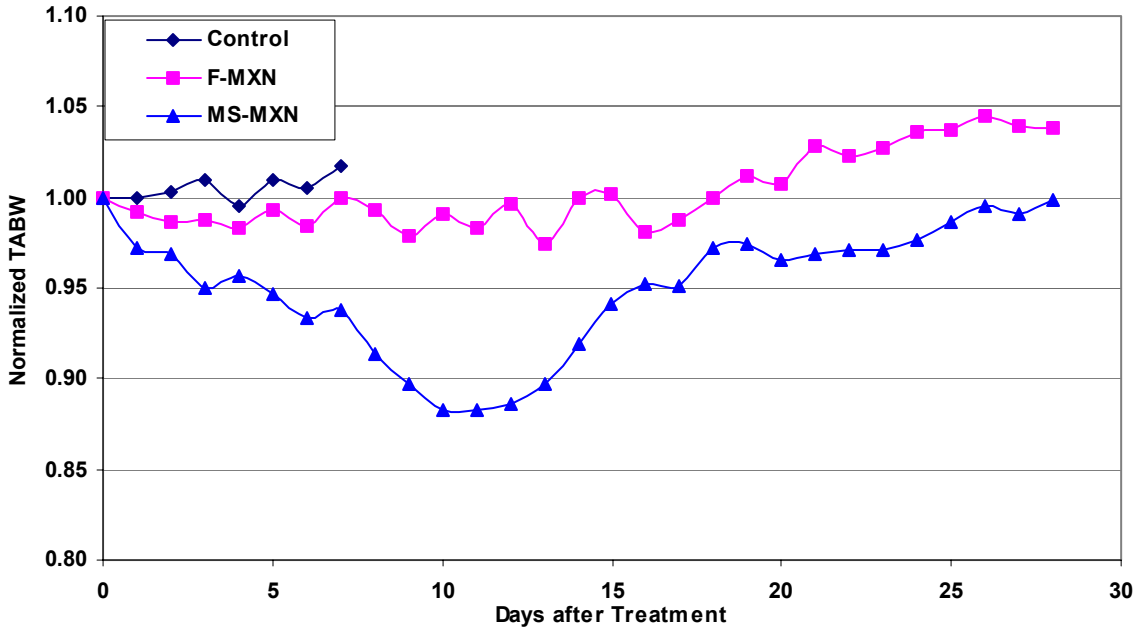

Figure 5-60 Average NTABW for mice treated with intratumoral injections of F-MXN or MS-MXN combined with F-MXN once a week for 3 weeks. Injections occurred on Days 0, 7, and 14.

5.8.3 Tumor Growth

Analysis of the tumor growth data shown in Figure 5-61 reveals that both IT MXN treatments effectively inhibited tumor growth. Data was analyzed on Days 5, 10, and 14 after the initial treatment to allow for direct comparison to the previous studies using a single IT injection, and on Day 7 in order to include the time of the second injection. Both the F-MXN alone and the combination treatment had significantly smaller tumors on Day 5 after IT injection compared to nontreated controls (one-way ANOVA, $p < 0.001$; followed by Tukey's MCT, family error < 0.05). No significant difference in tumor size was detected between the MS-MXN and F-MXN treatment groups on Days 5, 7, 10, 21, or 28. The tumors in the F-MXN treatment group were significantly smaller than those in the MS-MXN group on Day 14 (two-sample T-test, $p = 0.037$). However, this analysis is somewhat confounded by the flattening of the tumor mass after intratumoral injection with MXN, which leads to an overestimation of

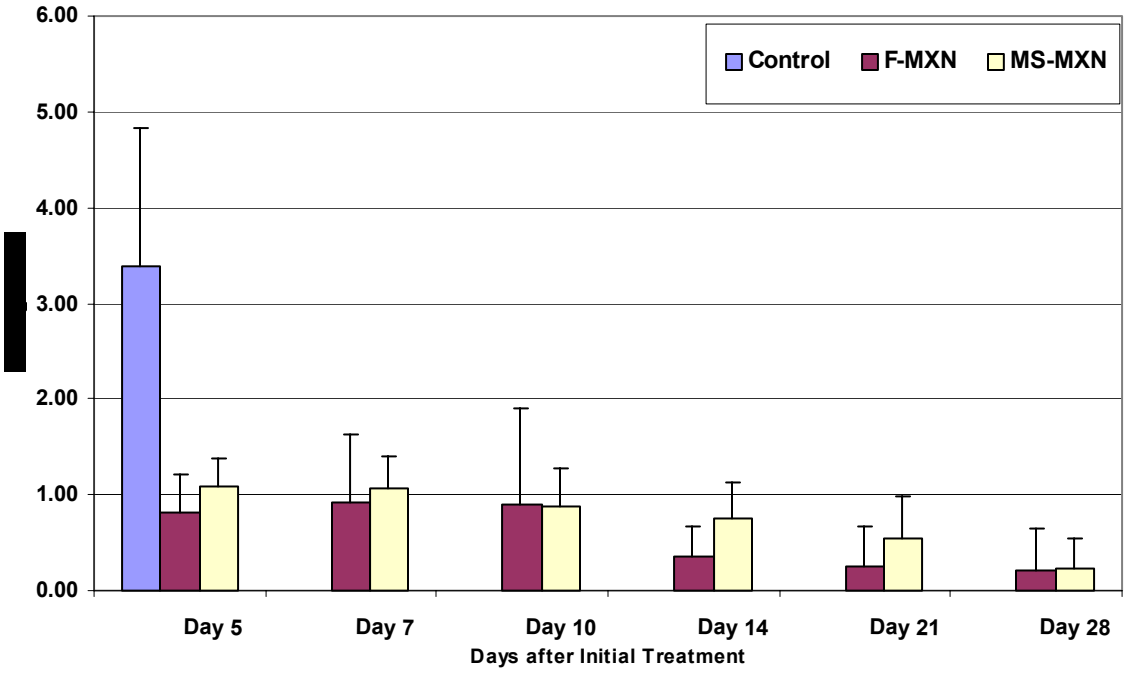

Figure 5-61 Average NTW for mice treated with intratumoral injections of F-MXN or MS-MXN combined with F-MXN once a week for 3 weeks.

the tumor size by the equation based on the volume of an ellipsoid. The MS-MXN treatment also seems more likely to produce a dense nodule, presumably of scar tissue, than the F-MXN treatment. The measurement of this noncancerous scar tissue also resulted in the size of the MS-MXN tumors being overestimated at the later time points the study.

5.8.4 Survival

Both of the MXN containing intratumoral treatment used in this study were very effective in curing the animals of their tumors. The Kaplan-Meier survival curves for each of the three treatments in this study are shown in Figure 5-62. Statistical analysis of these curves shows that both of the MXN treatments had a significantly better survival curve than the nontreated control group (log-rank test, $p < 0.0001$ for both groups). Neither the F-MXN alone or the combination MS and F-MXN containing IT treatments was statistically better than the other.

There were however qualitative differences between the effects of the two MXN treatments. The most significant problem with the MS-MXN containing treatment was toxicity, with 60% of the treated animals suffering from a greater than 15% decrease in their TABW. However, all three of the animals who did not receive the third injection due to body weight loss survived for at least 40 days and were judged cured of their tumors. Only one animal in this group was euthanized as a result of tumor growth. It survived for 38 days after the initial treatment, which represents a 375% increase in life span compared to the mean for the nontreated controls. Treatment failure in the F-MXN treated animals was due to tumor growth. One animal did not respond to treatment and it's tumor reached 10% of its body weight on Day 13. Two other animals' tumors initially responded to treatment, but eventually resumed growth. These animals survived for 32 and 36 days after the initial IT treatments. The survival outcomes for this study are summarized in Table 5-21.

Table 5-21 Survival statistics for 16/C MAC treated with scheduled injections.(three IT injections one week apart of either 8 mg/kg of F-MXN or a combination of 24 mg/kg MS-MXN and 4 mg/kg F-MXN). The one F-MXN group mouse that died before the third injection was due to tumor growth, whereas the two deaths in the MS-MXN + F-MXN group were due to TABWL > 20%. (TABWL = tumor-adjusted body weight loss > 15%, NM = no measurable tumor).

	Control	F-MXN	MS-MXN + F-MXN
# Randomized	10	10	10
# Receiving all 3 injections	N/A	6	5
Cause for missed injections (Death / TABWL/ NM)	N/A	1 / 0 / 3	2 / 3 / 1
Median survival [a]	8	**	**
ILS [b]		> 400%	> 400%
% Cures [c]	0%	70%	70%

[a] Time until reaching 50% survival after initial treatment (in days).

[b] Percent increase in median lifespan after surgery compared to median for controls.

[c] Animals alive 40 days after the intitial treatment.

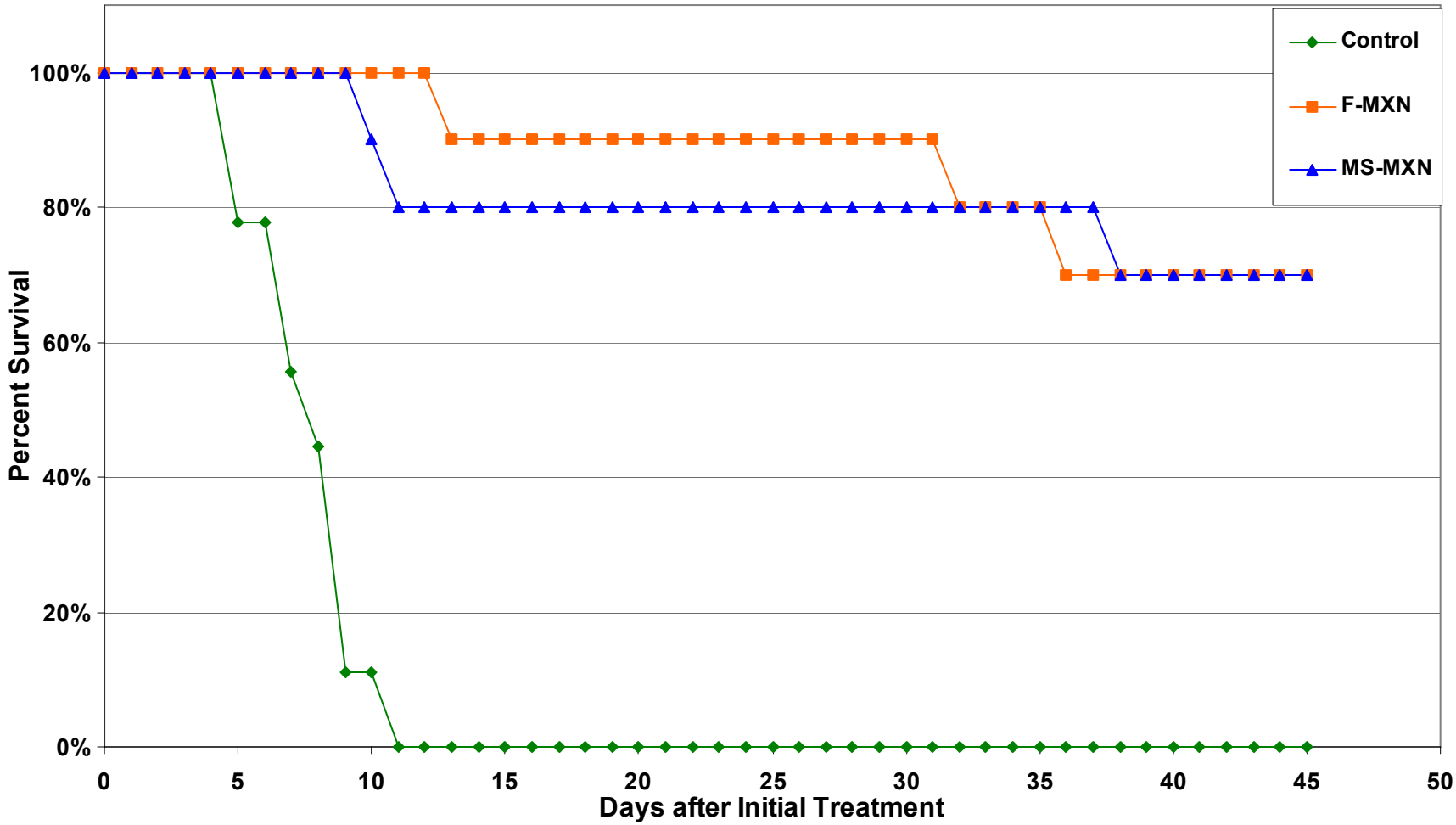

Figure 5-62 Survival plot for mice treated with three scheduled intratumoral injections of F-MXN or MS-MXN (24 mg/kg, 5 to 10 μm, 8% GTA)combined with F-MXN (4 mg/kg) delivered at one-week intervals for three weeks (on Days 0, 7, and 14).

CHAPTER 6
CONCLUSIONS

6.1 Introduction

The ultimate goal of these studies was to contribute to the establishment of a significant amount of preclinical data for intratumoral chemotherapy, which would facilitate the initiation of a Phase-I breast cancer trial in humans. With that goal in mind, the purpose of these studies was to evaluate the efficacy and toxicity of intratumoral chemotherapy using free and microsphere-loaded MXN formulations. Both IT chemotherapy alone and in combination with surgery (as a neoadjuvant therapy) were hypothesized to be efficacious treatments. The series of experiments was naturally divided into *in vitro* experiments and *in v*ivo experiments.

The specific aims for the *in vitro* experiments were as follows:

1. Synthesize MXN loaded albumin microspheres with the desired size and drug loading and release profiles for use in the *in vivo* studies.

2. To synthesize 5-FU loaded albumin microspheres as a "proof of concept" for possible use in future studies.

3. To characterize the particle size distribution and drug release of each of the drug loaded microsphere formulations synthesized.

The specific aims for the *in vivo* experiments were as follows:

1. Establish the improved efficacy of intratumoral chemotherapy compared to systemic (IV) chemotherapy both alone and as a neoadjuvant therapy.

2. To establish the efficacy of MXN loaded albumin microspheres and mesospheres for the treatment of breast cancer.

3. To compare the efficacy of intratumoral injection of free MXN and micro/mesosphere formulations loaded with MXN delivered alone, in combination, and as a neoadjuvant (preoperative) therapy.

4. To characterize the clinical and histological pathology associated with intratumoral chemotherapy.

5. To evaluate the efficacy of a series of scheduled intratumoral treatments for the treatment of breast cancer.

6.2 *In Vitro* Synthesis and Characterization of Microspheres

Mitoxantrone and 5-fluorouracil loaded albumin microspheres were successfully synthesized. All microspheres were synthesized using a suspension crosslinking technique with glutardehyde as the crosslinking agent following the general procedures previously described by Hadba.[9]

6.2.1 MXN-Loaded Albumin Microspheres

Both nonloaded and MXN-loaded BSA microspheres were produced with a mean diameter in the range of 5 to 10 μm. The particle size distribution of the microspheres was successfully controlled by adjusting the emulsion energy and the concentration of cellulose acetate butyrate, the emulsion stabilization agent. These 5 to 10μm microspheres were characterized along with larger 20 to 40 μm microspheres synthesized previously by Hadba. MXN-loaded microspheres in both size ranges crosslinked with 8% GTA were found to be smooth and spherical. The 5 to 10 μm microspheres crosslinked with 2% GTA were spherical and had a porous structure. The release of MXN from each of the three MXN-loaded albumin microsphere formulations used in the *in vivo* studies was measured in PBS at pH 7.4 and 37°C in an infinite sink condition. Both microsphere size and crosslink density (GTA concentration) were found to affect the *in vitro* release of the loaded drugs. Decreasing particle size and crosslink density

resulted in an increased rate of drug release and total percentage of loaded drug released. These results corroborate those of previous researchers studying microspheres loaded with MXN and other antineoplastic drugs.[77, 86, 89]

6.2.2 5-FU-Loaded Albumin Microspheres

Microspheres loaded with another chemotherapy drug commonly used to treat breast cancer, 5-FU, were also synthesized using an analogous protocol. These 5-FU–loaded microspheres were synthesized with three different crosslink densities, corresponding to 2, 4, and 8% GTA. Three samples of each crosslink density were prepared. The 5-FU–loaded microspheres were found to be generally spherical, with an increase in the amount of non-spherical particles observed with decreasing crosslink density. The average diameters ranged from 4 to 20 μm, and the mixer used to prepare the microspheres was found to have a greater influence on the particle size distribution than the GTA concentration.

The *in vitro* release of 5-FU from these microspheres was measured in PBS at pH 7.4 and 37°C under infinite sink conditions. The majority of the drug release occurred within the first hour, and the percentage of loaded drug released was dependant upon the crosslink density. As expected, the low crosslink-density microspheres were found to release the greatest amount of loaded drug. The rapid rate of drug release from the albumin microspheres was believed to result from the low affinity of 5-FU for the protein matrix and the presence of sodium ions within the microsphere increasing the degree of swelling.

Further studies to increase the loading and to prolong the time of release for 5-FU from albumin microspheres is warranted. The use of a combination of 5-FU and

MXN-loaded albumin microspheres in future *in vivo* studies may prove synergistic resulting in longer tumor growth remission times and higher cure rates.

6.3 *In Vivo* Evaluation of Intratumoral Chemotherapy

Based on these studies, it is concluded that intratumoral chemotherapy with free or microsphere loaded drugs is a promising modality for the treatment of solid tumors. The results presented here demonstrate that both intratumoral F-MXN and MS-MXN significantly improve survival in the 16/C murine mammary adenocarcinoma model. It is reasonable to believe that these results can generally be extended to other tumor models as well.

Intratumoral chemotherapy can localize the activity of mitoxantrone and greatly reduce systemic toxicity compared to intravenously delivered free drug. Intratumoral injections of free MXN were found to significantly improve survival and decrease toxicity. When given intratumorally in free drug form, the drug was tolerated in doses up to of 12 mg/kg compared to the published LD_{50} of 6.6 mg/kg for IV delivery. The most effective intratumoral dose of free MXN was found to be 8 mg/kg, which increased the median survival time, compared to controls. Increases of 175 to 529% were observed depending on the study. Comparatively, 4 mg/kg was the most effective IV dose. It only improved median survival 38% and produced no cured animals.

Two different size ranges of MXN-loaded microspheres were used in these studies: 5 to 10 μm mesospheres and 20 to 40 μm microspheres. Both microsphere formulations were found to significantly improve survival compared to untreated controls. Additionally, much higher doses of MXN could be delivered to the tumors using MS-MXN than were possible with F-MXN. The MTD for microsphere formulations was estimated to be around 48 mg/kg. The delivery of MS-MXN in

combination with F-MXN was found to offer improved efficacy compared to MS-MXN alone in at least one study. It is believed that this is because the F-MXN acts as a "loading dose" to the local tumor tissues and provides high local concentrations of MXN that may help to suppress the initial "burst" of drug from the microsphere formulations allowing for a more prolonged release. Cure rates as high as 80% were achieved following a single treatment with some microsphere formulations compared to 50% for IT injection of F-MXN and 0% for untreated animals. However, these studies have not conclusively shown an increased benefit from MS-MXN formulations compared to F-MXN when delivered IT.

The effect of IT MXN on blood cell counts was investigated in an attempt to elucidate the mechanism of toxicity associated with high dose MXN formulations. No evidence the expected toxicity, myelosuppression, was detected based on blood cell counts performed 1 and 14 days after a single intratumoral treatment. Changes in the leukocyte populations were found, which were consistent with a diagnosis of acute inflammation. However, this does not rule-out myelosuppression as a probable mechanism of IT therapy associated toxicity. This study may have failed to detect signs of myelosuppression because the MXN doses used were relatively well tolerated or due to the lack of data between days 1 and 14. Cell nadirs are known to occur between days 7 and 10 following IV administration of MXN. It is possible recovery may have occurred to an extent that the differences were not detected with the relatively small sample size used in this study. However, when Leftenstiener et al performed serial CBCs following the IP injection of MXN-loaded albumin microspheres they found the leukocyte nadirs persisted past 14 day after treatment.

The examination of tumors excised 1, 7, and 14 days after a single intratumoral injection of MXN showed significant differences from untreated tumors. The IT treated tumors were typically much smaller than the untreated tumors at days 7 and 14. The tumor tissue was also visibly stained dark blue to black by the injected MXN. These factors may facilitate the surgical excision of tumors in human patients. Histological examination of the IT treated tumors found them to have a significantly lower mitotic index than control tumors. However, the IT treatment was also associated with an increase in pleomorphism, which is generally considered to represent a higher grade neoplasm. The significance of the increased pleomorphism is uncertain at this time.

The most promising IT treatment modalities identified in these studies are the use of multiple scheduled injections and the combination of IT chemotherapy and surgery (as IT neoadjuvant therapy). The use of multiple scheduled injections of MXN was shown to be very effective in producing complete regression of the tumors without tumor recurrence. Both F-MXN and the combination of MS-MXN and F-MXN delivered in three courses at one-week intervals produce 70% survival rates. Even higher survival rates may be achieved with further research to identify optimal dose levels since 20% of the mice receiving combination therapy died of toxicity rather than resistance to treatment or tumor recurrence, which represents 2 out of the 3 failures for that treatment. The combination of neoadjuvant (preoperative) intratumoral injection of 5 to 10 μm mesospheres followed by surgical excision of the tumor 1 to 14 days later produced cure rates as high as 100% in several treatment groups. The neoadjuvant IT treatment of the tumors was also found to facilitate the excision of the tumor by causing regression in tumor size and local tissue involvement compared to the nontreated controls.

It is important to note that any potential new treatment for breast cancer must have a systemic effect, or be incorporated into a regimen that includes systemically active therapies. This statement is based upon the Fisher hypothesis of breast cancer, which states that human breast cancer should be considered a systemic disease because of the high probability that distant metastasis has already occurred by the time of diagnosis. This view has recently gained acceptance over the prior Halstead theory, which stated that breast cancer was a local disease that spread in an orderly fashion throughout the body. Halstead's point of view was used to justify the use of increasingly extensive surgeries in order to contain the locally metastasizing breast cancer. Fisher's hypothesis, which has been supported by a number of studies over the last thirty years, promotes the use of less extensive surgeries in combination with systemic therapies such as adjuvant chemotherapy.[15, 113]

The future role of intratumoral chemotherapy in the Fisher era of breast cancer treatment lies in the reconciliation of what at first glance appears to be a local therapy for the treatment of a systemic disease. This may be achieved by therapeutically monitoring the systemic concentration of drugs released from microspheres and supplementing with IV drug, as needed. Alternatively, microspheres may be used to locally deliver drugs such as MXN or adriamycin to the primary tumor mass, while other drugs currently used as part of the combination chemotherapy regimens, such as cyclophospamide or 5-FU, are delivered systemically (IV). Perhaps the most promising role for intratumoral therapy is as a neoadjuvant treatment in order to reduce the size and grade of the primary tumor mass prior to surgical excision, allowing for an increased use of tissue conserving operations. Finally, the most exciting role for IT therapy would be if formulations were

developed which consistently sensitized the immune system to the tumor cells, thereby allowing the body's natural defenses to clear it of systemic (metastatic) disease. A process that is greatly hindered in conventional therapies by the damage systemic cytotoxic therapy does to the immune system.

The results of these studies strongly support the improved efficacy of IT cytotoxic chemotherapy. Previous studies performed at the University of Florida also demonstrated that greatly increased survival and cure rates are produced by intratumoral chemotherapy using Mitomycin C, adriamycin, and mitoxantrone in a number of animal tumor models.[2] Additionally, intra- or peritumoral injection of free MXN with the goal of staining the sentinel lymph nodes has been reported to be safe and well tolerated in human breast cancer patients at doses up to 1.0 mg (four times the dose used in the 12 mg/kg F-MXN treated mice).[70] Based on the results of these preclinical studies in a murine mammary adenocarcinoma, it is believed that neoadjuvant intratumoral chemotherapy with either free or microsphere-loaded MXN would likely significantly decrease the size of the tumor mass at surgery, act as a stain to visibly identify the sentinel lymph nodes, and ultimately facilitate the use of increasingly tissue-conserving surgeries.

In view of the results reported here and in the literature, it is believed that a Phase-I human clinical study of neoadjuvant therapy of breast cancer, using either free or albumin microsphere-loaded MXN, may be warranted in the near future. The use of the 8% GTA 5 to 10 μm MXN-loaded albumin mesosphere formulation injected one to two weeks prior to the surgical excision of the primary tumor using a tissue conserving procedure with dissection of the sentinel lymph node(s) would be a viable protocol based upon these studies. Important response variables for such a study would include tumor

size/regression, extent of required surgery, positive staining of the primary tumor and the sentinel lymph nodes, and local-regional recurrence of breast cancer.

CHAPTER 7
FUTURE WORK

7.1 Introduction

During the course of performing these experiments, many new potential avenues for this research were put forward and many old concepts drew renewed attention. Those concepts that were deemed to deserve future attention and development are summarized here.

7.2 Future Directions in Microsphere Synthesis

First, there has always been interest in increasing the weight percent drug loading of the microsphere formulations. The early work by Longo and Iwata on albumin microspheres showed that one avenue to accomplish this was the preparation of microspheres whose matrix is compared of a blend of protein and polyionic polymers.[77, 78] The polyionic component allows for an increased affinity of the loaded drug for the microsphere matrix due to ionic interactions. For example, increased loading of cationic drugs such as MXN could be increased by the incorporation of polyanionic polymers, such as polyglutamic acid and polyacrylic acid, into the micosphere's matrix. This concept has not received much attention in the past few years and should be considered as a prime subject for future research efforts.

Second, interest has also arisen in the use of other crosslinking agents besides glutaraldehyde. Of particular recent interest is the use of the naturally occurring compound, Genipen. This compound is derived from the jasmine flower and has been shown to be significantly less cytotoxic than glutaraldehyde, in some studies.[114] Other

research groups have successfully developed genipen crosslinked chitosan (a positively charged polysaccharide) microspheres using genipen as a crosslinking material. These genipen crosslinked chitosan microspheres have been implanted into the skeletal muscle tissue of rats and were found to stimulate significantly less of an inflammatory reaction than similar glutaraldehyde crosslinked microspheres.[115] The real potential benefit of such less cytotoxic and inflammatory microspheres lies not in the treatment of cancer, but in other therapeutic areas where decreased cytotoxicity would be advantageous. For example, they could be loaded with antibiotics or anti-inflammatory drugs and injected within the joint capsule to treat septic or inflammatory joint diseases, such as occur in rheumatoid arthritis and other autoimmune diseases.

Third, renewed effort should be put forth to develop, and eventually test, microspheres loaded with immune-modulating agents, such as IL-2, IL-12, TNF, BCG cellwall preparations, lipopolysaccharides (LPS), and DMPL. It is through the use of such immune-modulators that the greatest chance of realizing the "*in vivo* vaccine-like" effects observed with some intratumoral therapies lies.[2, 61, 62, 86, 116] The development of such an *in vivo* vaccine could potentially be one of the most clinically beneficial new developments in the treatment of breast cancer.

Fourth, the studies detailed in this work consistently failed to demonstrate significant differences between most intratumoral treatment doses. This is possibly due to variability in the dose actually delivered to the tumor mass, in addition to the small size of most treatment groups. No studies thus far have addressed the amount of variation in the MS-MXN delivered to a tumor that results from such factors and the incomplete suspension of the microspheres prior to loading into the syringe, settling of

the microspheres within the syringe barrel, and the leaking of injected formulations from the injection site.

7.3 Future *In Vivo* Directions

First, the clinical effect of intratumoral chemotherapy needs to be further studied. Specifically, further studies should be conducted with the express intent of determining the mechanism of toxicity associated with intratumoral chemotherapy using MXN. Such as study should include serial CBCs with more time points than the study included herein and using higher dose levels that are known to produce significant, but not fatal, toxicity. Possible candidates would include doses of MS-MXN between 40 and 48 mg/kg. Furthermore, such studies should incorporate MS-MXN and F-MXN only treatments in order to determine the separate effects of each. Additionally, extensive histological examination of tissues known to be targets of cytotoxic drug associated toxicities should be conducted at predetermined time points corresponding to the time of greatest toxicity. Based on the body weight loss data gathered in these studies, time points of 7 to 10 days should be targeted. Specifically, tissues such as bone marrow, cardiac muscle, lung, and intestinal epithelium should be examined.

Second, further studies should be conducted to determine the mechanism of improved efficacy for IT chemotherapy. It is hypothesized that the treatment advantage is a pharmacokinetic one. Few studies to date have focused on the pharmacokinetics of IT chemotherapy with any drug, much less MXN. Specifically attempts should be made to determine the concentration of free MXN with the tumor tissues compared to the plasma. Potential techniques for this include microdialysis of the tumor tissue and the use of tissue-isolated perfused tumors.[117, 118] Additionally, it would be very interesting if this pharmacokinetic data could be correlated with the *in vivo* evaluation of intratumoral

injections. This could potentially be done using ^{31}P NMR to monitor the metabolism of the tumor and it's response to chemotherapy. Such analysis has been used before to study the effects of systemic chemotherapy, irradiation, and hyperthermia on the 16/C MAC tumor model.[119]

Third, it would be beneficial to conduct a small study to determine the volume of tumor tissue perfused by a single IT injection of MXN. The clinical opinion developed throughout these studies was that IT treatment failure was frequently a result of the incomplete perfusion of the tumor mass with the drug. This hypothesis was supported by the correlation between tumors observed to have incomplete perfusion (as determined by the dark blue staining of the tissue by MXN) and tumor recurrence following surgical resection in the histology and neoadjuvant therapy study. The volume of tumor perfused by MXN following a single injection should be readily discernable by observing sectioned tumors with the naked eye. It should be noted that the tumors must be observed either fresh or frozen, because the alcohol used in the embedding of tissues will extract (and redistribute) MXN from both microspheres and the stained MXN tissues. Such examination my prove that better perfusion is obtained with a single injection with a slow infusion of drug than with the five peripheral injections used in these studies. The multiple injections may function more to facilitate the leakage of the MXN (free or microsphere loaded) solution from the tumor than to ensure a diffuse distribution of microspheres and/or free drug as was originally intended.

Fourth, the development and testing of combination chemotherapy given in scheduled doses should be explored in the 16/C MAC and other metastatic cancer models. One such potential therapy would be cyclophosphamide (intraperitoneal)

combined with 5-FU and MXN-loaded albumin microspheres (delivered IT). It should be noted that cyclophosphamide is not a candidate for IT delivery because it must be activated within the liver before it has any therapeutic efficacy. Combination chemotherapy has been shown to have significant clinical advantages over monotherapy, and it is reasonable to believe that this treatment synergy would extend to combination intratumoral therapy.[17, 54, 120]

Fifth, ultimately an optimum intratumoral therapy should be identified for potential use in a Phase-I clinical study. In order to do this, a large study similar to the IV vs. IT chemotherapy study should be performed. This study should include the use of intratumoral chemotherapy in a neoadjuvant setting as this is most likely the best opportunity for future clinical use. Treatments should include IT MS-MXN formulations alone and in combination with F-MXN directly compared to F-MXN delivered IT and IV alone. Surgical excision should be performed at an early enough to allow direct comparison of survival with surgical control groups, but late enough to allow the acute inflammation observed one day after injection to subside.

7.4 Clinical Use

Ultimately the goal of any studies of the kind contained herein is to identify therapies that have a potential clinical benefit to patients. It is would be desirable to initiate Phase-I clinical trials of intratumoral chemotherapy, using MXN, for the treatment of breast cancer in the near future. Such a study should involve the use of IT MXN, either as free drug or loaded into microspheres, used in the neoadjuvant setting. The study should initially focus on the response of the primary tumor to therapy, specifically assessing treatment associated changes in tumor size and grade, the staining

and status of the sentinel lymph nodes, and the facilitation of more tissue conserving surgeries.

LIST OF REFERENCES

1. SEER Cancer Statistics Review, 1973-1997. Ries LAG, Eisner MP, Kosary CL, Hankey BF, Miller BA, Clegg L, Edwards BK, eds. http://seer.cancer.gov/Publications/CSR1973_1997/. Bethesda, MD: National Cancer Institute, 2000.

2. Goldberg EP, Hadba AR, Almond BA, Marotta JS. Intratumoral cancer chemotherapy and immunotherapy: opportunities for nonsystemic preoperative drug delivery. J Pharm Pharmacol 2002; 54:159-80.

3. Scanlon EF. The evolution of breast cancer treatment. JAMA 1991; 266:1280-1282.

4. Smith G, Henderson IC. New treatments for breast cancer. Semin Oncol 1996; 23:506-28.

5. Lewis C. Breast cancer: better treatments save more lives. FDA Consumer, http://www.fda.gov/fdac/499_toc.html 1999; 33:accessed 11/22/2002.

6. Carlson RW. Continuous intravenous infusion chemotherapy. In: Perry MC, ed. The chemotherapy source book. Baltimore: Williams & Wilkins, 2001:144-163.

7. Faulds D, Balfour JA, Chrisp P, Langtry HD. Mitoxantrone: a review of its pharmacodynamic and pharmacokinetic properties, and therapeutic potential in the chemotherapy of cancer. Drugs 1991; 41:400-449.

8. Hadba AR, Marotta JS, Goldberg EP. Effect of loading method on drug content and *in vitro* release of mitoxantrone from albumin microspheres, Trans Sixth World Biomat Cong, Kamela, Hawaii, 2000. Vol. 2.

9. Hadba AR. Synthesis, properties, and in vivo evaluation of sustained release albumin-mitoxantrone microsphere formulations for nonsystemic treatment of breast cancer and other high mortality cancers. Ph.D. Dissertation. Gainesville: Univ. of Florida, 2001.

10. Adjuvant therapy for breast cancer. NIH Consensus Statement Nov 1-3 2000; 17:1-35.

11. SEER Cancer Statistics Review, 1973-1998. Ries LAG, Eisner MP, Kosary CL, Hankey BF, Miller BA, Clegg L, Edwards BK, eds. http://seer.cancer.gov/Publications/CSR1973_1998/. Bethesda, MD: National Cancer Institute, 2001.

12. Breast cancer facts and figures 2001-2002. http://www.cancer.org/downloads/STT/BrCaFF2001.pdf. Atlanta, GA: American Cancer Society, 2001:accessed 11/22/02.

13. Lifetime probability of breast cancer in American women. http://cis.nci.nih.gov/fact/5_6.htm. Cancer Facts: Fact Sheet 5.6: National Cancer Institute, 2002:accessed 11/22/2002.

14. Kelsey JL, Horn-Ross PL. Breast cancer: magnitude of the problem and descriptive epidemiology. Epidemiol Rev 1993; 15:7-16.

15. Kardinal CG, Cole JT. Chemotherapy of breast cancer. In: Perry MC, ed. The chemotherapy source book. Baltimore: Williams & Wilkins, 2001.

16. Kelsey JL, Bernstein L. Epidemiology and prevention of breast cancer. Ann Rev Public Health 1996; 17:47-67.

17. Schwarz JK, Yarbro JW. Scientific foundation of chemotherapy. In: Perry MC, ed. The chemotherapy source book. Baltimore: Williams & Wilkins, 2001.

18. Skipper HE. Historic milestones in cancer biology: a few that are important in cancer treatment (revisited). Semin Oncol 1979; 6:506-14.

19. Goldie JH, Coldman AJ. A mathematic model for relating the drug sensitivity of tumors to their spontaneous mutation rate. Cancer Treat Rep 1979; 63:1727-33.

20. Kaufman DC, Chabner BA. Clinical strategies for cancer treatment: the role of drugs. In: Chabner B, Longo DL, eds. Cancer chemotherapy and biotherapy : principles and practice. Philadelphia: Lippincott Williams & Wilkins, 2001:1-16.

21. Skipper HE. Dose intensity versus total dose of chemotherapy: an experimental basis. Important Adv Oncol 1990:43-64.

22. Viens P, Maraninchi D. High-dose chemotherapy in advanced breast cancer. Crit Rev Oncol Hematol 2002; 41:141-9.

23. Antman KH. A critique of the eleven randomised trials of high-dose chemotherapy for breast cancer. Eur J Cancer 2001; 37:173-9.

24. Antman KH. Randomized trials of high dose chemotherapy for breast cancer. Biochim Biophys Acta 2001; 1471:M89-98.

25. Ensminger WD. Intraarterial therapy. In: Perry MC, ed. The chemotherapy source book. Baltimore: Williams & Wilkins, 2001:163-174.

26. Forman A, Levin VA. Intraventricular and intrathecal therapy. In: Perry MC, ed. The chemotherapy source book. Baltimore: Williams & Wilkins, 2001:132-141.

27. Markman M. Intraperitoneal chemotherapy. In: Perry MC, ed. The chemotherapy source book. Baltimore: Williams & Wilkins, 2001:141-144.

28. Markman M. Principles of regional antineoplastic drug delivery. In: Markman M, ed. Regional chemotherapy: clinical research and practice. Totowa, NJ: Humana Press, Inc., 2000:1-4.

29. Matsushima Y, Kanzawa F, Hoshi A, Shimizu E, Nomori H, Sasaki Y, Saijo N. Time-schedule dependency of the inhibiting activity of various anticancer drugs in the clonogenic assay. Cancer Chemother Pharmacol 1985; 14:104-7.

30. Fraile RJ, Baker LH, Buroker TR, Horwitz J, Vaitkevicius VK. Pharmacokinetics of 5-fluorouracil administered orally, by rapid intravenous and by slow infusion. Cancer Res 1980; 40:2223-8.

31. Meta-analysis Group In Cancer: Efficacy of intravenous continuous infusion of fluorouracil compared with bolus administration in advanced colorectal cancer. J Clin Oncol 1998; 16:301-308.

32. Durr FE, Wallace RE, Citarella RV. Molecular and biochemical pharmacology of mitoxantrone. Cancer Treat Rev 1983; 10 Suppl B:3-11.

33. Riggs CE. Antitumor antibiotic and related compounds. In: Perry MC, ed. The chemotherapy source book. Baltimore: Williams & Wilkins, 2001.

34. Beijen JH. Mitoxantrone hydrochloride. In: Florey K, ed. Analytical profiles of drug substances. Vol. 17. New York, N.Y.: Academic Press, 1988:221-258.

35. Birchall LA, Bailey NP, Blackledge GR. An overview of mitozantrone. Br J Clin Pract 1991; 45:208-211.

36. Wiseman LR, Spencer CM. Mitoxantrone. A review of its pharmacology and clinical efficacy in the management of hormone-resistant advanced prostate cancer. Drugs Aging 1997; 10:473-485.

37. Kolodziejczyk P, Reszka K, Lown JW. Enzymatic oxidative activation and transformation of the antitumor agent mitoxantrone. Free Radic Biol Med 1988; 5:13-25.

38. Barasch D, Zipori O, Ringel I, Ginsburg I, Samuni A, Katzhendler J. Novel anthraquinone derivatives with redox-active functional groups capable of producing free radicals by metabolism: are free radicals essential for cytotoxicity? Eur J Med Chem 1999; 34:597-615.

39. Dunn CJ, Goa KL. Mitoxantrone: a review of its pharmacological properties and use in acute nonlymphoblastic leukaemia. Drugs Aging 1996; 9:122-147.

40. Crossley RJ. Clinical safety and tolerance of mitoxantrone (Novantrone). Cancer Treat Rev 1983; 10 Suppl B:29-36.

41. Holland JF. Mitoxantrone--A critique. Cancer Treat Rev 1983; 10 Suppl B:77-79.

42. Posner LE, Dukart G, Goldberg J, Bernstein T, Cartwright K. Mitoxantrone: an overview of safety and toxicity. Invest New Drugs 1985; 3:123-32.

43. Ehninger G, Proksch B, Schiller E. Detection and separation of mitoxantrone and its metabolites in plasma and urine by high-performance liquid chromatography. J Chromatogr 1985; 342:119-127.

44. Ehninger G, Proksch B, Heinzel G, Woodward DL. Clinical pharmacology of mitoxantrone. Cancer Treat Rep 1986; 70:1373-8.

45. Ehninger G, Schuler U, Proksch B, Zeller KP, Blanz J. Pharmacokinetics and metabolism of mitoxantrone. A review. Clin Pharmacokinet 1990; 18:365-380.

46. Savaraj N, Lu K, Valdivieso M, Burgess M, Umsawasdi T, Benjamin RS, Loo TL. Clinical kinetics of 1, 4-dihydroxy-5,8-bis [(2-[(2-hydroxyethyl) amino] ethyl] amino]-9, 10-anthracenedione. Clin Pharmacol Therapeut 1982; 31:312-326.

47. Schleyer E, Kamischke A, Kaufmann CC, Unterhalt M, Hiddemann W. New aspects on the pharmacokinetics of mitoxantrone and its two major metabolites. Leukemia 1994; 8:435-440.

48. Loadman PM, Calabrese CR. Separation methods for anthraquinone related anti-cancer drugs. Journal of Chromatography B 2001; 764:193-206.

49. Priston MJ, Sewell GJ. Improved LC assay for the determination of mitozantrone in plasma: analytical considerations. J Pharm Biomed Anal 1994; 12:1153-1162.

50. Rentsch KM, Schwendener RA, Hanseler E. Determination of mitoxantrone in mouse whole blood and different tissues by high-performance liquid chromatography. J Chromatogr B Biomed Appl 1996; 679:185-92.

51. Connors KA, Amidon GL, Stella VJ. Chemical stability of pharmaceuticals: a handbook for pharmacists. New York: John Wiley & Sons, 1986.

52. Parker WB, Cheng YC. Metabolism and mechanism of action of 5-fluorouracil. Pharmacol Ther 1990; 48:381-95.

53. 5-Fluorouracil: Chemical Health & Safety. http://ntp-server.niehs.nih.gov/. National Toxicology Program: National Institute of Health, 2001:accessed 11/29/2002.

54. Chabner BA, Allegra CJ, Curt GA, Calabresi P. Chapter 51: antineoplastic agents. In: Goodman LS, Gilman A, Hardman JG, Gilman AG, Limbird LE, eds. Goodman & Gilman's the pharmacological basis of therapeutics. New York: McGraw-Hill Health Professions Division, 1996.

55. Gutheil JC, Finucane DM. Antimetabolites. In: Perry MC, ed. The chemotherapy source book. Baltimore: Williams & Wilkins, 2001.

56. Connors D, Gies D, Lin H, Gruskin E, Mustoe TA, Tawil NJ. Increase in wound breaking strength in rats in the presence of positively charged dextran beads correlates with an increase in endogenous transforming growth factor-beta1 and its receptor TGF-betaRI in close proximity to the wound. Wound Repair Regen 2000; 8:292-303.

57. Wattanatorn W, McLeod HL, Macklon F, Reid M, Kendle KE, Cassidy J. Comparison of 5-fluorouracil pharmacokinetics in whole blood, plasma, and red blood cells in patients with colorectal cancer. Pharmacotherapy 1997; 17:881-6.

58. Bateman J. Chemotherapy of solid tumors with triethyl phosphoramide. N Engl J Med 1955; 252:879-887.

59. Bateman J. Palliation of cancer in human patients by maintenance therapy with NN'N'-triethlyene thiophosphoramide and N-(3-oxapentamethylene)-N'N'-diethylene phosphoramide. Ann N Y Acad Sci 1958; 68:1057-1071.

60. McLaughlin CA, Cantrell JL, Ribi E, Goldberg EP. Intratumor chemoimmunotherapy with mitomycin C and components from mycobacteria in regression of line 10 tumors in guinea pigs. Cancer Res 1978; 38:1311-6.

61. Bast RC, Segerling M, Ohanian SH, Greene SL, Zbar B, Rapp HJ, Borsos T. Regression of established tumors and induction of tumor immunity by intratumor chemotherapy. J Natl Cancer Inst 1976; 56:829-32.

62. Borsos T, Bast RC, Jr., Ohanian SH, Segerling M, Zbar B, Rapp HJ. Induction of tumor immunity by intratumoral chemotherapy. Ann N Y Acad Sci 1976; 276:565-72.

63. Cantrell JL, McLaughlin CA, Ribi E. Efficacy of tumor cell extracts in immunotherapy of murine EL-4 leukemia. Cancer Res 1979; 39:1159-67.

64. McLaughlin CA, Goldberg EP. Local chemo- and immunotherapy by intratumor drug injection: Opportunities for polymer-drug compositions. In: Goldberg EP, ed. Targeted drugs. New York: John Wiley & Sons, 1983:231-268.

65. Tomita T. Interstitial chemotherapy for brain tumors: review. J Neurooncol 1991; 10:57-74.

66. Walter KA, Tamargo RJ, Olivi A, Burger PC, Brem H. Intratumoral chemotherapy. Neurosurgery 1995; 37:1128-45.

67. Haroun RI, Brem H. Local drug delivery. Curr Opin Oncol 2000; 12:187-193.

68. Theon AP. Intralesional and topical chemotherapy and immunotherapy. Vet Clin North Am Equine Pract 1998; 14:659-71, viii.

69. Brincker H. Direct intratumoral chemotherapy. Crit Rev Oncol Hematol 1993; 15:91-98.

70. Baitchev G, Gorchev G, Deliisky T, Popovska S, Raitcheva TZ. Perioperative locoregional application of mitoxantrone in patients with early breast carcinoma. J Chemother 2001; 13:440-3.

71. Saltzman WM. Drug delivery: engineering principles for drug delivery. New York: Oxford University Press, 2001:xi, 372.

72. Leach KJ. Cancer, drug delivery to treat--local & systemic. In: Mathiowitz E, ed. Encyclopedia of controlled drug delivery. Vol. 1. New York: John Wiley & Sons, Inc., 1999:119-143.

73. Harper E, Dang W, Lapidus RG, Garver RI, Jr. Enhanced efficacy of a novel controlled release paclitaxel formulation (PACLIMER delivery system) for local-regional therapy of lung cancer tumor nodules in mice. Clin Cancer Res 1999; 5:4242-8.

74. Longo WE, Iwata H, Lindheimer TA, Goldberg EP. Preparation of hydrophilic albumin microspheres using polymeric dispersing agents. J Pharm Sci 1982; 71:1323-8.

75. Goldberg EP, Longo WE, Iwata H. Microspheres for incorporation of therapeutic substances and methods of preparation thereof. Vol. June 9, 1987: U.S. Patent 4,671,954, 1987.

76. Longo WE, McCluskey RA, Goldberg EP. Magnetically responsive, hydrophilic microspheres for incorporation of therapeutic substances and methods of preparation thereof. Vol. October 3, 1989: U.S. Patent 4,871,716, 1989.

77. Longo WE. Albumin microspheres for the controlled release of therapeutic agents. Ph.D. Dissertation. Gainesville: University of Florida, 1983.

78. Goldberg EP, Iwata H, Longo W. Hydrophilic albumin and dextran ion-exchange microspheres for localized chemotherapy. In: Davis SS, Illum L, McVie JG, Tomlinson E, eds. Microspheres and drug therapy. pharmaceutical, immunological and medical aspects: Elsevier Science Publishers, 1984:309-325.

79. Longo WE, Goldberg EP. Hydrophilic albumin microspheres. Methods Enzymol 1985; 112:18-26.

80. Jayakrishnan A, Knepp WA, Goldberg EP. Casein microspheres: preparation and evaluation as a carrier for controlled drug delivery. Int J Pharmaceut 1994; 106:221-228.

81. Knepp WA. Synthesis and evaluation of casein and albumin microspheres for targeted drug and enzyme delivery. Ph.D. Dissertation. Gainesville: University of Florida, 1991.

82. Knepp WA, Jayakrishnan A, Quigg JM, Sitren HS, Bagnall JJ, Goldberg EP. Synthesis, properties, and intratumoral evaluation of mitoxantrone-loaded casein microspheres in Lewis lung carcinoma. J Pharm Pharmacol 1993; 45:887-91.

83. Latha MS, Jayakrishnan A. A new method for the synthesis of smooth, round, hydrophilic protein microspheres using low concentrations of polymeric dispersing agents. J Microencapsul 1995; 12:7-12.

84. Latha MS, Jayakrishnan A, Rathinam K, Mohanty M. Casein as a carrier matrix for 5-fluorouracil: drug release from microspheres, drug-protein conjugates and in-vivo degradation of microspheres in rat muscle. J Pharm Pharmacol 1994; 46:858-62.

85. Jameela SR, Latha PG, Subramoniam A, Jayakrishnan A. Antitumour activity of mitoxantrone-loaded chitosan microspheres against Ehrlich ascites carcinoma. J Pharm Pharmacol 1996; 48:685-688.

86. Kirk JF. Protein microspheres for controlled drug delivery and related analysis of biopolymers. Ph.D. Dissertation. Gainesville: University of Florida, 1997.

87. Hadba AR, Marotta JS, Goldberg EP. Synthesis of albumin microsphere drug carrier compositions: factors influencing particle size. Trans Soc Biomat 1999:434.

88. Hadba AR, Marotta JS, Goldberg EP. Optimization of albumin microsphere synthesis: factors influencing particle size, Trans Sixth World Biomat Cong, Kamela, Hawaii, 2000. Vol. 2.

89. Hadba AR, Almond BA, Goldberg EP. Intratumoral chemotherapy with mitoxantrone-loaded albumin microspheres in a murine mammary model, Trans Soc Biomat, Tampa, FL, 2002.

90. Luftensteiner CP, Viernstein H. Statistical experimental design based studies on placebo and mitoxantrone-loaded albumin microspheres. Int J Pharmaceut 1998; 171:87-99.

91. Luftensteiner CP, Schwendenwein I, Paul B, Eichler HG, Viernstein H. Evaluation of mitoxantrone-loaded albumin microspheres following intraperitoneal administration to rats. J Control Release 1999; 57:35-44.

92. Luftensteiner CP, Schwendenwein I, Eichler HG, Paul B, Wolfl G, Viernstein H. Toxicity of a particulate formulation for the intraperitoneal application of mitoxantrone. Int J Pharmaceut 1999; 180:251-260.

93. Fu Y-J, Shyu S-S, Su F-H, Yu P-C. Development of biodegradable co-poly(-lactic/glycolic acid) microspheres for the controlled release of 5-FU by the spray drying method. Colloids Surfaces B; In Press, Corrected Proof.

94. Hussain M, Beale G, Hughes M, Akhtar S. Co-delivery of an antisense oligonucleotide and 5-fluorouracil using sustained release poly (lactide-co-glycolide) microsphere formulations for potential combination therapy in cancer. Int J Pharmaceut 2002; 234:129-138.

95. Benoit J-P, Faisant N, Venier-Julienne M-C, Menei P. Development of microspheres for neurological disorders: From basics to clinical applications. J Control Release 2000; 65:285-296.

96. Zinutti C, Barberi-Heyob M, Hoffman M, Maincent P. In-vivo evaluation of sustained release microspheres of 5-FU in rabbits. Int J Pharmaceut 1998; 166:231-234.

97. Narayani R, Rao KP. Gelatin microsphere cocktails of different sizes for the controlled release of anticancer drugs. Int J Pharmaceut 1996; 143:255-258.

98. Arica B, Calis S, Kas HS, Sargon MF, Hincal AA. 5-Fluorouracil encapsulated alginate beads for the treatment of breast cancer. Int J Pharmaceut 2002; In Press, Uncorrected Proof.

99. Sugibayashi K, Morimoto Y, Nadai T, Kato Y, Hasegawa A, Arita T. Drug-carrier property of albumin microspheres in chemotherapy. II. Preparation and tissue distribution in mice of microsphere-entrapped 5-fluorouracil. Chem Pharm Bull (Tokyo) 1979; 27:204-9.

100. Festing MFW. Festing's List of Inbred Strains of Mice and Rats. www.informatics.jax.org/external/festing/search_form.cgi 2002:accessed 11/22/2002.

101. Jackson-Laboratories. Jax Mice: Product Specifications. www.jax.org/jaxmice 2000:accessed 11/22/02.

102. Ross SR. Using genetics to probe host-virus interactions; the mouse mammary tumor virus model. Microbes Infect 2000; 2:1215-23.

103. Matsuzawa A, Nakano H, Yoshimoto T, Sayama K. Biology of mouse mammary tumor virus (MMTV). Cancer Lett 1995; 90:3-11.

104. Sundberg JP, Boggess D, Sundberg MS. Neoplastic and hyperplastic lesions in the C3H/HeJ mouse strain. Jax Bulletin #461: The Jackson Laboratory, 1995.

105. Jackson-Laboratories. C3H/HeJ and C3H/HeOuJ mice free of exogenous MMTV. Jax Bulletin #7: The Jackson Laboratory, 2001.

106. Corbett TH, Griswold Jr DP, Roberts BJ, Peckham JC, Schabel Jr FM. Biology and therapeutic response of a mouse mammary adenocarcinoma (16/C) and its potential as a model for surgical adjuvant chemotherapy. Cancer Treat Rep 1978; 62:1471-88.

107. Corbett TH, Roberts BJ, Trader MW, Laster Jr WR, Griswold Jr DP, Schabel Jr FM. Response of transplantable tumors of mice to anthracenedione derivatives alone and in combination with clinically useful agents. Cancer Treat Rep 1982; 66:1187-200.

108. Schabel Jr FM, Corbett TH, Griswold Jr DP, Laster Jr WR, Trader MW. Therapeutic activity of mitoxantrone and ametantrone against murine tumors. Cancer Treat Rev 1983; 10 Suppl B:13-21.

109. Porter DA, Easterling KE. Phase transformations in metals and alloys. London: Chapman & Hall, 1992.

110. Reed-Hill RE, Abbaschian R. Physical metallurgy principles. Boston: PWS Publishing Co., 1994.

111. Justice M. Clinical hematology, accession # MPD:15. Mouse Phenome Database Web Site. Bar Harbor, ME: The Jackson Laboratory (http://www.jax.org/phenome), 2000:accessed 11/22/2002.

112. Physician's drug handbook. Springhouse, Pa.: Springhouse, 1999.

113. Fisher B. From Halsted to prevention and beyond: advances in the management of breast cancer during the twentieth century. Eur J Cancer 1999; 35:1963-73.

114. Sung HW, Liang IL, Chen CN, Huang RN, Liang HF. Stability of a biological tissue fixed with a naturally occurring crosslinking agent (genipin). J Biomed Mater Res 2001; 55:538-46.

115. Mi FL, Tan YC, Liang HF, Sung HW. In vivo biocompatibility and degradability of a novel injectable-chitosan-based implant. Biomaterials 2002; 23:181-91.

116. Goldberg EP, Longo WE, Almond BA, Hadba AR. Microsphere-drug compositions for localized chemotherapy and immunotherapy, Particles 2002: medical/biochemical diagnostic, pharmaceutical, and drug delivery applications of particle technology, Orlando, FL, 2002.

117. Kitazawa H, Sato H, Adachi I, Masuko Y, Horikoshi I. Microdialysis assessment of fibrin glue containing sodium alginate for local delivery of doxorubicin in tumor-bearing rats. Biol Pharm Bull 1997; 20:278-81.

118. Nishikawa M, Hashida M. Pharmacokinetics of anticancer drugs, plasmid DNA, and their delivery systems in tissue-isolated perfused tumors. Adv Drug Deliv Rev 1999; 40:19-37.

119. Evanochko WT, Ng TC, Lilly MB, Lawson AJ, Corbett TH, Durant JR, Glickson JD. In vivo 31P NMR study of the metabolism of murine mammary 16/C adenocarcinoma and its response to chemotherapy, x-radiation, and hyperthermia. Proc Natl Acad Sci U S A 1983; 80:334-8.

120. Chabner B, Longo DL. Cancer chemotherapy and biotherapy : principles and practice. Philadelphia: Lippincott Williams & Wilkins, 2001.

BIOGRAPHICAL SKETCH

Brett Anthony Almond was born in Panama City, Florida on August 16, 1974. He was raised in Lynn Haven, Florida, a suburb of Panama City. In 1996, he not only graduated valedictorian of his class at A. C. Mosley High School, but was also voted one of the "Top Ten" students by his peers. After high school, he spent the summer working at the Coastal Systems Station, a U.S. Naval research and development base, developing software to analyze data from simulations of underwater warfare systems. In the fall, he attended the University of Florida on National Merit, National Science, Robert C. Byrd, Anderson, and Florida Undergraduate scholarships. Shortly after entering college, he was designated an Advanced Placement Distinguished Scholar by the College Board. This designation was awarded to the top 14 freshman students in the nation based on the number of and performance on Advanced Placement Exams taken in high school. He originally intended to major in electrical engineering, but quickly developed an interest in biomedical engineering, which lead him to change his major to materials science and engineering in order to pursue a career in biomaterials research. While an undergraduate student in the Department of Material Science and Engineering, he was inducted into Tau Beta Pi, Golden Key, and Sigma Phi Epsilon national honor societies and received a Dow Chemical Scholarship. During his senior year, he conducted research on the pH controlled release of antibiotics and other substances from modified stents and catheters under the supervision of Dr. William Toreki for CApHCO, Inc. During this time, he also worked with Dr. Christopher Batich on his senior research project investigating the

controlled release of anti-cancer drugs from gelatin microspheres to treat inoperable hepatic carcinoma. Brett graduated from the University of Florida in May 1996 with a Bachelor of Science with High Honors in Materials Science and Engineering, specializing in polymer materials, and a minor in chemistry.

In the fall after graduation, Brett entered the MD/PhD program at the University of Florida. In the summers before and after his fist year of medical school he returned to the Coastal Systems Station as an engineer working on the SABRE project performing failure analysis and redesigning the polymeric components of an experimental warhead for the clearance of mines from the littoral zone (which includes the beach and surf zones).

In the fall of 1998 after the completion of his first two years of medical school, Brett returned to the Department of Materials Science and Engineering at the University of Florida to pursue his PhD in polymeric biomaterials research under the guidance of Dr. Eugene P. Goldberg. He performed his research on the controlled drug delivery from, and surface modification of, polymeric materials. His dissertation topic was the *in vivo* testing of intratumoral chemotherapy with drug-loaded albumin microspheres for the treatment of breast cancer. He received his Doctor of Philosophy degree in December 2002.

After defending his dissertation, Brett returned to medical school to complete his final two years. After graduation from medical school, he plans to perform his residency in surgery and pursue a career in academic medicine researching biomaterials and the body's interactions to them.